

ANALYSIS OF THE ROLE OF CARM1 IN TELOMERE MAINTENANCE

ANALYSIS OF THE ROLE OF CARM1 IN TELOMERE MAINTENANCE

BY

TALIA ASA, B.Sc.

A Thesis

Submitted to the School of Graduate Studies

in Partial Fulfillment of the Requirements

For the Degree

Master of Science

McMaster University

©Copyright by Talia Asa, July 2010

MASTER OF SCIENCE (2010)

McMaster University

(Biology)

Hamilton, Ontario

TITLE: Analysis of the role of CARM1 in telomere maintenance

AUTHOR: Talia Asa, B.Sc. (The University of Western Ontario)

SUPERVISOR: Professor Xu-Dong Zhu

NUMBER OF PAGES: xviii, 134

Abstract:

Recent data suggest that protein arginine methyltransferase 1 (PRMT1) plays a role in telomere length maintenance and telomere stability. PRMT1 has been shown to methylate the basic domain of TRF2 and depletion of PRMT1 leads to the formation of telomere doublets in primary cells and telomere shortening in cancer cells. Additionally mass spectrometry data suggest candidate arginine residues in TRF1 and TRF2 that are mono- or di-methylated. These data suggest that arginine methylation and thus PRMT enzymes may play a role in telomere biology.

Because PRMT1 has been shown to play a role in telomere maintenance, we decided to look for a role of another PRMT enzyme, coactivator associated arginine methyltransferase 1 (CARM1), on telomere biology. To determine if CARM1 plays a role in telomere length maintenance, hTERT-BJ cells were depleted for CARM1. Initially, a senescent phenotype was observed; however, this phenotype was not reproducible. Subsequently, I have shown that these cells do not accumulate telomere or genomic instability or a change in growth. To determine if CARM1 plays a role in telomere length maintenance, hTERT-BJ, HeLaII, and MCF-7 cells were depleted of CARM1 and cultured long term. Southern blot analysis indicated no change in telomere length dynamics over time upon depletion of CARM1 compared to control cells. Thus these results suggest that CARM1 does not play a role in telomere length maintenance.

The laboratory of Linger identified telomeres to be transcribed into telomere repeat-containing RNA termed TERRA. The mechanism of TERRA regulation is still to be elucidated. Because CARM1 is a transcriptional coactivator, we hypothesized that CARM1 play a role in TERRA transcription. Northern blot analysis conducted in hTERT-BJ and MCF-7 cells depleted of CARM1 revealed no role for CARM1 in TERRA regulation.

Acknowledgements:

I would like to start off by thanking my supervisor, Dr. Xu-Dong Zhu, for giving me the opportunity to complete my master's thesis in her lab. I have learned many useful laboratory and troubleshooting skills. Dr. Zhu is a very dedicated researcher and I appreciate the opportunity I had to learn with her. Additionally, I would like to thank the members of my supervisory committee, Drs. André Bédard and Karen Mossman, for their time and helpful advice. I would also like to thank the members of the biology department for all of their support and guidance.

I also owe thanks to my lab mates. I appreciate all the time you spent teaching me new techniques and helping me troubleshoot problems. Thanks to Megan and Taylor who taught me many protocols when I first started working in the laboratory. Thanks to Sichun who was always patient with me when I required assistance. I also owe thanks to Kajaparan and Mohammad who helped me through all the 'speed bumps' I encountered over the past two years.

Lastly, I would like to thank my family. To my parents, mum and dad, I love you and appreciate all of the love and support you have given me over the years. To my brothers, Benjamin and Jonathon, you two have always been there for me and I know that you always will be.

Table of Contents:

1.0 Introduction.....	1
1.1 The End Replication Problem, Telomeres, and Telomerase.....	1
1.2 The Shelterin Complex.....	2
1.2.1 TRF1 (Telomere Repeat Binding Factor 1).....	3
1.2.2 TRF2 (Telomere Repeat Binding Factor 2).....	6
1.2.3 Rap1 (Repressor-activator Protein 1).....	8
1.2.4 TIN2 (TRF1 Interacting Nuclear Protein 2).....	10
1.2.5 TPP1 (TINT1/PTOP/PIP1).....	13
1.2.6 POT1 (Protection of Telomeres).....	15
1.3 Telomere Repeat Containing RNA – TERRA.....	17
1.4 Arginine Methylation.....	22
1.5 Coactivator Associated Arginine Methyltransferase 1, CARM1.....	23
1.5.1 CARM1 and its Role as a Transcriptional Coactivator.....	26
1.5.2 CARM1 and its Role in RNA-Binding Properties.....	28
1.5.3 CARM1 and its Role in Breast and Prostate Cancer.....	32
1.6 Rationale and Hypothesis.....	36
2.0 Materials and Methods.....	49
2.1 Cloning of Constructs.....	49
2.1.1 Transformation.....	49
2.1.2 QIAGEN® Plasmid Purification Maxiprep Kit.....	49

2.2 Tissue Culture.....	51
2.2.1 Growth of Cell Lines.....	51
2.2.2 Retroviral Infection.....	51
2.3 Protein Study.....	52
2.3.1 Protein Extract.....	52
2.3.2 Bradford Assay.....	53
2.3.3 Western Blotting.....	53
2.3.4 Antibodies.....	54
2.4 Proliferation Assays.....	55
2.4.1 Short Term Cell Growth Assay.....	55
2.4.2 Long Term Cell Growth Assay.....	55
2.4.3 Senescence Associated β -Galactosidase Staining Assay.....	55
2.5 Immunofluorescence.....	56
2.5.1 Immunofluorescence Antibodies.....	57
2.6 Genomic DNA Analysis.....	57
2.6.1 Isolation of Genomic DNA.....	57
2.6.2 Digestion of Genomic DNA.....	59
2.6.3 Southern Blotting and Detection of Telomeric Fragments.....	59
2.7 RNA Analysis.....	60
2.7.1 Isolation of RNA.....	60
2.7.2 Northern Blotting and Detection of Telomeric RNA.....	61
3.0 Results.....	63

3.1 Depletion of CARM1 does not alter other PRMT protein levels.....	63
3.2 Depletion of CARM1 does not alter other the protein levels of shelterin proteins.....	64
3.3 Depletion of CARM1 initially induced cellular senescence.....	64
3.3.1 Cells depleted of CARM1 initially stained positive for senescence-associated β -galactosidase.....	64
3.3.2 Depletion of CARM1 does appear to not induce genomic instability.....	65
3.3.3 Depletion of CARM1 does not appear to alter telomere length.....	65
3.3.4 Depletion of CARM1 in hTERT-BJ cells does not appear to affect cell growth in the short term.....	66
3.4 Depletion of CARM1 in HeLaII cells does not appear to alter cellular proliferation or changes in telomere length dynamics.....	67
3.4.1 HeLaII cells infected with a retrovirus expressing shCARM1 show similar levels of CARM1 knockdown at early and late population doublings.....	67
3.4.2 HeLaII cells depleted of CARM1 do not appear to exhibit a growth defect.....	67
3.4.3 Depletion of CARM1 in HeLaII cells initially resulted in telomere elongation.....	68
3.5 Depletion of CARM1 in MCF-7 cells does not appear to alter cellular proliferation or changes in telomere length dynamics.....	69
3.5.1 The level of CARM1 knockdown in MCF-7 cells is altered from early to late population doublings.....	69
3.5.2 MCF-7 cells depleted of CARM1 do not appear to exhibit a growth defect.....	69
3.5.3 CARM1 depletion in MCF-7 cells does not appear to alter telomere length dynamics.....	70

3.6 Depletion of CARM1 in hTERT-BJ cells does not appear to alter cellular proliferation or changes in telomere length dynamics.....	70
3.6.1 hTERT-BJ cells infected with shCARM1 show similar levels of CARM1 knockdown at early and late population doublings....	70
3.6.2 hTERT-BJ cells depleted of CARM1 do not appear to exhibit a growth defect.....	71
3.6.3 CARM1 depletion in hTERT-BJ cells does not appear to alter telomere length dynamics.....	71
3.7 Depletion of CARM1 does not appear to alter TERRA levels.....	72
4.0 Discussion.....	115
4.1 Depletion of CARM1 initially induced cellular senescence.....	115
4.2 CARM1 does not appear to play a role in telomere length dynamics.....	115
4.3 CARM1 does not appear to play a role in TERRA regulation.....	116
4.4 Significance and Perspectives.....	117
4.5 Conclusion.....	118
5.0 References.....	120

Abbreviations:

2-D – 2 dimensional

53BP1 – p53-binding protein 1

AIB1 – Amplified in breast cancer 1

AdoMet – *S*-adenosylmethionine

AR – Androgen receptor

ATM – Ataxia telangiectasia mutated

ATP – Adenosine triphosphate

ATR – Ataxia telangiectasia and Rad3 related

AU-rich – Adenine Uracil-rich

BLM – Bloom syndrome protein

BRG1 – Brahma/SWI2-related gene 1

CARM1 – Coactivator associated arginine methyltransferase 1

CBP – CREB-binding protein

cdc25A - Cell division cycle 25 homolog A

cDNA – Complementary DNA

CREB - Cyclic adenosine monophosphate (cAMP) response element-binding

C-rich – Cytosine rich strand of DNA

ChIP – Chromatin immunoprecipitation

Chk1/2 – Checkpoint kinase 1/2

DAPI – 4' 6'-diamino-2-phenylindole

DEPC – Diethyl pyrocarbonate

D-loop – Displacement loop

DMEM – Dulbecco's Modified Eagle Medium

DNA – Deoxyribonucleic acid

DTT – Dithiothreitol

E (ex E6.5) – Embryonic day

E2 – 17 β -estradiol

EDTA – Ethylenediaminetetraacetic acid

EM – Electron microscopy

ER – Estrogen receptor

ER α – Estrogen receptor alpha

ER β – Estrogen receptor beta

ES cells – Embryonic stem cells

EST1A – Ever shorter telomeres 1A

FBS – Fetal bovine serum

Floxed – Flanked by LoxP sites

G1-phase – Gap 1 phase

G2-phase – Gap 2 phase

GADD45 – Growth arrest and DNA damage

GAPDH - Glyceraldehyde 3-phosphate dehydrogenase

GAR domain – Glycine- arginine-rich domain

G-rich – Guanine rich strand of DNA

GRIP1 – Glucocorticoid -receptor-interacting protein 1

GU-dinucleotides – Guanine uracil-dinucleotides

H3K4me – Histone H4 3 lysine 4 methylation

H3K9me3 – Histone H3 lysine 9 trimethylation

H3K18 – Histone H3 lysine 18

H3R17 – Histone H3 arginine 17

H3R17me – Histone H3 arginine 17 methylation

H3R26me – Histone H3 arginine 26 methylation

H4K20me3 – Histone H3 lysine 20 trimethylation

HBS – Hepes Buffered Saline

HEPES – 4-(2-hydroxyethyl)-1-piperazineethanesulfonic acid

HP1 – Heterochromatin protein 1

HP1 α – Heterochromatin protein 1 alpha

IP-10 – Interferon induced protein 10

iPABP – inducible poly-A-binding protein

IR – Ionizing radiation

LB – Lysogeny broth

M – Mitosis or mol/L

MDC1 – Mediator of DNA damage checkpoint protein 1

MEF – Mouse embryonic fibroblasts

MLL – Mixed lineage leukemia

MOPS – 3-(N-morpholino)propanesulfonic acid

MRN – Mre11/Rad50/Nbs1

mRNA – Messenger RNA

NF- κ B - Nuclear factor-kappa B

NHEJ – Nonhomologous end joining

NR – Nuclear receptor

NUMAC – Nucleosomal methylation activator complex

OB – oligonucleotide/oligosaccharide binding

Oct3 – Octamer binding protein 2

PABP – Poly-A-binding protein

PBS – Phosphate buffer saline

PD – Population doubling

PGM motif – Proline-, glycine-, methionine-, arginine-rich motifs

PIC_h - Proteomics of isolated chromatin segments

PIP1 – POT1-interacting protein 1

PMSF – Phenylmethanesulfonylfluoride

POT1 – Protection of telomeres

POT1 Δ OB – POT1 mutant lacking the OB domain

PRMT – Protein arginine methyltransferase

pRS – pRetro-Super

PSA – Prostate specific antigen

PTOP – POT1- and TIN2- organizing protein

R263K – Arginine 263 has been mutated to a lysine

Rap1 – Repressor-activator Protein 1

RNA – Ribonucleic acid

RPM - Revolutions per minute

RTEL1 – Regulator of telomere elongation helicase 1

RT-PCR – Reverse transcriptase polymerase chain reaction

S-phase – Synthesis phase

SDS - Sodium dodecyl sulphate

SDS-PAGE - Sodium dodecyl sulfate polyacrylamide gel electrophoresis

Ser – Serine

siRNA – Small interfering RNA

Sm proteins – Small ribonucleoprotein particle protein

SmB – Small ribonucleoprotein particle protein B

SMN – Survival of motor neuron

snRNP – Small nuclear ribonucleoproteins

Sox2 - SRY (sex determining region Y)-box 2

Suv39 – Suppressor of variegation 4-20

Suv4-20 – Suppressor of variegation 4-20

SWI/SNF – SWItch/Sucrose Nonfermentable

t-loop – Telomere loop

TBE – Tris borate EDTA

TE – Tris EDTA

TERRA – Telomeric repeat-containing RNA

TIF – Telomere dysfunction induced foci

TIN2 – TRF1 Interacting Nuclear Protein 2

TINT1 – TIN2 interacting protein 1

TPP1 – TINT1/PTOP/PIP1

TRF1 – Telomere repeat binding factor 1

TRF2 – Telomere repeat binding factor 2

TRF2 Δ B – TRF2 mutant lacking the basic domain

TRF2 Δ B Δ M – TRF2 mutant lacking the basic and DNA binding domain

TRFH – TRF homodimerization domain

SMG1 – Suppressor with morphogenetic defects in genitalia

snRNAs – Small nuclear ribonucleic acid

U1C – Small nuclear ribonucleoprotein polypeptide C

UPF1 – Up-frameshift mutation 1

UV – Ultraviolet

XRCC3 – X-ray repair cross-complementing protein group 3

Cell Lines:

293T – Human embryonic kidney cells transformed with SV40 large T-antigen

hTERT-BJ – Human fibroblast cells immortalized with telomerase

COS-7 – Monkey kidney cells transformed with SV40 large T-antigen

ES cells – Human embryonic stem cells

HCT75 – A derivative of HT1080 cells

HeLaII - Telomerase positive adenocarcinoma cell line

HT1080 – Telomerase positive human fibrosarcoma cell line

MCF-7 – Telomerase positive adenocarcinoma cell line

MEFs – Mouse embryonic fibroblast cells

U2OS – Telomerase negative human osteosarcoma cell line

List of Figures:

Figure 1.1 – The structure of human telomeric DNA

Figure 1.2 – Shelterin

Figure 1.3 – Shelterin protects telomeres from being recognized as damage DNA

Figure 1.4 – Arginine methylation by PRMTs

Figure 1.5 – Methylation of CBP/p300 by CARM1 regulates transcription of target genes

Figure 3.1 – HeLaII cells depleted for CARM1 do not show alterations in PRMT1, PRMT5, or PRMT6 protein levels

Figure 3.2 – hTERT-BJ cells depleted for CARM1 do not show alterations in shelterin protein levels

Figure 3.3 – Knockdown of CARM1 initially induced cellular senescence in hTERT-BJ cells

Figure 3.4 – Knockdown of CARM1 does not induce genomic instability or telomere instability in hTERT-BJ cells

Figure 3.5 – Southern blot analysis indicates that knockdown of CARM1 does not alter telomere length in the short term in hTERT-BJ cells

Figure 3.6 – hTERT-BJ cells depleted of CARM1 grow at the same rate as control cells over a 15-day period

Figure 3.7 – HeLaII cells depleted of CARM1 show equal levels of CARM1 knockdown at early and late population doublings

Figure 3.8 – HeLaII cells depleted of CARM1 do not exhibit defects in cells proliferation compared to control cells

Figure 3.9 – HeLaII cells depleted for CARM1 initially showed changes in telomere length dynamics; however, this was not reproducible.

Figure 3.10 – MCF-7 cells depleted of CARM1 show reduced levels of CARM1 knockdown at 40 population doublings compared to early population doublings

Figure 3.11 – MCF-7 cells depleted of CARM1 do not exhibit defects in cells proliferation compared to control cells

Figure 3.12 – MCF-7 cells depleted for CARM1 do not show changes in telomere length dynamics.

Figure 3.13 – hTERT-BJ cells depleted of CARM1 show equal levels of CARM1 knockdown at early and late population doublings

Figure 3.14 – hTERT-BJ cells depleted of CARM1 do not exhibit defects in cells proliferation compared to control cells.

Figure 3.15 – hTERT-BJ cells depleted for CARM1 do not show changes in telomere length dynamics

Figure 3.16 – Depletion of CARM1 does not alter TERRA levels in MCF-7 cells

Figure 3.17 – Depletion of CARM1 does not alter TERRA levels in hTERT-BJ cells.

1.0 Introduction:

1.1 The End Replication Problem, Telomeres, and Telomerase:

The end replication problem, noted by Olovnikov and Watson in 1972, stems from the inability of the standard mechanism of DNA replication to successfully complete its function (Olovnikov *et al.*, 1971; Watson *et al.*, 1972; Olovnikov *et al.*, 1973). With each round of replication, a gap at the extreme 5' ends of chromosomes is anticipated to occur due to the removal of the last RNA primer (Olovnikov *et al.*, 1971; Watson *et al.*, 1972; Olovnikov *et al.*, 1973). If cells are unable to compensate, chromosome ends will shorten with each successive round of replication (Olovnikov *et al.*, 1971; Watson *et al.*, 1972; Olovnikov *et al.*, 1973). In 1987 Greider and Blackburn discovered telomerase, a ribonucleoprotein responsible for adding TTAGGG repeats to the ends of chromosomes to combat the end replication problem (Greider *et al.*, 1987). Thus, upon DNA replication essential information is not lost.

The length of human double stranded telomeric DNA at birth is approximately 10-15 kilobases and consists of a 50-500 base pair 3' G-rich single stranded overhang (de Lange *et al.*, 1990; Lejinine *et al.*, 1995; McElligott *et al.*, 1997; Wright *et al.*, 1997) (Figure 1.1A). Mammalian telomeric DNA does not contain a blunt-ended free floating end but rather exists in a telomere-loop (t-loop) configuration in which the 3' overhang invades the duplex DNA to form a t-loop (Griffith *et al.*, 1999). The 3' overhang base pairs with the C-rich duplex

DNA and displaces the G-strand at this site to create the displacement loop (D-loop) (Griffith *et al.*, 1999) (Figure 1.1B). The t-loop is thought to act to sequester the natural ends of linear chromosomes from being recognized as DNA damage (Griffith *et al.*, 1999).

Telomeres not only serve as a buffer to combat the end replication problem but also function as a tumor suppressor mechanism to limit the cell's proliferative abilities (Olovnikov *et al.*, 1971; Watson *et al.*, 1972; Olovnikov *et al.*, 1973). Telomere DNA is lost with each cell division and when telomeres reach a critical length replicative senescence occurs (Greider *et al.*, 1987; Blackburn *et al.*, 1989; Greider *et al.*, 1989). Telomerase is typically active only in stem and germ cells, but is activated in many cancers (Greider *et al.*, 1987; Blackburn *et al.*, 1989; Greider *et al.*, 1989; Counter *et al.*, 1992; de Lange 2006). This allows cancer cells to overcome the replication barrier imposed by telomere loss (Greider *et al.*, 1987; Blackburn *et al.*, 1989; Greider *et al.*, 1989).

1.2 The Shelterin Complex:

The TTAGGG telomeric tract associates with a six membered protein complex termed shelterin (Liu *et al.*, 2004, de Lange, 2005; Palm *et al.*, 2008). Shelterin prevents the natural chromosome ends from being recognized as sites of DNA damage and allows for telomerase-mediated telomere length maintenance (de Lange, 2005). The specificity of the shelterin complex for telomeric repeats is due to the affinity of the proteins to bind to the TTAGGG repeats (Palm *et al.*,

2008). Telomere repeat binding factors 1 and 2 (TRF1 and TRF2) bind to the duplex telomeric DNA while protection of telomeres 1 (POT1) binds to the 3' G-rich single stranded overhang and the single stranded DNA in the D-loop upon t-loop formation (Bilaud *et al.*, 1997; Smith *et al.*, 1997; Baumann *et al.*, 2001; Loayza *et al.*, 2003). TIN2/PTOP/PIP1 (TPP1), TRF1 interacting nuclear protein 2 (TIN2), and repressor activator protein 1 (Rap1) are other members of the shelterin complex (Kim *et al.*, 1999; Li *et al.*, 2000; Houghtaling *et al.*, 2004; Liu *et al.*, 2004; Ye *et al.*, 2004; O'Connor *et al.*, 2006). TPP1 associates with POT1 whereas Rap1 associates with TRF2 (Li *et al.*, 2000; Liu *et al.*, 2004; Ye *et al.*, 2004; O'Connor *et al.*, 2006; Hockemeyer *et al.*, 2007). TIN2 serves as a bridging protein to connect the shelterin complex (Broccoli *et al.*, 1997; Smogorzewska *et al.*, 2000; vanSteensel *et al.*, 1997; Ye *et al.*, 2004) (Figure 1.2).

1.2.1 TRF1 (Telomere Repeat Binding Factor 1):

TRF1 was shown to be a component of human telomeres through its ability to bind a TTAGGG substrate *in vitro* and its ability to localize to telomeres in both interphase and metaphase cells (Chong *et al.*, 1995). TRF1 contains an N-terminal acidic domain, a TRFH homodimerization domain, a linker region, and a C-terminal Myb domain (Chong *et al.*, 1995; Bianchi *et al.*, 1997). TRF1 was shown to bind double stranded telomeric DNA as a dimer and induce bending to allow for pairing of the telomere tracts during t-loop formation (Bianchi *et al.*, 1997; Broccoli *et al.*, 1997; Griffith *et al.*, 1998). TRF1 has shown to be an

essential gene since mice depleted for TRF1 die before E6.5 (Karlseder *et al.*, 2003). Telomerase deficiency does not appear to rescue embryonic lethality suggesting TRF1 may play a role during development that is independent of telomere length regulation (Karlseder *et al.*, 2003).

TRF1 functions as a negative regulator in telomere length maintenance (Smith *et al.*, 1997; van Steensel and de Lange 1997). Overexpression of TRF1 in HT1080 cells resulted in telomere shortening whereas introduction of a dominant negative form of TRF1 resulted in gradual telomere elongation (van Steensel and de Lange 1997). Thus TRF1 controls telomere length in *cis* by inhibiting telomerase from acting on the ends of telomeres (van Steensel and de Lange 1997). This idea lead to the protein counting model in which longer telomeres have more TRF1 bound, thus inhibiting telomerase access from chromosome ends, resulting in shorter telomeres (Smogorzewska *et al.*, 2000). Conversely, shorter telomeres have less TRF1 molecules bound and thus have a greater chance of being elongated (Smogorzewska *et al.*, 2000). In this manner telomerase positive cells maintain a balance of telomerase positive and negative signals based on telomere length by virtue of the amount of TRF1 recruited.

Tankyrase, a TRF1-interacting ankyrin-related ADP-ribose polymerase, has been shown to poly(ADP-ribosyl)ate TRF1 causing its removal from telomere tracts and subsequent ubiquitination and degradation (Smith *et al.*, 1998; Smith *et al.*, 1999; Smith *et al.*, 2000; Chang *et al.*, 2003). Tankyrase was found to

interact with the N-terminal of TRF1 through a yeast-two-hybrid analysis (Smith *et al.*, 1998). *In vitro* assays show that tankyrase poly(ADP-ribosyl)ates TRF1 and gel-shift assays show that ribosylation causes the removal of TRF1 from telomeric DNA (Smith *et al.*, 1998). Overexpression of tankyrase resulted in reduced TRF1 at telomeres and telomere elongation in telomerase positive cells whereas overexpression of a PARP-deficient form of tankyrase failed to alter telomere length dynamics (Smith *et al.*, 2000). Once TRF1 is released from the telomeres through ADP-ribosylation, TRF1 is ubiquitinated and degraded by the proteasome pathway (Chang *et al.*, 2003).

Telomeric repeats have the potential to create problems during DNA replication (Martínez *et al.*, 2009; Sfeir *et al.*, 2009). Sfeir and colleagues identified a potential role of TRF1 in the progression of the replication fork at telomeres (Sfeir *et al.*, 2009). Using fluorescence *in situ* hybridization they report that deletion of TRF1 in MEFs caused an increase in multitelomeric signals per chromatid end (Sfeir *et al.*, 2009). This phenotype suggests that lack of TRF1 may result in replication defects (Sfeir *et al.*, 2009). Using *in vivo* labeling to assess replication fork progression, they show that deletion of TRF1 resulted in replication fork stalling (Sfeir *et al.*, 2009). Additionally, they show that bloom syndrome protein (BLM) and regulator of telomere elongation helicase 1 (RTEL1) deficient MEFs induced multitelomeric signals acting epistatic to TRF1 (Sfeir *et al.*, 2009). Thus, they propose a mechanism suggesting that TRF1

recruits helicases BLM and RTEL1 to replication forks to prevent the formation of a fork barrier (Sfeir *et al.*, 2009).

1.2.2 TRF2 (Telomere Repeat Binding Factor 2):

The architectural similarities between TRF1 and TRF2 helped to identify TRF2 as a telomere protein. TRF2 contains a C-terminal DNA binding domain, a TRFH homodimerization domain, and an N-terminal basic domain (Bilaud *et al.*, 2007 and Broccoli *et al.*, 1997). Three experiments indicate that TRF2 is a component of human telomeres: gel-shift assays identified TRF2 binds to TTAGGG telomeric repeats, immunofluorescence indicated that TRF2 forms punctuate nuclear staining, and fluorescence *in situ* hybridization of metaphase chromosomes revealed that TRF2 is located at the ends of mitotic chromosomes (Bilaud *et al.*, 2007 and Broccoli *et al.*, 1997). Yeast-two-hybrid analysis and *in vitro* immunoprecipitation experiments indicated that like TRF1, TRF2 is able to homodimerize through its TRFH domain (and Broccoli *et al.*, 1997). Like TRF1, TRF2 also acts as a negative regulator of telomere length as overexpression of TRF2 in telomerase positive HCT75 cells induced telomere shortening (Smogorzewska *et al.*, 2000).

TRF2 has been shown to be critical in the formation of the t-loop structure. Electron microscopy (EM) showed that when TRF2 is incubated with a telomeric substrate, TRF2 is able to form a t-loop like structure (Stansel *et al.*, 2001). This is hypothesized to occur through some unique features of TRF2

(Palm and de Lange, 2008). Firstly, TRF2 has been shown to have a high affinity to bind telomeric DNA containing a 3' overhang (Stansel *et al.*, 2001). Secondly, TRF2 is able to promote t-loop formation through *in vitro* studies by condensing the DNA and generating positive supercoiling to promote strand invasion (Fouche *et al.*, 2006). Lastly, the basic domain of TRF2 has been shown to bind to Holiday junctions (Amiard *et al.*, 2007). The basic domain has been shown to be vital to the formation of t-loops (Wang *et al.*, 2004). Deletion of the basic domain of TRF2 (TRF2 Δ B), results in sudden telomere loss and 2-D gel electrophoresis revealed that the TRF2 Δ B mutants contain large circular telomeric DNA (Wang *et al.*, 2004). These large t-loop sized deletions are dependent on XRCC3, a protein implicated in having resolvase activity (Wang *et al.*, 2004). Therefore it is hypothesized that the basic domain of TRF2 plays a role in binding and stabilizing the Holiday junction structure formed within the t-loop, thus preventing resolution of the junction and destabilization of the t-loop (Wang *et al.*, 2004).

TRF2 has been shown to act in maintaining genomic stability and preventing a DNA damage response at telomeres. The use of the dominant negative TRF2 Δ B Δ M protein (a mutant lacking the N- and C-terminal basic and DNA binding domains) allowed for identification of the role for TRF2 in maintaining genomic stability (Karlseder *et al.*, 1999; vanSteensel *et al.*, 1998). Induction of TRF2 Δ B Δ M revealed an increase in p53-dependent senescence and apoptosis, anaphase bridges, and lagging chromosomes (Karlseder *et al.*, 1999;

vanSteensel *et al.*, 1998). Additionally, cells deficient for ATM failed to undergo apoptosis upon expression of TRF2 Δ B Δ M implying that induction of apoptosis through telomere dysfunction requires functional ATM as an upstream activator of p53 (Karlseder *et al.*, 1999) (Figure 1.3). Genomic instability was also assessed through the fluorescence *in situ* hybridization of metaphase chromosomes (vanSteensel *et al.*, 1998). Expression of exogenous TRF2 Δ B Δ M was shown to induce chromosome fusions that occur with intact telomeres (vanSteensel *et al.*, 1998). These trains of chromosomes were dependent on functional ATM as MEFs deficient for ATM and TRF2 abrogate the ability of cells to form telomere dysfunction induced foci (TIFs) and fused chromosomes (Denchi and de Lange, 20007). Additionally, these fusions were shown to occur through the nonhomologous end joining (NHEJ) repair pathway as depletion of ligase IV and TRF2 decreased the percentage of fused chromosomes (Celli and de Lange, 2005; Denchi and de Lange, 20007). Thus, depletion of TRF2 has been shown to result in an ATM-mediated DNA damage response.

1.2.3 Rap1 (Repressor-activator Protein 1):

Rap1 was discovered through a yeast-two-hybrid analysis using TRF2 as the bait (Li *et al.*, 2000). Deletion mapping revealed that amino acids spanning the TRFH domain and linker region in TRF2 and the C-terminus of Rap1 were responsible for their interaction (Li *et al.*, 2000; O'Connor *et al.*, 2003). Immunoprecipitation followed by mass spectrometry identified Rap1 and TRF2 to

associate in a 1:1 complex (Zhu *et al.*, 2000). The presence of Rap1 at telomeres is dependent on TRF2 as depletion of TRF2 resulted in loss of TRF2 and Rap1 from telomeric DNA (Celli *et al.*, 2006). Additionally, immunofluorescence analysis indicated that Rap1 associates with telomeres in interphase and metaphase cells, and gel-shift analysis indicated that Rap1 associates with telomeric DNA only in the presence of TRF2 (Li *et al.*, 2000; Li *et al.*, 2003). Rap1 has been shown to play a role in telomere length dynamics as induction of Rap1 in a telomerase-positive cell line caused telomere elongation at a rate of 30 base pairs/population doubling (Li *et al.*, 2000; Li *et al.*, 2003).

The work by McClintock suggests that an essential function of telomeres is to repress chromosomal fusions from DNA breaks or other chromosome ends (McClintock, 1941). Therefore telomeres must inhibit DNA damage signaling (Denchi and de Lange, 2007). Bae and Baumann showed that both Rap1 and TRF2 are required to prevent chromosome ends from undergoing NHEJ (Bae and Baumann, 2007). However, since Rap1 fails to localize to telomeres in the absence of TRF2, the ability of Rap1 alone to repress NHEJ could not be addressed (Greenwood and Cooper, 2009). In attempts to determine if Rap1 was responsible for ablating NHEJ at telomeres, Sarthy *et al.* targeted Rap1 to telomeres in the absence of TRF2 (Sarthy *et al.*, 2009). Fluorescence *in situ* hybridization of metaphase chromosomes revealed that in the presence of TRF2 Δ BAM, chromosomal fusions occurred; however, when Rap1 was tethered to telomeres in the TRF2 Δ BAM background, a partial rescue of this fusion

phenotype was observed (Smogorzewska *et al.*, 2002; Sarthy *et al.*, 2009). These data suggest that one role of Rap1 at telomeres may be to inhibit NHEJ-mediated telomere fusions (Sarthy *et al.*, 2009).

Recently, the laboratory of de Lange challenged this idea. They showed that removal of Rap1 from Rap1^{Floxed/Floxed} MEFs does not result in NHEJ as analyzed by fluorescence *in situ* hybridization of metaphase chromosomes (Sfeir *et al.*, 2010). They propose that the sole purpose of Rap1 at telomeres is to inhibit homologous recombination (Sfeir *et al.*, 2010). They showed that removal of TRF2 in a Ku depleted background caused an increase in telomeric sister chromatid exchanges and that this phenotype cannot be rescued by a TRF2 mutant unable to associate with Rap1 (Celli *et al.*, 2006; Sfeir *et al.*, 2010). Furthermore, MEFs depleted for Rap1 in a Ku deficient background also showed an increase in sister telomeric chromatid exchange (Sfeir *et al.*, 2010).

1.2.4 TIN2 (TRF1 Interacting Nuclear Protein 2):

TIN2 was identified through a yeast-two-hybrid screen as a TRF1 interacting factor (Kim *et al.*, 1999). Deletion mapping of TRF1 indicated that TIN2 binds to TRF1 through its TRFH homodimerization domain (Kim *et al.*, 1999; Chen *et al.*, 2008). Immunofluorescence of interphase cells and immunostaining of metaphase chromosomes showed that TIN2 is present at human telomeres (Kim *et al.*, 1999). Overexpression of TIN2 in HT1080 cells revealed a slight telomere shortening phenotype and knockdown of TIN2 in

HTC75 cells showed telomere elongation suggesting that TIN2 acts as a negative regulator of telomerase-mediated telomere elongation (Kim *et al.*, 1999; Ye and de Lange 2004). Genetic studies in mice indicate that TIN2 is an essential gene (Chiang *et al.*, 2004). Mice depleted of TIN2 die before E7.5 in a telomerase independent manner as telomerase-deficient mice do not rescue embryonic lethality (Chiang *et al.*, 2004).

Gel-shift assays revealed that TIN2 alone does not bind to telomeric DNA, but rather enhances the ability of TRF1 to base pair with telomeric DNA (Kim *et al.*, 1999; Kim *et al.*, 2003). Knockdown of TIN2 also led to a reduction in the punctate staining of TRF1 as depicted by immunofluorescence and a reduction in TRF1 protein levels (Ye and de Lange 2004). Interestingly, these phenotypes resemble that of tankyrase 1 overexpression: telomere elongation and reduced TRF1 protein levels (Ye and de Lange 2004). Thus it was thought that the effect of TRF1 upon TIN2 depletion is potentially mediated by tankyrase 1 activity (Ye and de Lange 2004). To test this hypothesis, tankyrase 1 was inhibited in the presence of TIN2 knockdown (Ye and de Lange 2004). Inhibition of tankyrase 1 reverted the depletion of TRF1 protein levels in the presence of TIN2 knockdown (Ye and de Lange 2004). Using an *in vitro* ADP-ribosylation assay, it was shown that the presence of TIN2 inhibits the ability of tankyrase to poly(ADP-ribosyl)ate TRF1 causing its release from telomeric DNA (Ye and de Lange 2004). Therefore, it has been suggested that TIN2 acts as a negative regulator of telomere-length regulation by allowing for the accumulation of TRF1 at telomeric

DNA and by protecting TRF1 from being poly(ADP-ribosyl)ated by tankyrase 1 (Ye and de Lange 2004).

Immunoprecipitation of exogenously expressed TIN2 resulted in the association of TRF1 and TRF2, indicating that potentially TRF2 is a TIN2 interacting factor (Kim *et al.*, 2004). Immunofluorescence showed that depletion of TIN2 not only led to a decreased TRF1 signal at telomeres but also resulted in a reduced telomere association of TRF2 (Ye *et al.*, 2004). These data suggest that TRF1 and TRF2 are linked through a molecular bridge containing TIN2 (Kim *et al.*, 2004; Ye *et al.*, 2004). Additional support for this model came in the form of immunoprecipitation studies which showed that the absence of TIN2 results in reduced association of TRF1 and TRF2 with telomeric DNA *in vivo* (Kim *et al.*, 2004). Disrupting the ability of TIN2 to bind to either TRF1 or TRF2 results in the detection of a DNA damage response at telomeres as seen by the formation of TIFs (Kim *et al.*, 2004). These results indicate that TIN2 is important for telomere capping through its association with TRF1 and TRF2 (Kim *et al.*, 2004).

TIN2 also recruits TPP1 to the TRF1-TRF2 complex. Mass spectrometry analysis showed that the TRF1/TIN2 complex is able to pull down TPP1 (Chen *et al.*, 2008). The TIN2-TPP1 interaction is involved in regulating formation of shelterin and mediating telomere length (O'Connor *et al.*, 2006).

1.2.5 TPP1 (TINT1/PTOP/PIP1):

Smith and colleagues used TIN2 as bait in a yeast-two-hybrid screen and identified TIN2 interacting protein 1 (TINT1); Songyang's laboratory identified POT1- and TIN2- organizing protein (PTOP) through immunoprecipitation of TIN2 followed by mass spectrometry; and lastly, de Lange's group identified POT1-interacting protein 1 (PIP1) through immunoprecipitation of the TRF1/TIN2 complex (Houghtaling *et al.*, 2004; Liu *et al.*, 2004; Ye *et al.*, 2004). Collectively they named the novel protein TPP1. TPP1 associates with POT1 and TIN2 with its N- and C-terminus respectively and immunofluorescence data suggest that TPP1 is a component of mammalian telomeres (Houghtaling *et al.*, 2004; Liu *et al.*, 2004; Ye *et al.*, 2004). TPP1 is an essential protein as mice deficient for TPP1 die before E14.5 (Kibe *et al.*, 2010). Depletion of TPP1 from MEFs resulted in telomere dysfunction phenotypes identical to that of depletion of POT1 (Kibe *et al.*, 2010). Chromatin immunoprecipitation (ChIP) analysis showed that depletion of TPP1 results in less POT1 association with telomeric DNA, suggesting that TPP1 acts to recruit POT1 to telomeres (Kibe *et al.*, 2010). Fluorescence *in situ* hybridization of metaphase chromosomes and immunofluorescence reveal that TPP1 is essential for maintaining genomic stability as depletion of TPP1 results in telomere fusions and an increase in TIF-formation that occurs in an ATR-dependent manner (Kibe *et al.*, 2010).

As per all shelterin proteins, TPP1 acts as a negative regulator of telomerase-mediated telomere elongation. Overexpression of TPP1 in HTC75 cells has been shown to result in telomere shortening whereas depletion of TPP1 in HTC75 cells resulted in telomere elongation (Houghtaling *et al.*, 2004; Ye *et al.*, 2004). TPP1 may in part act as a negative regulator of telomere length through its role in POT1 recruitment to telomeric DNA.

TPP1 has also been implicated in regulating telomerase activity at telomeres (Wang *et al.*, 2007; Xin *et al.*, 2007). Immunoprecipitation showed that TPP1 associates with hTERT *in vitro* (Xin *et al.*, 2007). TPP1 contains an N-terminal oligonucleotide/oligosaccharide binding (OB) fold (Wang *et al.*, 2007; Xin *et al.*, 2007). Furthermore, a telomere repeat amplification protocol assay identified that TPP1 immunoprecipitates could give rise to telomerase activity and that TPP1 mutants lacking the OB fold led to a reduction in telomerase activity (Xin *et al.*, 2007). These data support the idea that TPP1 acts to recruit telomerase to telomeres allowing for telomerase-mediated telomere elongation (Xin *et al.*, 2007). The POT1-TPP1 complex has also been shown to increase the processivity of telomerase by decreasing dissociation of the template from telomerase and increasing translocation of the substrate as shown by the telomere repeat amplification protocol assay (Wang *et al.*, 2007; Latrich and Cech 2010).

Recently, the TIN2-TPP1 interaction has been shown to be important for the recruitment of telomerase to telomeres (Abreu *et al.*, 2010). ChIP and

immunofluorescence analysis showed that depletion of TPP1 resulted in less association of telomerase to telomeres (Abreu *et al.*, 2010; Tejea *et al.*, 2010). It is suggested that this is dependent on the association of TPP1 and TIN2 since depletion of TIN2 also resulted in less telomerase at telomeres (Abreu *et al.*, 2010).

1.2.6 POT1 (Protection of Telomeres):

POT1 was discovered by Peter Baumann through its homology to the *Schizosaccharomyces pombe* protein (Baumann and Cech, 2001). POT1 was identified to be a telomere protein through its ability to form punctate staining in interphase cells and its ability to colocalize with Rap1 (Baumann *et al.*, 2002). Gel-shift assays revealed that POT1 binds to single-stranded TTAGGG telomeric repeats *in vitro* and ChIP assays showed that POT1 binds telomeres *in vivo* (Baumann and Cech, 2001; Loayza and de Lange, 2003). Furthermore, ChIP assays revealed that depletion of TRF1 from telomeric DNA through tankyrase 1 overexpression results in a decreased telomeric association of POT1, suggesting that the TRF1 complex acts to recruit POT1 to telomeres (Loayza and de Lange, 2003). *In vivo* ChIP experiments showed that POT1 mutants that retain the ability to associate with the TRF1 complex but are defective in binding telomeric DNA (POT1 Δ OB mutants) cause telomere elongation in telomerase positive cell lines, implying that TRF1 functions as a measuring device of telomere length and the

information about telomere length is transduced from TRF1 to telomerase through POT1 that binds to the 3' overhang (Loayza and de Lange, 2003).

POT1 is required to maintain genomic stability. Depletion of POT1 through RNAi revealed a slight increase in telomere fusions as seen by fluorescence *in situ* hybridization and immunofluorescence shows a significant increase in TIF formation (Hockemeyer *et al.*, 2005). These TIFs occur primarily in G1-phase indicating a role for POT1 in preventing a DNA damage response during G1 (Hockemeyer *et al.*, 2005). Additionally, TIF formation occurs in an ATR-dependent manner as POT1a/b null ATR-depleted MEFs abrogate TIF foci (Denchi and de Lange, 2007). Because ATR is the DNA damage signaling pathway activated in response to single stranded DNA, it is not surprising that POT1 acts to suppress an ATR response at telomeres (Denchi and de Lange, 2007). In concordance with this notion, POT1a/b null MEFs show an increase in Chk1 and Chk2 signaling (Denchi and de Lange, 2007). Deletion of POT1 causes decreased cell growth and p53-dependent senescence (Hockemeyer *et al.*, 2006; Wu *et al.*, 2006). Western blot shows a typical ATR activation resulting in ATM-Ser1981 phosphorylation and activation of Chk1 and Chk2 (Wu *et al.*, 2006) (Figure 1.3).

Additionally, southern blot analysis revealed that depletion of POT1b in MEFs results in a loss of the 3' overhang (Hockemeyer *et al.*, 2005). Furthermore, POT1 has been shown to regulate the length of the 3' overhang, thus

allowing for t-loop formation by means of strand invasion and the generation of a Holiday junction (Wu *et al.*, 2006). MEFs depleted for POT1a/b in a p53-deficient background showed an increase in telomere sister chromatid exchange (lengthening of one chromosome at the expense of another through homologous recombination between sister chromatids) and an increase in telomere circles (homologous recombination occurring with interstitial sites) (Hockemeyer *et al.*, 2006; Wu *et al.*, 2006; Palm *et al.*, 2009).

1.3 Telomere Repeat Containing RNA – TERRA:

Telomeres have been shown to resemble sites of constitutive heterochromatin as they are enriched for heterochromatin marks such as H3K9me3, H4K20me3, and HP1 (Schoeftner and Blasco, 2010). Subtelomeric DNA has also been shown to undergo DNA methylation (Schoeftner and Blasco, 2010). Because telomeres resemble sites of constitutive heterochromatin and do not appear to contain genes, it was suspected that telomeres would remain transcriptionally silent. In 2007, the laboratory of Linger identified telomeres to be transcriptionally active, giving rise to non-coding telomere repeat containing RNA termed TERRA (Azzalin *et al.*, 2007). Northern blot analysis identified TERRA transcripts ranging from ~100 base pairs to 9 kilobases in length (Azzalin *et al.*, 2007). TERRA length seems to be conserved among different cell lines; however, its abundance varies greatly among tissues suggesting that telomere length is positively correlated with TERRA abundance (Azzalin *et al.*, 2007;

Azzalin and Lingner, 2008; Schoeftner and Blasco, 2008). TERRA transcripts are primarily G-rich; however, C-rich TERRA has been shown to exist at low levels (Azzalin *et al.*, 2007; Azzalin and Lingner, 2008; Schoeftner and Blasco, 2008). Hybridization of a probe derived from the subtelomeric region of human chromosome Xp/Yp to a northern blot revealed a TERRA-like hybridization pattern suggesting that TERRA is transcribed in a centromere to telomere direction (Azzalin *et al.*, 2007; Nergadze *et al.*, 2009). This gave some evidence indicating the transcriptional start site lies within the subtelomeric region. Recently, Azzalin and colleagues identified a CpG-island rich region within the subtelomeric 61-29-37 repeats (Nergadze *et al.*, 2009). Promoter assays reveal that the 29- and 37- base pair repeats are sufficient to drive the transcription of TERRA (Nergadze *et al.*, 2009). A defined start site of TERRA transcription within the subtelomeric region suggests that the heterogeneity of TERRA stems from its 3' end indicating that the transcripts are differentially processed or that transcription can terminate at multiple sites along the telomeric repeats (Luke and Linger, 2009).

TERRA colocalizes with Rap1 and TRF1 indicating that TERRA remains associated with telomeres and RNA-fluorescence *in situ* hybridization revealed that only a subset of telomeres associate with TERRA (Azzalin *et al.*, 2007; Schoeftner and Blasco, 2008). It has been suggested that TERRA can bind to telomeres either through formation of a RNA-DNA hybrid or through RNA-protein interactions (Luke and Linger, 2009). Yeast experiments indicate that

TERRA binds to telomere DNA as introduction of RNaseH (which degrades RNA-DNA hybrids) in a *rat1-1* mutant background (which would normally allow for an accumulation of TERRA) allows for the degradation of TERRA transcripts as depicted through northern blot analysis (Luke *et al.*, 2008). *In vitro* evidence suggests that TERRA is able to bind to G-quadruplexes suggesting a RNA-DNA interaction (Xu *et al.*, 2008). RNA-immunoprecipitation and RNA-ChIP revealed that TERRA interacts with both TRF1 and TRF2; however, TERRA was unable to associate with Rap1, TPP1, or POT1 (Deng *et al.*, 2009). RNA-fluorescence *in situ* hybridization revealed that TERRA associates with telomeres through its interaction with the basic domain of TRF2 as depletion of the basic domain in TRF2 causes diffused TERRA staining and less TERRA at telomeres (Deng *et al.*, 2009). The removal of TERRA from yeast telomeres has been shown to require the 5' to 3' Rat1p exonuclease (Luke *et al.*, 2008). In addition, depletion of SMG1, EST1A, and UPF1, components of the nonsense mediated decay pathway, in mammalian cells results in increased TERRA foci at telomeres (Azzalin *et al.*, 2007).

ChIP analysis revealed the association of RNA polymerase II at telomeres and RNA dot blots revealed that treatment with alpha-amanitin (an RNA polymerase II inhibitor) significantly reduced the levels of TERRA (Schoeftner and Blasco, 2008). These data suggest that TERRA is an RNA polymerase II derived transcript (Luke *et al.*, 2008; Schoeftner and Blasco, 2008). Immunoprecipitation analysis revealed an interaction between RNA polymerase II

and TRF1 and depletion of TRF1 significantly reduces the levels of TERRA as seen by Northern blot (Schoeftner and Blasco, 2008). CHIP analysis revealed that recruitment of RNA polymerase II to telomeres was unaffected by the depletion of TRF1, indicating that TRF1 promotes RNA polymerase II progression through the telomeric tract but it does not directly recruit RNA polymerase II to telomeres (Schoeftner and Blasco, 2008). TERRA has been shown to be polyadenylated and Pap-1, the canonical polyadenylation polymerase in yeast, has been shown to be responsible for this in *Saccharomyces cerevisiae* (Luke *et al.*, 2008). Northern blot analysis revealed that the poly-A-tail is required for TERRA stability, as temperature-sensitive *pap-1* mutants no longer reveal a TERRA signal and poly-dT columns no longer bind TERRA RNA (Luke *et al.*, 2008). Nuclear RNA extracted through a poly-dT resin followed by northern blot analysis suggest that about 7% of HeLa TERRA molecules are polyadenylated and these TERRA molecules appear to be greater than 2 kilobases in length (Azzalin and Lingner, 2008). To date, TERRA molecules have not been shown to have a 5'methylguanosine cap.

It has been suggested that the heterochromatin state controls TERRA transcription. As previously mentioned, telomeres contain heterochromatin features such as H3K9me3, H4K20me3, and subtelomeric DNA methylation (Schoeftner and Blasco, 2010). Treatment of cells with Trichostatin A, a histone deacetylase inhibitor, resulted in increased TERRA transcription as depicted by northern blotting (Azzalin and Lingner, 2008). RNA dot blot analysis revealed

that mouse cells depleted for Suv39 (H3K9 methyltransferase) and Suv4-20 (H4K20 methyltransferase) show reduced TERRA levels (Schoeftner and Blasco, 2008). These data indicate that the heterochromatin structure of telomeric DNA can influence TERRA transcription. The epigenetic status of the telomeric chromatin has not only been shown to influence TERRA transcription, but TERRA has also been shown to alter the epigenetic status of chromatin. ChIP data showed that depletion of TERRA caused a significant loss in H3K9me2 and H3K9me3 histone marks at telomeres (Deng *et al.*, 2009). RNA-ChIP was used to determine the role of TERRA in heterochromatin formation and this study revealed that TERRA associates with H3K9me3 and HP1 α , suggesting that TERRA is within a heterochromatic region (Deng *et al.*, 2009).

The exact function of TERRA within cells has not yet been clearly elucidated. TERRA has been shown to be involved in prevention of a DNA damage response at telomeres since depletion of TERRA through siRNA resulted in an ~5-fold increase in TIFs as measured through colocalization of 53BP1 foci at telomeres (Deng *et al.*, 2009). Additionally, fluorescence *in situ* hybridization of metaphase chromosomes identified that depletion of TERRA caused an increase in telomere aberrations such as sister telomere loss, telomere doublets, and telomere double minutes (Deng *et al.*, 2009). Moreover, telomerase activity has been shown to be regulated through TERRA (Luke *et al.*, 2008; Schoeftner and Blasco, 2008). It was hypothesized that the G-rich nature of TERRA might associate with the RNA template of telomerase, thus inhibiting its function.

Increasing RNA oligonucleotides has been shown to inhibit telomerase activity *in vitro* suggesting a role for TERRA in telomerase-mediated telomere elongation (Schoeftner and Blasco, 2008). Recently, the laboratory of Linger demonstrated through immunoprecipitation that endogenous telomerase can associate with TERRA *in vivo* (Redon *et al.*, 2010). They showed *in vitro* that TERRA associates with the RNA template of telomerase and competes with telomeric DNA to bind telomerase (Redon *et al.*, 2010).

The presence of the histone lysine methyltransferase Mixed Lineage Leukemia, MLL, at telomeres and its corresponding methylation mark (H3K4me) gave insight to the regulation of TERRA (Caslini *et al.*, 2009). RNA slot blot revealed that depletion of MLL results in less TERRA transcription at telomeres indicating that MLL might act as a transcriptional coactivator of TERRA (Caslini *et al.*, 2009). In addition, CHIP studies showed that depletion of MLL induces a telomere-damage response as indicated by the association of 53BP1 with telomeric DNA (Caslini *et al.*, 2009). Telomere uncapping has been shown to increase transcription of TERRA that is dependent upon the cooperation of p53 and MLL (Caslini *et al.*, 2009).

1.4 Arginine Methylation:

Arginine methylation is a common post-translational modification found on both nuclear and cytoplasmic proteins (Bedford, 2007). Protein arginine methyltransferases (PRMTs) are the enzymes that utilize *S*-adenosyl methionine

(AdoMet) as a methyl donor and catalyze the transfer of a methyl group to one or two of the guanidino nitrogen atoms of arginine residues (McBride *et al.*, 2001; Bedford *et al.*, 2005). PRMTs fall into two categories based on the nature of the methylation introduced (Pal *et al.*, 2007). Type I PRMTs catalyze asymmetric dimethylation whereas type II PRMTs catalyze arginine dimethylation symmetrically (Pal *et al.*, 2007) (Figure 1.4). Arginine methylation primarily occurs on GAR (glycine-, arginine-rich) domains although PRMT4/CARM1 is an exception and is unable to methylate GAR domains (Bedford *et al.*, 2005). Instead CARM1 has been demonstrated to have a high affinity to methylate PGM (proline-, glycine-, methionine-, arginine-rich) motifs (Bedford *et al.*, 2005). To date, eleven PRMTs have been identified in mammalian cells, the majority of which have been shown to catalyze arginine methylation (Pal *et al.*, 2007).

1.5 Coactivator Associated Arginine Methyltransferase 1, CARM1:

CARM1 was identified through its ability to interact with p160 transcriptional coactivators. The p160 coactivators are a group of three related proteins that interact with nuclear hormone receptors (Tsai *et al.*, 1994; Torchia *et al.*, 1998). These coactivators modify chromatin structure and help recruit RNA polymerase II (Torchia *et al.*, 1998; Struhl, 1998). The activating signal from the nuclear hormone is mediated through the p160 protein to the activation domains 1 and 2 (Onate *et al.*, 1998; Webb *et al.*, 1998; Ma *et al.*, 1999). The first activation domain was shown to recruit the histone acetyltransferase

p300/CBP and the second activation domain was found to interact with CARM1 (Yao *et al.*, 1996; Chen *et al.*, 1997; Chen *et al.*, 1999). Yeast-two hybrid analysis identified a 608-amino acid protein, CARM1, which bound to the C-terminus of the GRIP1 binding protein (Chen *et al.*, 1999). The CARM1 sequence contains homology to the PRMT family members and thus was tested both *in vitro* and *in vivo* to methylate histones (Chen *et al.*, 1999; Bauer *et al.*, 2002). CARM1 has a high affinity to asymmetrically dimethylate histone H3 at arginines 2, 17, and 26 (Schurter *et al.*, 2001). Luciferase assays revealed that CARM1 is able to allow for increased activation of genes under the control of the estrogen response element and the androgen response element (Chen *et al.*, 1999).

Genetic studies showed that CARM1 is an essential protein as knockout mice are smaller in size than their wild-type counterparts, are born alive, but exhibit lung defects and therefore die before taking their first breath (Yadav *et al.*, 2003). CARM1 deficient embryos isolated by Caesarian section exhibit defects in lung development as their lungs fail to inflate with air, but respond to stimulus when pinched with forceps (Yadav *et al.*, 2003). Interestingly, CARM1 methyltransferase dead knockin mice phenocopies the CARM1 knockout mice suggesting that the methyltransferase activity of CARM1 is essential (Kim *et al.*, 2010).

CARM1 has been shown to be involved in the genetic reprogramming of early embryos (Torres-Padilla *et al.*, 2007). At the four-cell blastomere stage,

immunofluorescence showed that increased levels of H3R17 methylation contributes to the inner cell mass implying that pluripotent cells have increased CARM1 activity (Torres-Padilla *et al.*, 2007). To test this model, Torres-Padilla and colleagues injected CARM1 mRNA into one cell at the two-cell stage (Torres-Padilla *et al.*, 2007). They noted that cells expressing higher levels of CARM1 almost exclusively contributed to the inner cell mass and had an increase in Nanog and Sox2 protein, two proteins responsible for maintaining a pluripotent state (Torres-Padilla *et al.*, 2007; Wu *et al.*, 2009). Additionally, microarray data suggested that depletion of CARM1 shows an increase in genes responsible for differentiation and a decrease in genes required to maintain pluripotency (Wu *et al.*, 2009). ChIP data suggested CARM1 and its methylation marks associate with the promoters of Sox2 and Oct3 in wild-type ES cells suggesting that CARM1 mediates transcription of these genes and is thus required for maintaining a pluripotent state (Wu *et al.*, 2009).

ATP-dependent chromatin remodeling complexes have been shown to alter the chromatin state by affecting nucleosome position or mobility (Travers 1999). Immunoprecipitation of Flag-tagged CARM1 revealed it associates with a multisubunit complex termed NUMAC, nucleosomal methylation activator complex (Xu *et al.*, 2004). NUMAC was shown to contain members of the SWI/SNF chromatin-remodeling complex, including the ATPase BRG1, and has been shown to preferentially methylate nucleosomes as opposed to free histones (Xu *et al.*, 2004). ChIP analysis identified CARM1 and BRG1 to be recruited to

estrogen regulated target genes and reporter assays illustrated that BRG1 and CARM1 cooperate to activate estrogen-dependent gene transcription (Xu *et al.*, 2004).

1.5.1 CARM1 and its Role as a Transcriptional Coactivator:

CARM1 has been shown to bind to p160 family coactivators and its histone methyltransferase activity has been shown to be important for nuclear receptor-driven gene transcription (Chen *et al.*, 1999). Xu *et al.* propose that CARM1 acts as a transcriptional coactivator for nuclear hormone genes while acting as a corepressor in cyclin adenosine monophosphate signaling genes (Xu *et al.*, 2001). They showed *in vitro* and *in vivo* that CARM1 associates directly with the CBP/p300 complex and that CARM1 is able to methylate the KIX domain of CBP/p300 (Xu *et al.*, 2001). *In vivo* transcription assays and northern blot analysis revealed that CARM1 negatively regulates CREB-mediated transcription in a methyltransferase dependent manner (Xu *et al.*, 2001). Thus, they propose that CARM1 methylation of the KIX domain interferes with the ability of CBP/p300 to regulate CREB-response genes (Xu *et al.*, 2001). Thus, when CBP/p300 is methylated by CARM1, this increases the association of CARM1 and CBP/p300 to nuclear hormone activated genes and hyperactivation (Xu *et al.*, 2001) (Figure 1.5). Additionally, methylation of CBP by CARM1 at an arginine residue outside of the KIX domain increases nuclear hormone-mediated gene transcription (Chevallard-Briet *et al.*, 2002). CBP is also methylated at R742 *in*

vitro and *in vivo* in a CARM1 dependent manner (Chevillard-Briet *et al.*, 2002). Methylation of CBP appeared to be important for CARM1-mediated ER gene transcription as a methylation-resistant form abolished luciferase activity when luciferase was under the control of the estrogen response element and cells were treated with estrogen (Chevillard-Briet *et al.*, 2002).

In addition to regulating nuclear hormone regulated gene transcription, CARM1 has been shown to be involved in transcriptional regulation of other genes. Immunoprecipitation experiments conducted by An *et al.* identified CARM1 to associate with the C-terminus of the p53 protein (An *et al.*, 2004). Additionally, they suggest that CARM1 is responsible for transcription of p53-dependent genes (An *et al.*, 2004). ChIP analysis showed that p53-deficient cells lack CARM1 and its methylation mark at the promoter of the p53 response gene, GADD45 (An *et al.*, 2004). When the cells are complemented with p53, CARM1 and H3R17me are enriched at the GADD45 gene (An *et al.*, 2004). In concordance with this notion, U2OS cells subjected to ChIP revealed that CARM1 is recruited to the GADD45 promoter four hours after UV treatment (An *et al.*, 2004). In agreement for a potential role of CARM1 in response to p53 activation, ChIP analysis showed that inhibition of CARM1 resulted in decreased H3R17 methylation at the p21 promoter and northern blot showed that inhibition of CARM1 results in decreased levels of p21 mRNA (Selvi *et al.*, 2010).

CARM1 has also been shown to play a role in regulation of the NF- κ B gene (Covic *et al.*, 2005; Miao *et al.*, 2006). NF- κ B is a transcription factor that regulates genes involved in apoptosis, cell proliferation, and immune and inflammatory responses (Ghosh *et al.*, 1998; Baldwin *et al.*, 1996). RT-PCR shows a subset of NF- κ B target genes that are downregulated in CARM1 null MEFs (Covic *et al.*, 2005). Additionally, CARM1 null MEFs do not exhibit NF- κ B-dependent luciferase activity (Covic *et al.*, 2005). Immunoprecipitation studies identified an interaction between NF- κ B and CARM1, and ChIP data identified recruitment of CARM1 and H3R17 methylation at the promoter of the NF- κ B-response gene, IP-10 (Covic *et al.*, 2005; Miao *et al.*, 2006).

1.5.2 CARM1 and its Role in RNA-Binding Properties:

The first protein substrate of CARM1 to be identified was PABP1, poly(A)-binding protein 1 (Lee *et al.*, 2002). *In vitro* methylation assay allowed for recombinant CARM1 and tritium labeled AdoMet to be incubated with a protein array containing a human brain protein library consisting of 37, 200 clones (Lee *et al.*, 2002). Fluorography identified PABP1 as a CARM1 substrate (Lee *et al.*, 2002). The ability of CARM1 to methylate PABP1 was further verified through *in vivo* methylation assays and deletion mapping revealed that the methylation occurred within residues 384-478 (Lee *et al.*, 2002). *In vivo* methylation assays performed in HeLa cells verified that the region of methylation within PABP1 occurs between amino acids 384-478 as deletion of

these residues abrogated the ability of CARM1 to methylate PABP1 (Lee *et al.*, 2002). To date, the role of CARM1 methylation of PABP1 has not yet been elucidated.

The laboratory of Bedford used a small-pool screening technique to identify methylated proteins (Cheng *et al.*, 2007). A plasmid cDNA library was divided into small pools of ten clones and *in vitro* transcription-translation allowed for the cDNA to be converted into protein (Cheng *et al.*, 2007). Each protein pool was identified to contain PRMT enzymes, thus if *in vitro* transcription-translation was performed in the presence of tritium labeled AdoMet, fluorography could be used to identify methylated proteins (Cheng *et al.*, 2007). This small-pool screening technique revealed methylated substrates that did not contain a GAR-motif and were thus hypothesized to be methylated by CARM1 (Cheng *et al.*, 2007). *In vitro* methylation assays were then used to determine that CA150, SmB, U1C, iPABP, and SAP49 are substrates of CARM1 (Ohkura *et al.*, 2005; Cheng *et al.*, 2007). Interestingly, these proteins all appear to be involved in mRNA regulation. CA150 has been shown to bind to the C-terminus of RNA polymerase II and acts to negatively regulate transcriptional elongation, SmB is part of the core snRNP core protein complex, U1C is responsible for base pairing with the GU dinucleotides at the 5' splice site, iPABP is closely related to PABP1 (a previously identified CARM1 substrate), and SAP49 is involved in U2 snRNP function (Ruby *et al.*, 1988; Yang *et al.*, 1995; Huntriss *et al.*, 1994; Das *et al.*, 1999; Suñé and Garcia-Blanco, 1999; Lee *et al.*,

2002).

The ability of CARM1 to methylate proteins involved in splicing suggests that it may be a regulator of alternative splicing. The use of the CD44 minigene as a model for splicing allows one to analyze the role of CARM1 in alternative splicing (Auboeuf *et al.*, 2002). COS-7 cells transfected with the CD44 minigene primarily give rise to two splice products containing either one or both variable exons (Ohkura *et al.*, 2005). Alternatively, upon transfection of rat CARM1 variant-3, the relative proportions of the splice products were altered suggesting that CARM1 plays a role in alternative splicing (Ohkura *et al.*, 2005). Ohkura *et al.* suggest that the ability of CARM1 to regulate splicing is independent of its methyltransferase activity as CARM1 methyltransferase dead mutants show a similar pattern of splicing as cells transfected with wild type CARM1. Alternatively, Bedford and colleagues propose that CARM1's ability to regulate alternative splicing is dependent on its methyltransferase activity (Cheng *et al.*, 2007). Bedford again used the CD44 minigene as a model to analyze alternative splicing; however, they used CARM1 knockout MEF cells complemented with CARM1 or methyltransferase dead CARM1 (Cheng *et al.*, 2007). Again they noticed that CARM1 caused an increase in exon skipping; however, the methyltransferase dead CARM1 did not show an exon skipping pattern, rather these cells retained the variable exons of the CD44 minigene at ratios comparable to CARM1 knockout MEFs (Cheng *et al.*, 2007). They showed that CARM1 methylation within the N-terminal PGM motif of CA150 is required for exon

skipping as cells transfected with the CD44 minigene, CARM1, and wild type CA150 promote exon skipping whereas cells transfected with a mutated form of CA150 in which the PGM motif has been deleted have a higher exon inclusion ratio (Cheng *et al.*, 2007). Far western analysis suggested that CARM1 mediated CA150 methylation allows for the interaction of the SMN proteins with CA150 (Cheng *et al.*, 2007). The SMN proteins have been shown to be involved in assembling the Sm proteins and the U snRNAs into snRNPs to allow for the proper formation of the spliceosome (Paushkin *et al.*, 2002; Eggert *et al.*, 2006; Pellizzoni, 2007). Thus, the CARM1 dependent interaction of CA150 and SMN allows for the coupling of transcription and splicing and CARM1 mediated methylation has been shown to play a role in regulating alternative splicing (Cheng *et al.*, 2007).

CARM1 has also been shown to play a role in regulating mRNA stability. Hu proteins have been shown to bind AU-rich elements in the 3' untranslated regions of some labile mRNAs altering their stability and translational efficiency (Hinman and Lou, 2008). There are four mammalian Hu proteins: HuR (HuA), HuB, HuC, and HuD (Szabo *et al.*, 1991; Levine *et al.*, 1993; Lie *et al.*, 1995; Ma *et al.*, 1996). HuR is ubiquitously expressed whereas the latter three are neuronal-specific proteins (Keene *et al.*, 1999; Ma *et al.*, 1996; Okano *et al.*, 1997). *In vitro* and *in vivo* methylation assays identified HuR and HuD as CARM1 substrates (Li *et al.*, 2002; Fujiwara *et al.*, 2006). The functional role of methylated HuR has not been elucidated while HuD methylation by CARM1 maintains PC12 cell

proliferation by committing p21 transcripts to mRNA decay (Li *et al.*, 2002; Fujiwara *et al.*, 2006). Depletion of CARM1 in PC12 cells has been shown by western blot analysis to increase p21 protein levels (Fujiwara *et al.*, 2006). Immunoprecipitation followed by RT-PCR showed that CARM1 methylation-resistant HuD (R263K) bound more p21 transcripts than the wild type HuD (Fujiwara *et al.*, 2006).

1.5.3 CARM1 and its Role in Breast and Prostate Cancer:

CARM1 is involved in activating hormone-dependent gene transcription and CARM1 has been shown to be upregulated in breast and prostate cancers (Chen *et al.*, 1999; Hong *et al.*, 2004; and Majumder *et al.*, 2004; El Messaoudi *et al.*, 2006). Thus it is likely that CARM1 plays a role in the development of these cancers. Breast cancer proliferation is controlled by a number of different components including hormones, growth factors, and other signaling components (Doisneau-Sixou *et al.*, 2003). E2, 17 β -estradiol, regulates the activation of the ER α and ER β , estrogen receptors α and β , which act as ligand-regulated transcription factors (Klinge *et al.*, 2001). The pS2 gene is typically overexpressed in breast cancers and is a potential marker for hormone-dependent breast cancers (Stack *et al.*, 1988). Reporter assays in 293T cells identified CARM1 and its methyltransferase activity as having a positive effect on transcription of the pS2 gene in the presence of the estrogen receptor (Bauer *et al.*, 2002). Additionally, MCF-7 cells were shown by northern blot analysis to

induce pS2 mRNA upon treatment with estrogen (Bauer *et al.*, 2002). In agreement for the role of CARM1-mediated methylation in transcription of the pS2 gene, ChIP analysis identified that CARM1 and its methylation mark, H3R17me, are recruited to the pS2 gene only in the presence of estrogen (Bauer *et al.*, 2002; Daujat *et al.*, 2002). The recruitment of CARM1 to the pS2 promoter was shown to be dependent on CBP recruitment and prior H3K18 acetylation (Daujat *et al.*, 2002). Breast cancer cells have been shown to have increased levels of E2F due to E2-activated ER α mediated transcription thus allowing for G1/S-phase cell cycle progression (Musgrove *et al.*, 1993; Altucci *et al.*, 1996; Wang *et al.*, 1999; Eeckhoutte *et al.*, 2006). Additionally, grade-3 breast cancer cells have been shown to have increased levels of CARM1, ACTR (a p160 coactivator), and cyclinE1 mRNA (El Messaoudi *et al.*, 2006).

The cyclinE1 gene has been shown to be required for G1/S-phase cell cycle progression and has been shown to be a target of CARM1-mediated transcription (Nielsen *et al.*, 2001; Bandyopadhyay *et al.*, 2002; Fabbrizio *et al.*, 2002; Morrison *et al.*, 2002; El Messaoudi *et al.*, 2006). ChIP analysis identified the promoter of the cyclinE1 gene to be enriched for CARM1, H3R17me, and H3R26me during G1/S-phase indicating that CARM1 may act to regulate this gene during cell cycle progression (El Messaoudi *et al.*, 2006). Consistent with this idea, CARM1 knockout MEF cells and U2OS cells depleted for CARM1 display reduced cyclinE1 mRNA (El Messaoudi *et al.*, 2006). Luciferase assays confirmed the idea that CARM1-mediated methylation is required for cyclinE1

gene transcription as mouse fibroblasts depleted for CARM1 show less luciferase activity (and thus less cyclinE1 mRNA) than the wild type fibroblast cell lines (El Messaoudi et al., 2006). Additionally, CARM1 methyltransferase dead mutants are unable to rescue the decrease luciferase activity (El Messaoudi et al., 2006). U2OS cells depleted for the p160 ACTR coactivator also show reduced levels of cyclinE1 mRNA (El Messaoudi et al., 2006). CHIP analysis showed reduced association of CARM1 and its methylation mark at the cyclinE1 promoter in U2OS cells depleted for ACTR (El Messaoudi et al., 2006). These results indicate that ACTR is required to recruit CARM1 to the cyclinE1 promoter to initiate cyclinE1 transcription.

CARM1 has been shown to be involved in E2-induced breast cancer cell proliferation (Frietze *et al.*, 2008). MCF-7 cells depleted for CARM1 and treated with E2 were shown to undergo cell cycle arrest and decreased cell viability as measured by cell sorting analysis and cell viability assays (Frietze *et al.*, 2008). It has been suggested that CARM1 is capable of regulating E2-mediated cell cycle progression in part by maintaining proper levels of E2F and E2F-reponse genes (Frietze *et al.*, 2008). Real-time PCR data suggested that depletion of CARM1 in MCF-7 cells treated with E2 results in decreased levels of E2F, cdc25A, cyclinE1, and cyclinE2 mRNA (El Messaoudi et al., 2006; Frietze *et al.*, 2008). Additionally, CHIP data suggested that upon estrogen treatment, the E2F promoter is enriched for CARM1 as well as its methylation mark, H3R17me2 (Frietze *et al.*, 2008). Interestingly, the p160 AIB1 coactivator was required for the

recruitment of CARM1 to the E2F promoter under E2 stimulation as depletion of AIB1 though siRNA in MCF-7 cells significantly reduced CARM1 enrichment at the E2F promoter (Frietze *et al.*, 2008).

Additional evidence for a role in CARM1 in estrogen-positive breast cancer stems from the fact that CARM1 is capable of regulating transcription of the estrogen receptor (Shirley *et al.*, 2009). The laboratory of Fuchs-Young showed that p53 is capable of regulating the ER gene (Shirley *et al.*, 2009). Stimulation of p53 through either ionizing radiation or doxorubicin increased p53 mRNA and protein levels in MCF-7 cells (Shirley *et al.*, 2009). Likewise, depletion of p53 reduces ER mRNA and ER protein levels (Shirley *et al.*, 2009). ER induction by DNA damaging agents is dependent on p53 as depletion of p53 failed to upregulate ER mRNA and protein upon treatment of DNA damage (Shirley *et al.*, 2009). ChIP analysis in MCF-7 cells showed that CARM1 and CBP are recruited to the ER promoter and this recruitment is dependent upon p53 (Shirley *et al.*, 2009). Thus recruitment of CARM1 (and other factors) to the ER promoter in a p53-dependent manner allows for transcription of the estrogen receptor.

Androgen plays an important role in the regulation of some prostate cancers (Jenster, 1999). The hormone signal is mediated through the androgen receptor, AR, which acts as a hormone dependent transcription factor (Evans

1988). The androgen-AR complex will then recruit coactivators/corepressors to elicit changes in cell behavior (Evans 1988).

Studies completed by Hong *et al.* identified that CARM1 levels are upregulated in prostate cancers, as assessed by immunohistochemistry (Hong *et al.*, 2004; and Majumder *et al.*, 2004). They thus hypothesized that CARM1 functions with other transcriptional coactivators in the regulation of androgen response genes. CHIP analysis on the PSA promoter, a prostate cancer specific marker, revealed the recruitment of CARM1 and its methylation mark one hour after androgen stimulation (Kang *et al.*, 2004; Majumder *et al.*, 2006). Additionally, depletion of CARM1 abrogated the increase in androgen-induced PSA mRNA levels as assessed by real-time PCR (Majumder *et al.*, 2006). These data suggest that CARM1 is recruited to androgen responsive enhancers following androgen stimulation and that CARM1 is required for AR-dependent gene transcription in prostate cancer cells (Majumder *et al.*, 2006). In addition, depletion of CARM1 leads to decreased cell proliferation and increased apoptosis in androgen treated cells suggesting that prostate cancer cells require CARM1 for their proliferation and viability (Majumder *et al.*, 2006).

1.6 Rationale and Hypothesis:

PRMT1 was initially identified to associate with human telomeres through proteomics of isolated chromatin segments (PICh) (Déjardin and Kingston, 2009). The PICh technique allows for solubilized chromatin that has undergone

formaldehyde treatment to preserve protein-protein and protein-DNA interactions to be pulled down using a biotin labeled specific probe (Déjardin and Kingston, 2009). The hybridized chromatin is then captured on magnetic beads and the hybrids are eluted (Déjardin and Kingston, 2009). The eluted proteins are then analyzed through mass spectrometry. When Déjardin and Kingston pulled down telomeric sequences, they found PRMT1 to be associated with telomeric DNA (Déjardin and Kingston, 2009). Their findings suggest a role for PRMT1 in telomere maintenance.

Immunoprecipitations revealed an *in vivo* association between TRF2 and PRMT1 (Mitchell *et al.*, 2009). Additionally, an *in vitro* methylation assay revealed that recombinant PRMT1 is able to methylate the basic domain of recombinant TRF2 (Mitchell *et al.*, 2009). Depletion of PRMT1 in normal human cells resulted in growth arrest with no change in telomere length (Mitchell *et al.*, 2009). Fluorescence *in situ* hybridization of metaphase chromosomes using a telomere specific probe revealed that depletion of PRMT1 and overexpression of TRF2 mutants unable to undergo arginine methylation in the basic domain primarily results in the formation of two telomere signals per chromatid end (Mitchell *et al.*, 2009). The formation of telomere doublets is thought to be involved in replication defects, thus it is suspected that methylation of the basic domain of TRF2 may be involved in telomere replication (Mitchell *et al.*, 2009; Sfeir *et al.*, 2009). Interestingly, depletion of PRMT1 in transformed cell lines showed no change in cell proliferation; however, telomere shortening occurred

indicating that PRMT1 is a regulator of telomere length maintenance in cancer cells (Mitchell *et al.*, 2009). Additionally, ChIP analysis showed that depletion of PRMT1 causes an increased association of TRF2 to telomeric DNA, which may allow for telomere shortening (Mitchell *et al.*, 2009).

The role of PRMT1 in telomere length regulation and stability lead to the hypothesis that potentially other PRMT enzymes may be involved in telomere regulation. Mass spectrometry data also suggest that there are a number of arginine residues in TRF1 and TRF2 that are mono- and dimethylated (Zhu, unpublished data). Therefore it was hypothesized that CARM1 may play a role in telomere length maintenance. MLL, a prominent lysine methyltransferase, has been shown to play a role in the regulation of TERRA transcription (Caslini *et al.*, 2009). Since CARM1 is also involved in the transcriptional activation of genes, it was hypothesized that CARM1 may play a role in the regulation of TERRA.

Figure 1.1: The structure of human telomeric DNA. (A) Human chromosomes end in TTAGGG repeats that vary in length and contain a 3' overhang. Proximal to the telomeric repeats lies degenerate TTAGGG repeats and subtelomeric DNA. (B) Depiction of the t-loop. The size of the t-loop varies in length. The 3' overhang invades the duplex telomeric DNA and forms the D-loop within the t-loop (Palm and de Lange, 2008)

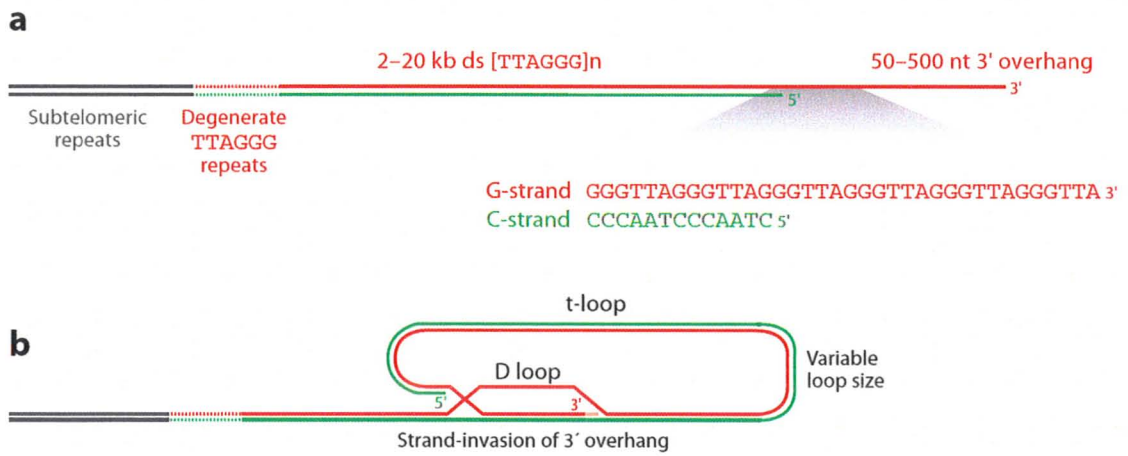


Figure 1.2: Shelterin. Depicted here is a schematic of how shelterin is hypothesized to bind to telomeric DNA. TRF1 and TRF2 bind to the duplex telomere tracts while POT1 binds to the single stranded 3' overhang. TPP1 associates with POT1. TIN2 connects the double stranded DNA binding proteins to the POT1-TPP1 complex. Additionally, Rap1 associates with TRF2 in a 1:1 complex (de Lange, 2005).

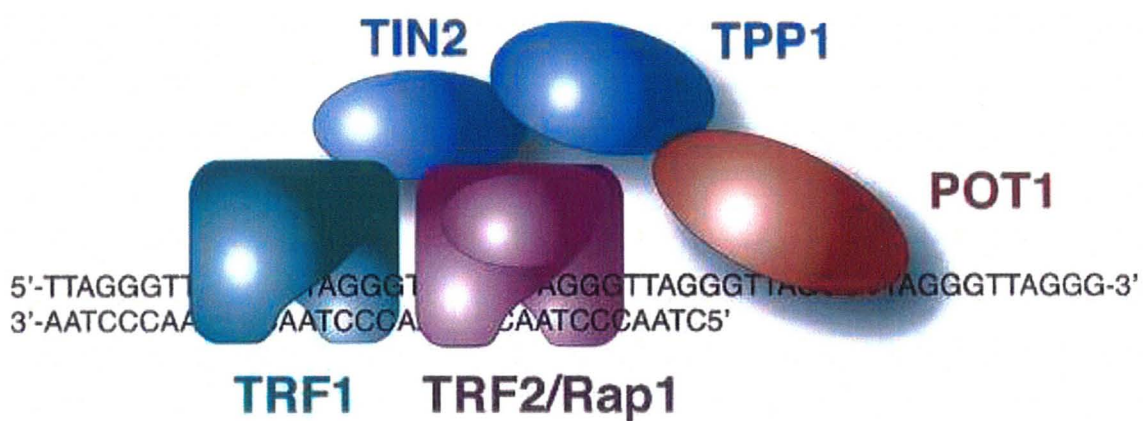


Figure 1.3: Shelterin protects telomeres from being recognized as damage DNA. Both ATM and ATR kinases phosphorylate histone H2AX on Serine 139 to promote the accumulation of MDC1, 53BP1, and the MRN complex at sites of DNA damage. ATM and ATR phosphorylate Chk1 and Chk2, which will inhibit Cdc25 phosphatases and enforce G1/S or G2/M arrest. Chk1 and Chk2 activate, along with ATM and ATR, p53 to inhibit cell cycle progression. TRF2 and POT1 act to inhibit ATM and ATR signaling pathways respectively at telomeres. Depletion of TRF2 results in cell cycle arrest through the activation of the ATM kinase whereas depletion of POT1 activates the ATR signaling pathway (Palm and de Lange, 2008).

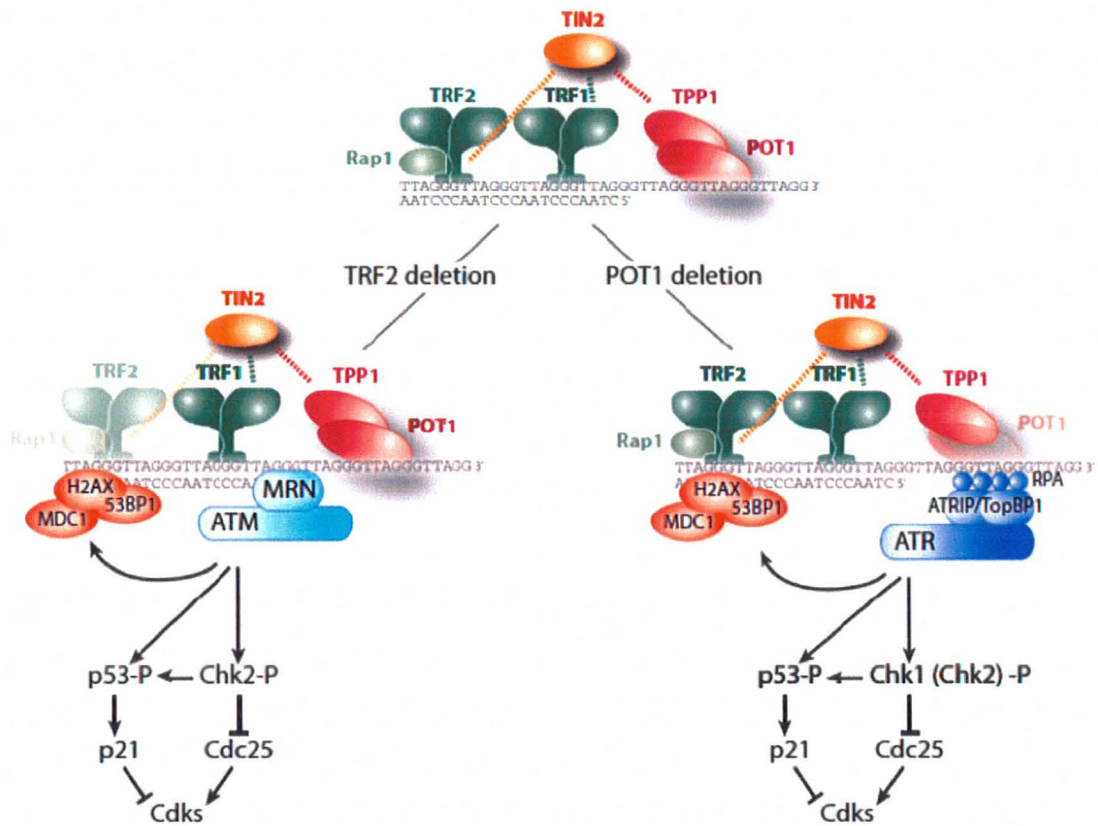


Figure 1.4: Arginine methylation by PRMTs. Both type I and type II PRMTs are capable of catalyzing monomethylation of arginine residues; however, type I is responsible for asymmetric dimethylation whereas type II is responsible for symmetric dimethylation (Adapted from Zhang *et al.*, 2001).

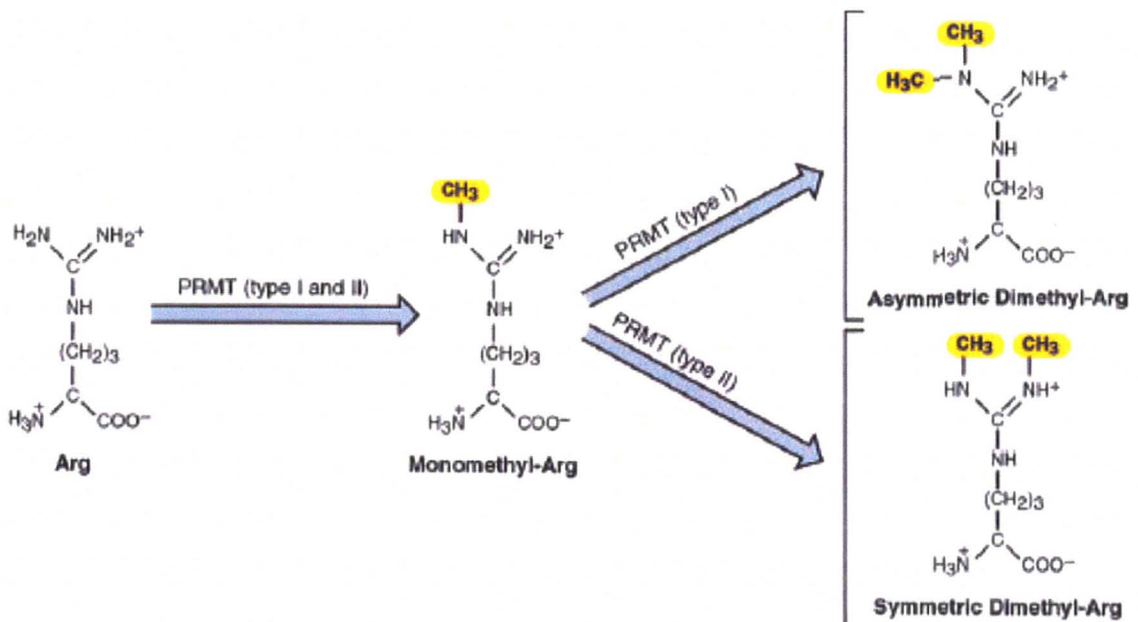
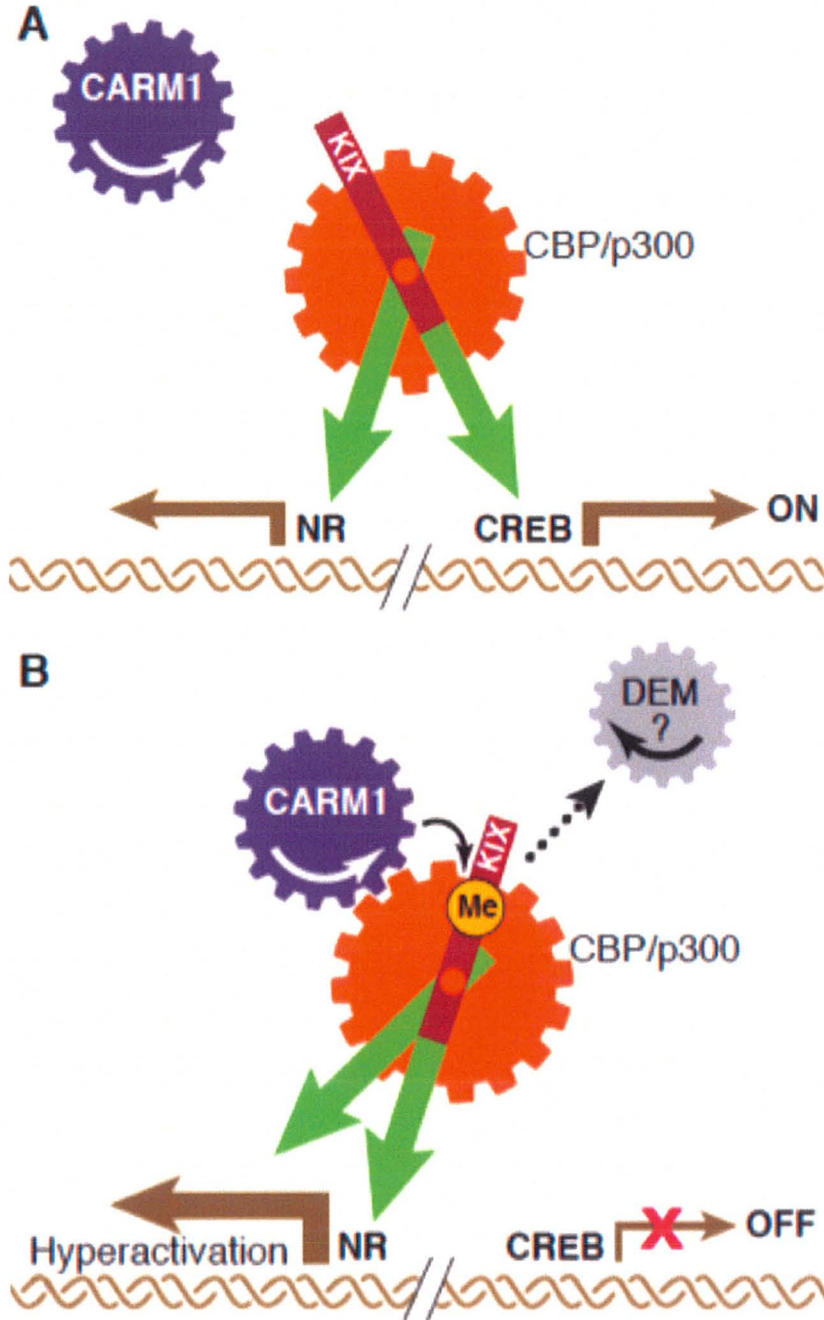


Figure 1.5: Methylation of CBP/p300 by CARM1 regulates transcription of target genes. (A) When CBP/p300 is not methylated, it is able to transcribe both nuclear hormone regulated genes (NR) and CREB-dependent genes. (B) When CARM1 methylates the KIX domain of CBP/p300, CBP/p300 is no longer able to act as a coactivator for CREB-dependent genes. In this scenario, CBP/p300 is able to only activate NR genes thus resulting in their hyperactivation (Nishioka and Reinberg 2001).



2.0 Materials and Methods:

2.1 Cloning of Constructs:

2.1.1 Transformation:

pRS-shCARM1 (plasmid #3029) and pRS-shScramble (plasmid #3031) were cloned by Kajaparan Jeyanthan. One microliter of miniprep plasmid DNA was incubated with 100 μ l Top10 competent *E. coli* cells on ice for 30 minutes. The samples were heat shocked at 42°C for 45 seconds and placed back on ice for 2 minutes. Nine hundred microliters of LB media (1% Bacto™ tryptone, 0.5% Bacto™ yeast extract, 17.1 mM NaCl, 2.8 mM NaOH) was added to the tube and the cells were incubated in a 37°C shaker at 200 RPM for 1 hour. The cells were spun down at 13, 000 RPM for 30 seconds, 900 μ l of the LB supernatant was removed, the cells were vortexed, and plated on LB agar plates containing 0.1 mg/ml ampicillin (1% Bacto™ tryptone, 0.5% Bacto™ yeast extract, 17.1 mM NaCl, 2.8 mM NaOH, 1.5% agar). Plates were incubated for 16 hours at 37°C.

2.1.2 QIAGEN® Plasmid Purification Maxiprep Kit:

A single transformed bacterial colony was inoculated in 3 ml of LB media containing 0.1 mg/ml ampicillin and placed in a 37°C shaker at 200 RPM for 8 hours. The culture was then diluted 1:1000 in 200 ml of LB media containing 0.1 mg/ml ampicillin and was left shaking at 225 RPM for 16 hours at 37°C. The

bacterial cells were collected by centrifugation at 4000 RPM for 15 minutes at room temperature. The supernatant was removed and the pellets were resuspended in 10 ml of buffer P1 (50 mM Tris-HCl [pH 8.0], 10 mM EDTA, and 100 µg/ml RNase A). Ten milliliters of buffer P2 (200 mM NaOH, 1% SDS) was added, the tubes were mixed through inversion, and incubated at room temperature for 5 minutes. Ten milliliters of chilled buffer P3 (3.0 M potassium acetate [pH 5.0]) was added to the samples and incubated on ice for 20 minutes. The samples were spun at 12, 500 RPM for 30 minutes at 4°C to remove the cell debris, the supernatant was centrifuged again at 12, 500 RPM for 15 minutes at 4°C, and the final remaining supernatant was loaded into a QIAGEN column equilibrated with 10 ml of buffer QBT (750 mM NaCl, 50 mM MOPS [pH 7.0], 15% isopropanol, 0.15% Triston^RX-100). The columns were washed twice with 30 ml of buffer QC (1.0 M NaCl, 50 mM MOPS [pH 7.0], 15% isopropanol). The plasmid DNA was then eluted with 15 ml of buffer QF (1.25 M NaCl, 50 mM Tris-HCl [pH8.5], 15% isopropanol). Ten and a half milliliters of isopropanol was added to the plasmid DNA and centrifuged at 12, 500 RMP for 30 minutes at 4°C. The DNA pellet was washed with 7 ml of 70% ethanol and centrifuged for 12, 500 RMP for 10 minutes at 4°C. The DNA was dried and resuspended in 1 ml of TE buffer (10 mM Tris-HCl [pH 8.0], 1 mM EDTA [pH 8.0]). The purity and concentration of the DNA was measured using the A_{260}/A_{280} ratio.

2.2 Tissue Culture:

2.2.1 Growth of Cell Lines:

hTERT-BJ, HeLaII, MCF-7, and Phoenix cells were grown in DMEM media containing 10% FBS, 1X L-glutamine, penicillin (100 U/ml), streptomycin (0.1 mg/ml), and 1% non-essential amino acids. Stable cell lines infected with pRS, pRS-shScramble, or pRS-shCARM1 were grown in selection media containing 2 µg/ml puromycin. All cell lines were grown in 37°C incubators containing 5% CO₂ and 100% humidity.

2.2.2 Retroviral Infection:

Three and a half million Phoenix amphotropic retroviral cells were seeded 12-24 hours preceding transfection experiments on 10cm plates. Prior to transfection, 20 µg of plasmid DNA was ethanol precipitated per construct. Plasmid DNA was mixed with 438 µl of ddH₂O and 62 µl of 2M CaCl₂. While bubbling, 500 µl of 2X HBS [pH 7.05] (50 mM HEPES, 10 mM KCl, 12 mM dextrose, 280 mM NaCl, 1.5 mM Na₂PO₄) was added drop wise to the DNA. The mixture was bubbled for 30 seconds post the addition of the last drop of 2X HBS [pH 7.05] and a total of 1 ml of mix was added drop wise to a 70% confluent plate of Phoenix cells. Twelve hours post-transfection, the media was changed with 9 ml of fresh media and 12-hours later to 4 ml of fresh media. The first infection occurred 36-hours post transfection. The virus containing media was collected,

supplemented with 4 ml FBS and 100 µg/ml of polybrene, and filtered through a 0.45 µm filter. The filtered media was then plated onto recipient cells. Over the next 48-hour period, five more infections were completed. After the last infection, the media was changed with 9 ml of fresh media and 12-hours later the cells were placed in selection media. Seven hundred and fifty thousand MCF-7 and hTERT-BJ cells and 500, 000 HeLaII cells were seeded on 10 cm plates 24-hours prior to the first transfection.

2.3 Protein Study:

2.3.1 Protein Extract:

Confluent plates of cells grown on 10 cm plates were scraped and the cells were collected. The cells were spun in a 15 ml Falcon tube at 1000 RPM for 5 minutes at 4°C. The cells were then transferred to a microcentrifuge tube, washed in 1 ml of 1X PBS [pH 7.4], and collected by centrifugation at 3000 RPM for 2 minutes at 4°C. Cell pellets were resuspended in buffer C (20 mM Hepes-KOH [pH7.9], 0.42 M KCl, 25% glycerol, 0.1 mM EDTA, 5 mM MgCl₂, 0.2% NP40, 1 mM DTT, 0.5 mM PMSF, 1 µg/ml leupeptin, 1 µg/ml aprotinin, 1 µg/ml pepstatin, 10 mM NaF, 1 mM NaVO₄, 20 mM Na-β-glycerol phosphate) in a volume that was equal to five times the pellet size and incubated on ice for 30 minutes. The cells were then centrifuged at 13, 000 RPM for 10 minutes at 4°C and the supernatant was collected. 2X Laemmli buffer (100 mM Tris-HCl [pH

6.8], 20% glycerol, 3% SDS, 0.01% bromophenol blue, 0.02% β -mercaptoethanol) was added to each sample to allow for a final protein concentration of 1-2 $\mu\text{g}/\mu\text{l}$. Samples were stored at -20°C .

2.3.2 Bradford Assay:

The concentration of the protein extract was determined through Bradford assay. One microliter of protein extract was added to 199 μl of water followed by 800 μl of Bradford (BioRad) reagent for a total of 1 ml. The mixture was incubated at room temperature for 15 minutes followed by an absorbance measurement at 595 nm. Water was used as a standard. The concentration of the protein extract was determined based on the standard curve of the Bradford reagent.

2.3.3 Western Blotting:

Protein extract was heated for 5 minutes at 90°C and loaded onto an 8% SDS polyacrylamide gel (SDS-PAGE gel) with a 5% stacking gel and run in running buffer (25 mM Tris, 250 mM glycine, 1% SDS) for 1.5 to 2 hours at 100 V. The proteins were then transferred to a nitrocellulose membrane at 90 V for 1.5 hours in blotting buffer (25 mM Tris, 125 mM glycine, 20% methanol, 0.02% SDS). The membranes were blocked for a minimum of 45 minutes at room temperature in 1X PBS containing 10% skim milk and 0.5% Tween-20. The membranes were rinsed quickly in the incubation buffer (1X PBS containing

0.1% skim milk and 0.1% Tween-20) and incubated in primary antibody for 2 hours at room temperature or overnight at 4°C. The membrane was subsequently washed 3 times for 5 minutes at room temperature in incubation buffer. The membrane was then incubated in the appropriate horse radish peroxidase-conjugated secondary anti-rabbit or anti-mouse secondary antibody at a 1:20,000 dilution for 1 hour at room temperature. The membranes were exposed using enhanced chemiluminescence reagent (GE Healthcare). Membranes were stripped for 1 hour at room temperature in 2 M glycine [pH 2.2] and subsequently blocked.

2.3.4 Antibodies:

CARM1 rabbit-polyclonal antibody was purchased from Cell Signaling (catalogue number 4438S) and used at a dilution of 1:500 in incubation buffer. PRMT1 and PRM5 rabbit-polyclonal antibodies were purchased from Upstate and used at a dilution of 1:4000 and 1:2000 respectively in incubation buffer. PRMT5 rabbit-polyclonal antibody was purchased from Bethyl Laboratories Inc. and was used at a dilution of 1:6000 in incubation buffer. TRF1 (371), TRF2 (647), Rap1 (765), and TIN2 (864) are all rabbit-polyclonal antibodies were generously provided by Titia de Lange, Rockefeller University, and used at a dilution of 1:1000 in incubation buffer. Mouse monoclonal anti- γ -tubulin from Sigma was used as a loading control. Anti-mouse and anti-rabbit IgG peroxidase-linked secondary antibodies were purchased from Amersham Biosciences.

2.4 Proliferation Assays:

2.4.1 Short Term Cell Growth Assay:

Twenty thousand hTERT-BJ cells were seeded per well into a 12-well plate in duplicate on the third day of selection. This was done for each of the 7-time points 3-days post selection. Every other day, the cells were trypsinized and counted using a Beckman Z1 Coulter[®] Particle Counter. Every 4 days the cells were provided with fresh media and when required, the cells were split 1-to-2.

2.4.2 Long Term Cell Growth Assay:

Seven hundred and fifty thousand hTERT-BJ and MCF-7 cells and 1 million HeLaII cells were seeded in 10 cm plates within two weeks post the start of selection. Every 4 days, the cells were trypsinized and counted using a Beckman Z1 Coulter[®] Particle Counter. The appropriate number of cells was then reseeded.

2.4.3 Senescence Associated β -Galactosidase Staining Assay:

The senescence associated β -galactosidase staining assay was completed using the Cell Signaling Technology kit #9860. One hundred thousand hTERT-BJ cells were seeded onto 3.5 cm plates. Twenty-four hours later, the cells were washed twice in 1X PBS [pH 7.4] and fixed in 1 ml of fixing solution (2% formaldehyde, 0.2% glutaraldehyde in 1X PBS) for 15 minutes at room

temperature. The cells were washed again twice in 1X PBS [pH 7.4] and incubated in 1 ml of staining solution (1 mg/ml X-gal diluted in DMF, 40 mM Na₂HPO₄ [pH 7.5], 150 mM NaCl, 2 mM MgCl₂, 5 mM K₃Fe(CN)₆, 5 mM K₄Fe(CN)₆) for 16 hours at 37°C. Cells were then rinsed twice in ddH₂O, dried, and stored at room temperature. Images were obtained from a phase contrast microscope (Nikon Eclipse TE2000-S) and a digital camera (Nikon DXM1200F).

2.5 Immunofluorescence:

Twenty-four hours prior to fixing the cells, cells were seeded on coverslips in 6 cm plates. Cells were washed in 1X PBS and fixed in 3% paraformaldehyde and 2% sucrose in 1X PBS for 10 minutes at room temperature. Cells were washed in 1X PBS for 5 minutes at room temperature. Cells were then permeabilized in 0.5% Triton-X 100 in 1X PBS (0.5% Triton X-100, 20 mM HEPES-KOH [pH 7.9], 50 mM NaCl, 3 mM MgCl₂, 300 mM Sucrose) for 10 minutes at room temperature. Cells were washed 2 times for 5 minutes in 1X PBS and stored in 4°C in 1X PBS with 2% sodium azide.

Coverslips were placed in a container lined with wet paper towels and parafilm. Coverslips were blocked in PBG (0.2% (w/v) cold water fish gelatin, 0.5% (w/v) BSA in 1X PBS) for a minimum of 30 minutes at room temperature. Cells were then incubated in primary antibody diluted in PBG for 2 hours at room temperature. Cells were washed 3 times for 5 minutes in PBG and incubated in secondary antibody diluted 1:300 in PBG for 45 minutes at room temperature.

Subsequently, cells were washed in PBG 2 times for 5 minutes and incubated in DAPI diluted in PBG at 100 mg/ml. Lastly, cells were washed in 1X PBS for twice for 5 minutes. After completion, coverslips were mounted on microscope slides using a 20-30 μ l drop of embedding medium and sealed with nail polish. Slides were stored at -20°C. Immunofluorescence was visualized with a Zeiss Axioplan 2 microscope with Openlab software (Improvision) connected to Hamamatsu C4742-05 camera.

2.5.1 Immunofluorescence Antibodies:

53BP and γ H2AX mouse–monoclonal antibodies were purchased from BD Transduction Laboratories and Upstate respectively and were diluted 1:4000 and 1:6000 in PBG respectively. Rap1 (765) rabbit-polyclonal antibody was used at a dilution of 1:1000 in PBG. Secondary antibodies Fluorescein (FITC)-conjugated affinity pure fragment donkey anti-rabbit IgG and Rhodamine (TRITC)-conjugated affinity pure donkey anti-mouse IgG were purchased from Jackson ImmunoResearch Laboratories Inc. and were diluted 1:300 dilution in PBG.

2.6 Genomic DNA Analysis:

2.6.1 Isolation of Genomic DNA:

Confluent plates of hTERT-BJ, HeLaII, and MCF-7 cells grown on 10 cm plates were scraped and the cells were collected. The cells were spun in a 15 ml Falcon tube at 1000 RPM for 5 minutes at 4°C. The cells were then transferred to

a microcentrifuge tube, washed in 1 ml of 1X PBS [pH 7.4], and collected by microcentrifugation at 3000 RPM for 2 minutes at 4°C. The cell pellets were stored in -80°C.

The cell pellets were quickly thawed at room temperature, resuspended in 1 ml of TNE (10 mM Tris [pH 7.4], 100 mM NaCl, 10 mM EDTA), and placed into a 15 ml phase lock tube (5 Prime) containing 1 ml of freshly prepared TENS buffer containing proteinase K (10 mM Tris [pH 7.4], 100 mM NaCl, 10 mM EDTA, 1% SDS, 100 µg/ml proteinase K). The cells were incubated overnight at 37°C.

Sixteen hours later, 2 ml of phenol:chloroform was added to the tubes and they were mixed until the phases were indistinguishable. The tubes were spun at 3000 RPM for 10 minutes at 4°C. The aqueous phase was then poured into a new phase lock tube, 2 ml of phenol:chloroform was added, the tubes were inverted several times until one phase was apparent, and spun at 3000 RPM for 10 minutes at 4°C. The aqueous phase was then poured off into a 15 ml tube containing 2 ml isopropanol and 22 µl of 2 M NaAc [pH 5.5]. The bundle of DNA was fished out of the tubes and transferred into a microcentrifuge tube containing 300 µl of TNE with 100 µg/ml RNase A. The DNA was incubated for 2.5 hours at 37°C. The DNA was then mixed with 300 µl of TENS buffer containing proteinase K and was incubated for one hour at 37°C. Six hundred microliters of phenol:chloroform was then added to the microcentrifuge tube and the tubes were

mixed until one phase appeared. The DNA was then spun at 13, 000 RPM for 10 minutes at 4°C. The aqueous phase was transferred to a microcentrifuge tube containing 600 µl of isopropanol with 66 µl of NaAc [pH 5.5]. The bundle of DNA was then fished out and placed in 100-200 µl of T₁₀E_{0.1} (10 mM Tris-HCl [pH 8.0], 0.1 mM EDTA). The DNA was left to dissolve for a few hours at 37°C and left in 4°C overnight. Samples were then stored at -20°C.

2.6.2 Digestion of Genomic DNA:

A total of 30 µl of dissolved genomic DNA was digested with 2.5 µl of RasI, HinfI, and 0.2 ng RNase A. The genomic DNA was digested overnight at 37°C. The DNA concentration was measured by Hoechst fluorometry using calf thymus DNA as a standard.

2.6.3 Southern Blotting and Detection of Telomeric Fragments:

Based on the Hoechst measurement, 4 µg of digested genomic DNA was loaded onto a 20x20 cm 0.7% agarose gel in 0.5X TBE (45 mM Tris-borate, 1 mM EDTA). The gel was run for ~1000-1100 V until the 1.3 kb marker almost ran off the gel. For pulse-field gels, 4 µg of digested genomic DNA was added to 2% agarose and loaded into wells to create plugs. The plugs were loaded into a 1% agarose gel in 0.5X TBE and the gel was run at 5.4 V/cm for 20 hrs with an initial and final pulse of 5 seconds in a pulse-field gel electrophoresis apparatus (BioRad Electrophoresis Cell model #1703649).

The gel was dried for 2 hours at 55°C using a gel drier (SGD200 Slab Gel Drier model #QS2576). The gel was denatured for 30 minutes in denaturing solution (1.5 M NaCl, 0.5 M NaOH) and neutralized twice for 15 minutes in neutralization buffer (3 M NaCl, 0.5 M Tris-HCl [pH 7.0]). The gel was quickly rinsed in ddH₂O and placed in 20-25 ml of Church mix (0.5 M NaPi [pH7.2], 1 mM EDTA [pH 8.0], 7% SDS, 1% BSA) for a minimum of 1 hour at 55°C. The gel was hybridized overnight in a γ -³²P end labeled telomere C-rich probe.

The following day, the gel was washed three times for 20 minutes in 4X SSC (0.6 M NaCl, 60 mM sodium citrate) and then twice for 20 minutes in 4X SSC containing 0.1% SDS. The gel was placed in a PhosphorImager screen (GE Healthcare) overnight and scanned the following day using a PhosphorImager (Storm 820, Amersham Pharmacia Biotch). The southern blots were quantitated using ImageQuant software version 5.2.

2.7 RNA Analysis:

2.7.1 Isolation of RNA:

Confluent plates of hTERT-BJ and MCF-7 cells grown on 10 cm plates were scraped with 1 ml Trizol reagents (Invitrogen) and the cells were collected in a microcentrifuge tube. The cells were incubated for 5 minutes at room temperature. Two hundred microliters of chloroform were quickly added to the homogenized samples, the samples were then vortexed, and centrifuged at 13, 000

RPM for 15 minutes at 4°C. The aqueous phase was transferred to a new microcentrifuge tube and 500 µl of isopropanol was added. The samples were incubated for 10 minutes at room temperature and then spun at 13, 000 RPM for 10 minutes at 4°C. The RNA pellets were washed twice with 1 ml of DEPC-treated 75% ethanol and air-dried at room temperature. The RNA was dissolved in 15 µl of DEPC-treated ddH₂O for 10 minutes at 60°C. The RNA purity and concentration was measured based on the A_{260}/A_{280} ratio. Samples were stores at -80°C in 20 µg aliquots.

2.7.2 Northern Blotting and Detection of Telomeric RNA:

Two microliters of 10X MOPS (200 mM MOPS [pH 7.0], 50 mM NaAc, 10 mM EDTA [pH 8.0])., 4 µl of 37% formaldehyde, 10 µl of formamide, and 0.05 µg of ethidium bromide were added to 20 µg of RNA. The RNA was incubated at 55°C for 15 minutes. The samples were run on a 1.2% agarose gel containing 12.5 ml 10X MOPS and 3.75 ml of 37% formaldehyde. The gel was run at 40 V for 8 hours in 1X MOPS (20 mM MOPS [pH 7.0], 5 mM NaAc, 1 mM EDTA [pH 8.0]). The gel was soaked in 0.05 M NaOH for 20 minutes and then in 20X SSC (3 M NaCl, 0.3 M sodium citrate) for 40 minutes. The RNA was transferred overnight onto Hybond^{TE}-M (GE Healthcare) membrane using 20X SSC as the transfer buffer.

The next day, the RNA was crosslinked to the gel using a UV crosslinker

(UV Stralinker 1800). The membrane was quickly rinsed in DEPC-treated ddH₂O and placed in 10-15 ml of Church mix (0.5 M NaPi [pH7.2], 1 mM EDTA [pH 8.0], 7% SDS, 1% BSA) for a minimum of 1 hour at 60°C. The gel was hybridized overnight in a α -³²P labeled telomere C-rich probe.

The next day, the membrane was washed 10 minutes in 1X SSC with 0.1% SDS (150 mM NaCl, 15 mM sodium citrate, 0.1% SDS) then 3 times for 10 minutes in 0.5X SSC with 0.1% SDS (75 mM NaCl, 7.5 mM sodium citrate, 0.1% SDS). The gel was placed in a PhosphorImager screen (Amersham Biosciences) overnight and scanned the following day using a PhosphorImager (Storm 820, Amersham Pharmacia Biotch).

Northern blots were stripped in stripping buffer (10 mM Tris-HCl [pH 7.4], 0.2% SDS) for 1.5 hours at 75°C. Northern blots were quickly rinsed in DEPC-treated ddH₂O and placed in 10-15 ml of Church mix (0.5 M NaPi [pH7.2], 1 mM EDTA [pH 8.0], 7% SDS, 1% BSA) for a minimum of 1 hour at 60°C. The gel was hybridized overnight in a α -³²P labeled GAPDH probe. The next morning the membrane was washed four times for 5 minutes in 2X SSC (0.3 M NaCl, 30 mM sodium citrate). The northern blots were quantitated using ImageQuant software version 5.3.

3.0 Results:

3.1 Depletion of CARM1 does not alter other PRMT protein levels:

The effect of arginine methylation on telomere dynamics has not been well characterized. Recently, it was demonstrated that PRMT1 plays a role in telomere length maintenance and stability in part through the methylation of TRF2 (Mitchell *et al.*, 2009). This led us to study the effect of CARM1 on telomere length and stability.

To knockdown CARM1, plasmid DNA was transfected into Phoenix retroviral packaging cells. Retroviral particles containing a puromycin resistance gene, shScramble, or shCARM1 were infected into HeLaII cells. Cells were then selected in media containing puromycin for 3 days to generate stable cell lines. Retroviral infections of shCARM1 into HeLaII cells created stable cell lines depleted of CARM1 (Figure 3.1). As a control, cells were also infected with virus containing shScramble or vector alone (Figure 3.1). Figure 1 also shows that the shRNA designed to target CARM1 is specific to this PRMT enzyme and not the PRMT family as cells infected with virus containing shCARM1 did not alter the expression levels of PRMT1, PRMT5, or PRMT6 compared to control cells.

3.2 Depletion of CARM1 does not alter other the protein levels of shelterin proteins:

Retroviral infections of shCARM1 into hTERT-BJ cells were used to create stable cell lines depleted of CARM1 (Figure 3.2). Control cells were also infected with virus containing shScramble or vector alone (Figure 3.2). Since CARM1 is a transcriptional coregulator we thought it would be important to determine if CARM1 played a role in transcription of telomere proteins. Figure 2 also shows that depletion of CARM1 in hTERT-BJ cells does affect the protein expression of telomeric proteins TRF1, TRF2, TIN2, or Rap1.

3.3 Depletion of CARM1 initially induced cellular senescence:

3.3.1 Cells depleted of CARM1 initially stained positive for senescence-associated β -galactosidase

hTERT-BJ cells depleted for CARM1 became large, flat, and often showed multiple nuclei, a phenotype reminiscent of cellular senescence. Two weeks post selection cells were stained with β -galactosidase, a marker of cellular senescence. Almost 100% of cells depleted for CARM1 underwent cellular senescence while control cells exhibited approximately 10% senescent cells (Figure 3.3).

In attempts to reproduce this phenotype, three different maxi preps were prepared and sequenced. The plasmid DNA was transfected into viral packaging

cells and hTERT-BJ cells were infected with retrovirus containing vector alone, shScramble, or shCARM1. Cells were then selected in media containing antibiotics for 3 days to generate stable cell lines. This time, the senescent phenotype was not reproducible in spite of CARM1 knockdown.

3.3.2 Depletion of CARM1 does not appear to induce genomic instability:

Immunofluorescence was used to determine if genomic instability is the cause of cellular senescence. Four days after selection, the number of 53BP1 and γ H2AX foci markers of DNA damage, was analyzed in hTERT-BJ cells depleted for CARM1. hTERT-BJ cells expressing shScramble or vector alone were used as a control. hTERT-BJ cells stably expressing shCARM1 did not display an increase in either 53BP1 foci or γ H2AX foci compared to vector control or cells infected with shScramble, arguing that depletion of CARM1 does not appear to result in an increase in genomic instability (Figure 3.4 A and B). In order to determine if CARM1 depletion increases telomere dysfunction, cells were costained for Rap1 and γ H2AX. TIF formation was not altered in cells depleted of CARM1 relative to control (Figure 3.4C). These results indicate that depletion of CARM1 does not appear to induce genomic instability.

3.3.3 Depletion of CARM1 does not appear to alter telomere length:

To determine if cells expressing shCARM1 show acute changes in telomere length, southern blot analysis was performed. Nine days post selection,

cells were harvested for genomic DNA to determine if CARM1 depletion affects telomere length. The genomic DNA was digested leaving telomeric DNA intact, run on an agarose gel, dried, denatured, and probed with a radioactively labeled C-rich telomere probe. In gel hybridization analysis revealed no acute change in telomere length in cells depleted of CARM1 relative to control cells.

hTERT-BJ cells have an average telomere length of ~20kb. It is thought that the large fragments might not have separated well on the agarose gel, thus masking any potential change in telomere length. Pulse-field gel electrophoresis allows for better separation of large DNA fragments compared to conventional agarose gels and was thus used to study changes in telomere length. In gel hybridization analysis of telomere length by pulse-field gel electrophoresis in hTERT-BJ cells indicates no acute change in telomere length in CARM1-depleted cells compared to control cells (Figure 3.5).

3.3.4 Depletion of CARM1 in hTERT-BJ cells does not appear to affect cell growth in the short term:

Since hTERT-BJ cells show a strong senescent phenotype upon depletion of CARM1, it is expected that these cells will have altered growth dynamics compared to control cells. hTERT-BJ cells were retrovirally infected with virus expressing shCARM1, shScramble, or vector control and selected for three days. Upon completion of selection, cells were seeded into 12-well plates and counted every two days to monitor changes in growth rate. Cells depleted for CARM1

proliferate at the same rate as control cells (Figure 3.6). These results suggest that depletion of CARM1 does not appear to alter proliferation over the short term.

3.4 Depletion of CARM1 in HeLaII cells does not appear to alter cellular proliferation or changes in telomere length dynamics:

3.4.1 HeLaII cells infected with a retrovirus expressing shCARM1 show similar levels of CARM1 knockdown at early and late population doublings:

Retroviral infections with a virus containing shCARM1, shScramble, or empty vector were used to create stable HeLaII cell lines. Western blot analysis reveals that CARM1 is knocked down in cells expressing shCARM1 compared to control cells (Figure 3.7). Immunoblotting also reveals that the level of CARM1 knockdown at 0 population doublings is roughly equal to the level of knockdown 60 population doublings later (Figure 3.7).

3.4.2 HeLaII cells depleted of CARM1 do not appear to exhibit a growth defect:

HeLaII cells depleted for CARM1 were cultured long term to determine if CARM1 depletion altered cell proliferation. As shown in figure 3.8, HeLaII cells depleted of CARM1 do not appear to have altered growth dynamics compared to control cells.

3.4.3: Depletion of CARM1 in HeLaII cells initially resulted in telomere elongation:

To assess if CARM1 plays a role in telomere length maintenance, HeLaII cells depleted for CARM1 were cultured long term, 60 population doublings, to monitor changes in telomere length. Because HeLaII cells have short telomeres they are an ideal candidate cell line to monitor telomere length dynamics, as subtle changes in length will be more apparent.

Cells were collected at several different population doublings and the genomic DNA was extracted. The genomic DNA was digested with frequent cutting enzymes leaving the telomeres intact. The digested DNA was run on an agarose gel, the gel was dried down, denatured, and probed with a radioactively end labeled telomere specific probe. Figure 3.9 A and B depict a southern blot suggesting that depletion of CARM1 causes telomere elongation. Southern blot analysis suggests that at 40 population doublings, HeLaII cells depleted of CARM1 show a sudden increase in telomere length at a rate of ~300 base pairs/population doubling compared to control cells. In attempts to reproduce this telomere elongation phenotype, the experiment was repeated. HeLaII cells depleted for CARM1 along with control cell lines were subjected to long-term culturing and southern blot analysis in duplicate. Figure 3.9 C and D depict a southern blot showing changes in telomere length over time in cells infected with virus expressing empty vector, shScramble, and shCARM1. CARM1 depleted

cell lines did not show telomere elongation when compared to control cells. These cells; however, maintained a similar average telomere length over the 60 population doublings when compared to control cells.

3.5 Depletion of CARM1 in MCF-7 cells does not appear to alter cellular proliferation or changes in telomere length dynamics:

3.5.1 The level of CARM1 knockdown in MCF-7 cells is altered from early to late population doublings:

Stable cell lines depleted of CARM1 and vector control were created using retroviral infections. Western blot analysis shows a high efficiency of CARM1 knockdown in MCF-7 cells at the beginning of cell culture experiments (Figure 3.10). As the cells were passaged, knockdown efficiency weakened; however, there still appears to be a substantial knockdown of CARM1 compared to vector control by 40 population doublings.

3.5.2 MCF-7 cells depleted of CARM1 do not appear to exhibit a growth defect:

MCF-7 cells depleted for CARM1 were cultured long term. As shown in figure 3.11, MCF-7 cells depleted of CARM1 do not appear to have altered growth dynamics compared to control cells.

3.5.3 CARM1 depletion in MCF-7 cells does not appear to alter telomere length dynamics:

To determine if CARM1 may play a role in regulating telomere length, telomere experiments were conducted in a different cell line, MCF-7. MCF-7 cells depleted for CARM1 along with control cells were cultured for 40 population doublings, at which point southern blot analysis was conducted. Genomic DNA was extracted from cells collected at different population doublings. The genomic DNA was digested with frequent cutting restriction enzymes leaving the telomeres intact. The digested genomic DNA was run on an agarose gel and the gel was dried down to perform in gel hybridization. The gel was denatured and probed with a telomere specific probe. As depicted in figure 3.12, depletion of CARM1 in MCF-7 cells does not appear to alter telomere length dynamics. CARM1 depleted cells maintained an average telomere length of 3kb over 40 population doublings similar to control cells.

3.6 Depletion of CARM1 in hTERT-BJ cells does not appear to alter cellular proliferation or changes in telomere length dynamics:

3.6.1 hTERT-BJ cells infected with shCARM1 show similar levels of CARM1 knockdown at early and late population doublings:

Retroviral infections with a virus containing shCARM1 or empty vector were used to create stable hTERT-BJ cell lines. Western blot analysis reveals that

CARM1 is knocked down in cells expressing shCARM1 compared to control cells (Figure 3.13). Immunoblotting also reveals that the level of CARM1 knockdown at 0 population doublings is roughly equal to the level of knockdown 30 population doublings later (Figure 3.13).

3.6.2 hTERT-BJ cells depleted of CARM1 do not appear to exhibit a growth defect:

hTERT-BJ cells depleted for CARM1 do not appear to show altered growth dynamics compared to control cells over long-term culture (Figure 3.14).

3.6.3 CARM1 depletion in hTERT-BJ cells does not appear to alter telomere length dynamics:

Thus far, it appears that depletion of CARM1 does not affect telomere length dynamics in cancer cells. To determine if immortalized cell lines exhibit alternations in telomere length maintenance upon depletion of CARM1, hTERT-BJ cells were cultured for long term. Cells were collected at various population doublings and the genomic DNA was extracted. The DNA was digested leaving the telomeres intact and run on a 0.7% agarose gel. The gel was dried, denatured, and probed with a telomere specific probe. Southern blot analysis revealed no change in telomere length over 30 population doublings in hTERT-BJ cells depleted of CARM1 compared to control cells (Figure 3.15). Control and

CARM1 depleted cell lined maintained an average telomere length of 17-18kb over the 30 population doublings.

3.7 Depletion of CARM1 does not appear to alter TERRA levels:

Telomeres are transcribed into UUAGGG repeat-containing telomeric RNA that commence within the subtelomeric region (Azzalin *et al.*, 2007). Recently, it has been shown that the MLL complex, a lysine methyltransferase, methylates H3K4 and that methylation contributes to TERRA transcription in a telomere length-dependent manner (Caslini *et al.*, 2009). We therefore hypothesized that CARM1, an arginine methyltransferase transcriptional coactivator, might contribute to telomere transcription.

To determine if CARM1 plays a role in the regulation of TERRA, northern blot analysis was conducted. RNA was extracted from MCF-7 and hTERT-BJ cell lines depleted of CARM1 along with vector control cells from early population doublings. The RNA was run on an agarose denaturing gel, transferred to a nitrocellulose membrane, cross linked, and probed with a telomere specific probe. Northern blot analysis revealed that CARM1 does not appear to play a role in the regulation of TERRA in immortalized or cancer cells compared to vector control cells (Figure 3.16 and 3.17).

Figure 3.1: HeLaII cells depleted for CARM1 do not show alterations in PRMT1, PRMT5, or PRMT6 protein levels. Plasmids containing a CARM1-specific shRNA, a control shRNA, or vector control were transfected into retroviral packaging cells, the virus was collected, and HeLaII cells were infected. Western blot analysis on protein extracts from HeLaII cells containing shCARM1 results in a significant reduction in CARM1 protein levels compared to control cells. To ensure that the shRNA is specific to CARM1 and not PRMT enzymes in general, western blots were completed to show that depletion of CARM1 does not cause alterations in PRMT1, PRMT5, and PRMT6 protein levels. Western blots were completed after 80 population doublings.

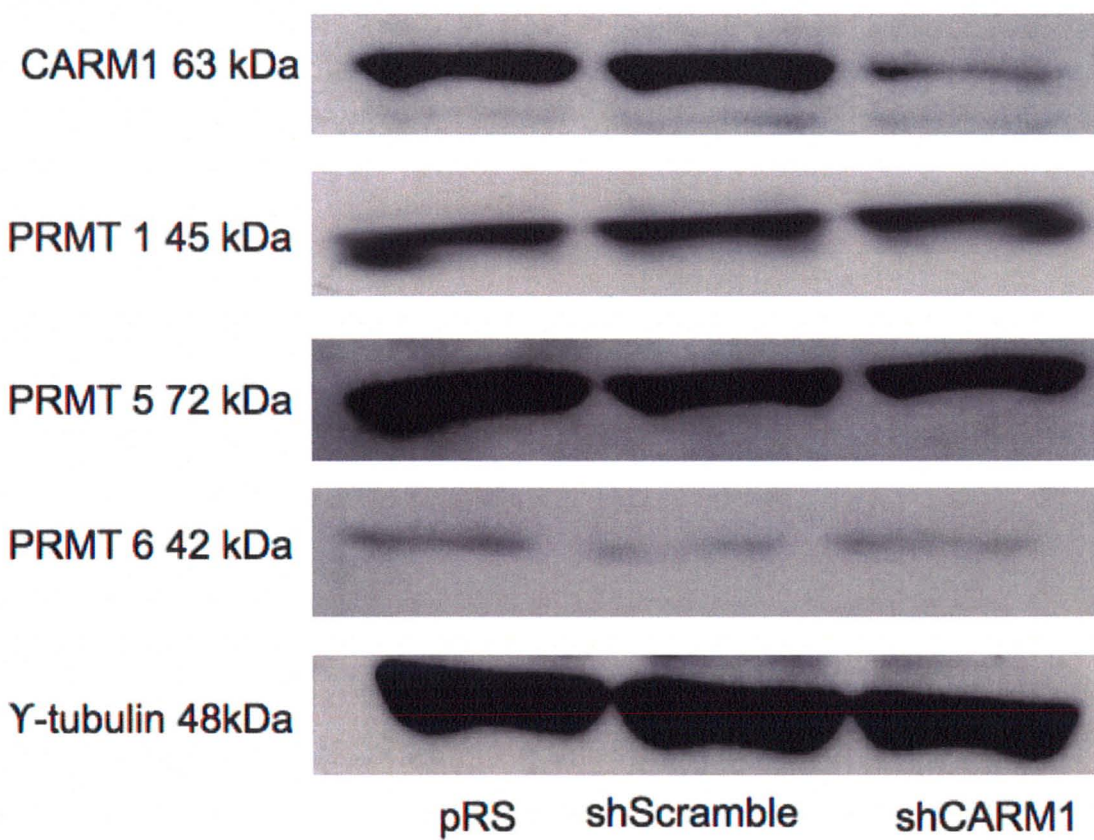


Figure 3.2: hTERT-BJ cells depleted for CARM1 do not show alterations in shelterin protein levels. hTERT-BJ cells underwent a retroviral infection of CARM1-specific shRNAs, control shRNAs, or vector control. Twelve days post selection cells were harvested for protein extracts. Western blot depicts hTERT-BJ cells containing shCARM1 show a significant reduction in CARM1 protein level compared to control cells. Western blot indicates that CARM1 depletion does not alter protein expression of telomeric proteins TRF1, TRF2, Rap1, and TIN2.

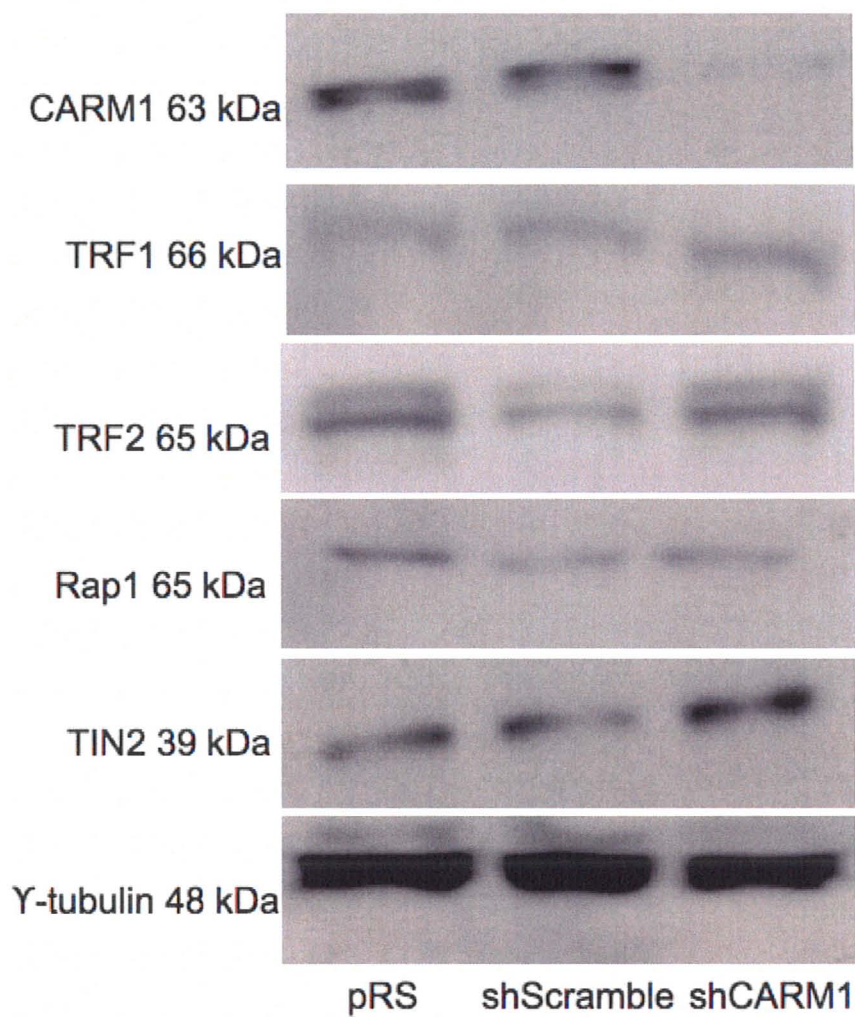


Figure 3.3: Knockdown of CARM1 initially induced cellular senescence in hTERT-BJ cells. hTERT-BJ cells infected with the indicated viruses were stained for 16 hours with senescence-associated β -galactosidase two weeks post selection. One thousand cells were counted per experiment and standard deviations derived from three independent experiments are shown.

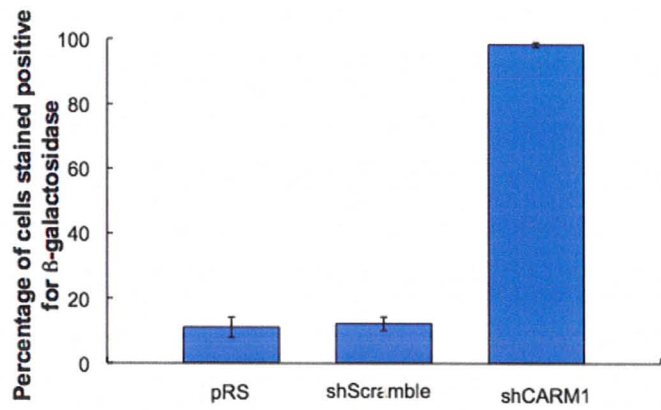
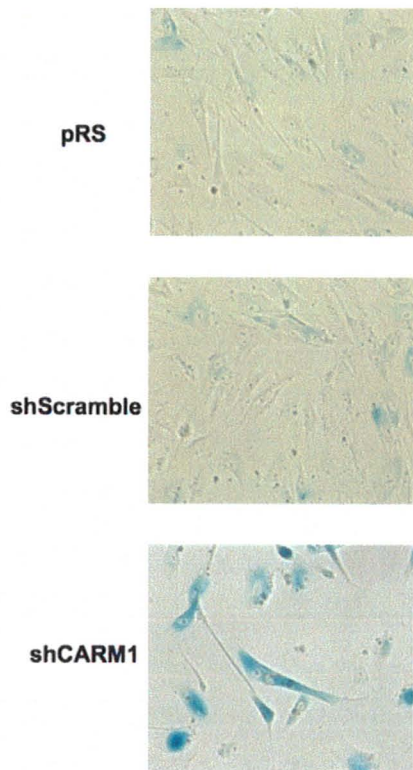
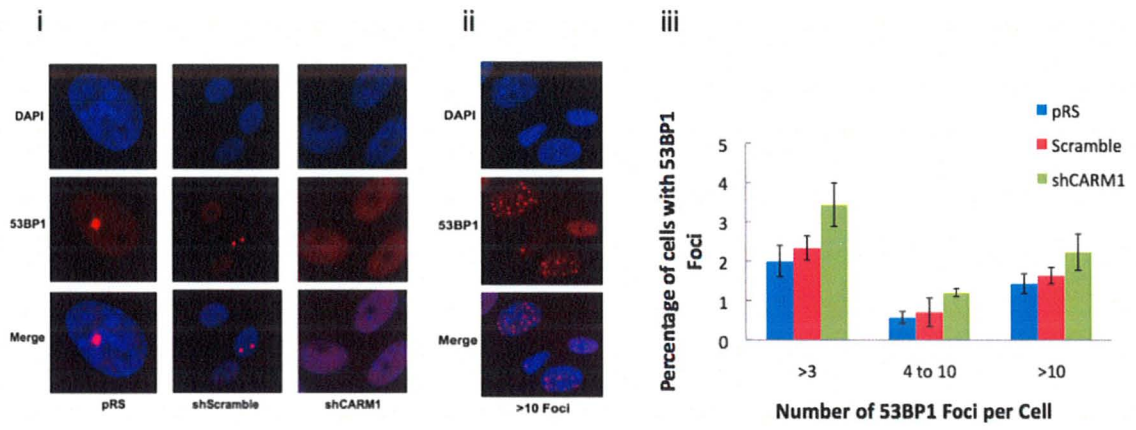
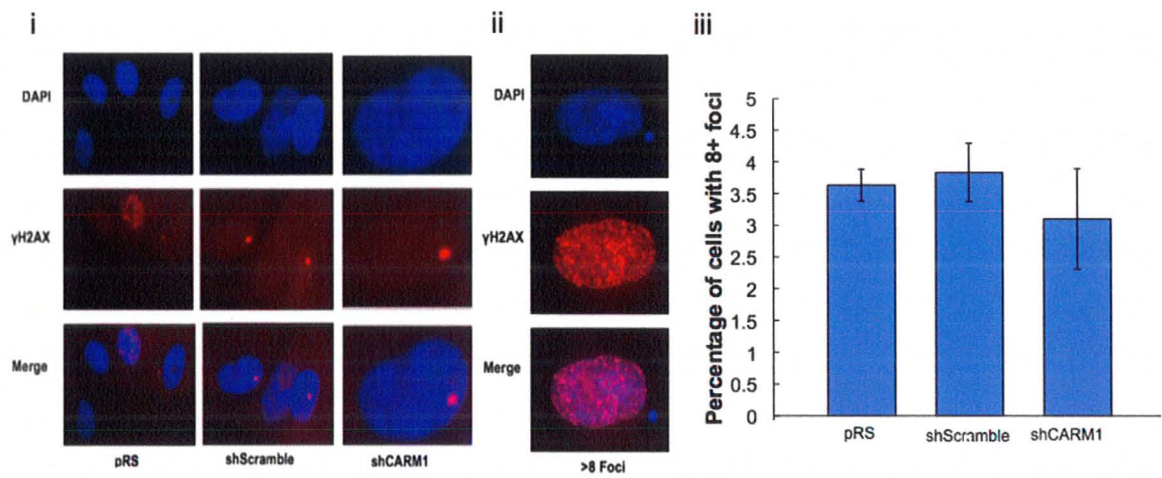


Figure 3.4: Knockdown of CARM1 does not induce genomic instability or telomere instability in hTERT-BJ cells. Immunofluorescence was completed on hTERT-BJ cells infected with the indicated viruses 4 days post the start of selection. CARM1 depleted cell lines did not show an increase in genomic instability as depicted through the formation of 53BP1 foci (A) γ H2AX foci (B) when compared to control cells. To determine if cells depleted of CARM1 preferentially form these DNA damage foci at telomeres, cells were costained with γ H2AX and Rap1 (C). Cells depleted for CARM1 do not show an elevated level of TIF formation compared to control cells. One thousand cells were counted per experiment and standard deviations derived from three independent experiments are shown.

A



B



C

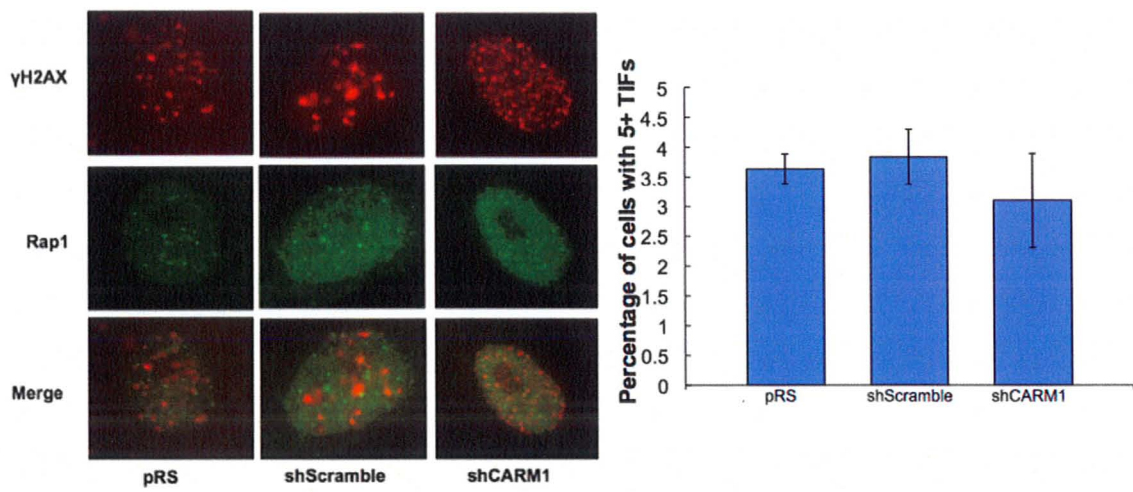


Figure 3.5: Southern blot analysis indicates that knockdown of CARM1 does not alter telomere length in the short term in hTERT-BJ cells. Genomic DNA isolated from hTERT-BJ cells infected with the indicated virus was subjected to southern blot analysis nine days post selection. The genomic DNA was digested, run on a pulse-field gel electrophoresis, dried, denatured, and probed with a telomere specific probe. The southern blot reveals that cells depleted for CARM1 do not show immediate alterations in telomere length compared to control cells. Loading control (ethidium bromide staining) is shown below.

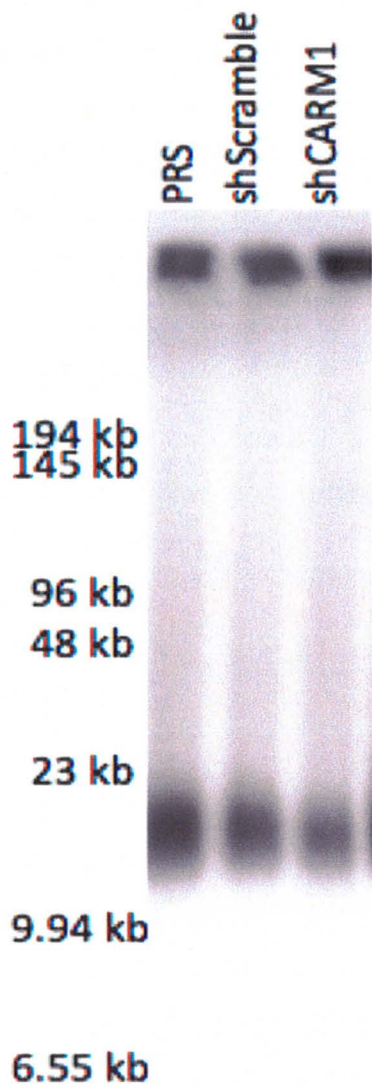


Figure 3.6: hTERT-BJ cells depleted of CARM1 grow at the same rate as control cells over a 15-day period. Three days after the start of selection, 20,000 cells were seeded in 12-well plates in duplicate. Every other day the cells were counted and the average of the duplicate experiments was used to determine the final cell number. Standard deviations derived from three independent experiments are shown.

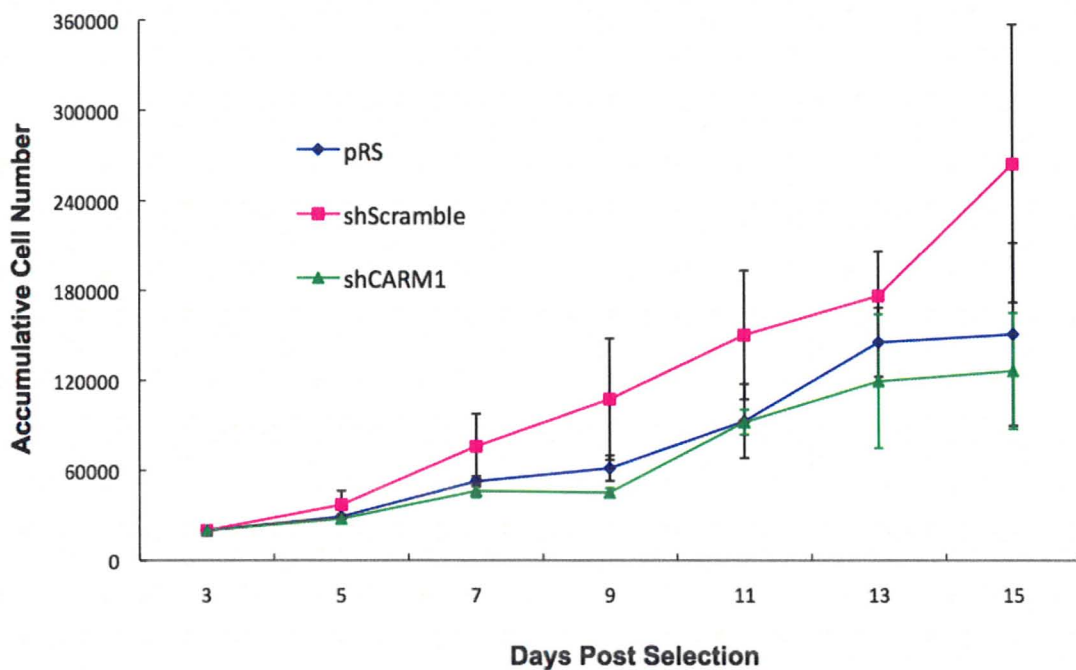


Figure 3.7: HeLaII cells depleted of CARM1 show equal levels of CARM1 knockdown at early and late population doublings. Protein extract was collected at early and late population doublings to compare the level of CARM1 knockdown. As depicted, the level of CARM1 knockdown appears to be stable from population doubling 0 to 60.

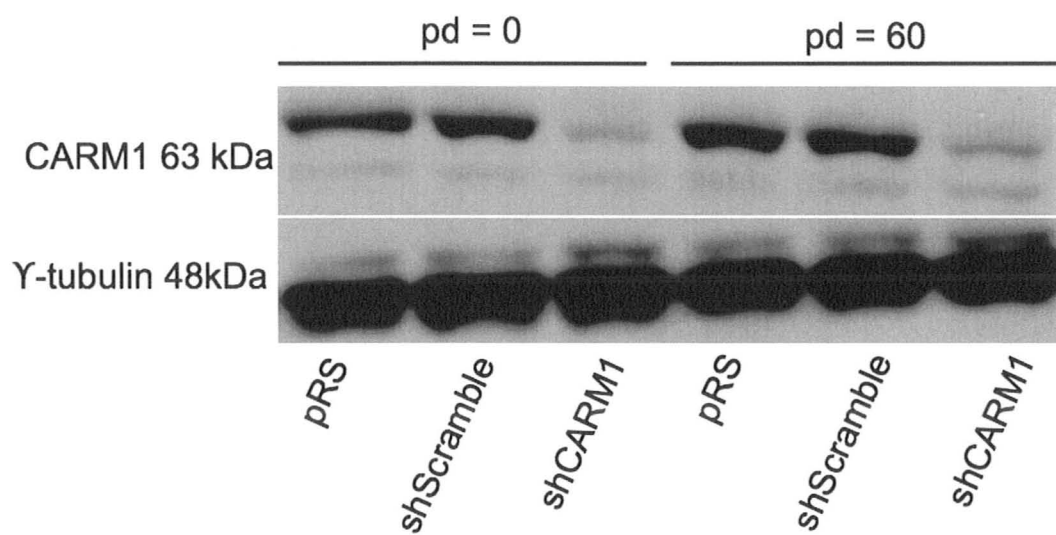


Figure 3.8: HeLaII cells depleted of CARM1 do not exhibit defects in cells proliferation compared to control cells. HeLaII cells infected with the indicated virus were cultured long term. Every four days the cells were counted and 1 million cells were seeded. The number of population doublings was plotted against the number of days in culture. Standard deviations derived from three independent experiments are shown.

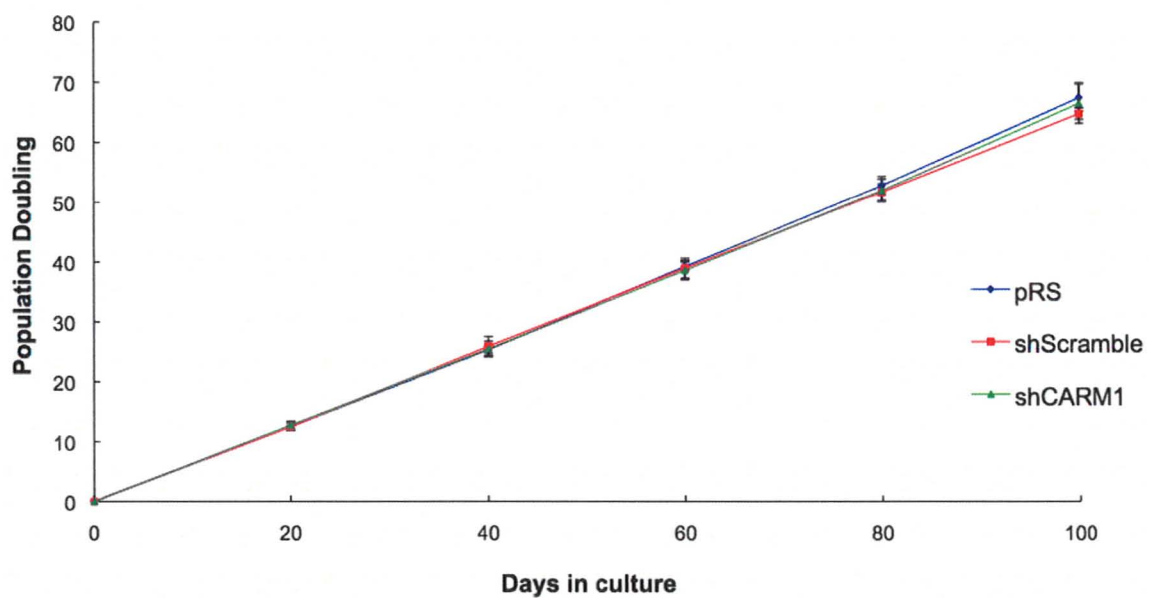
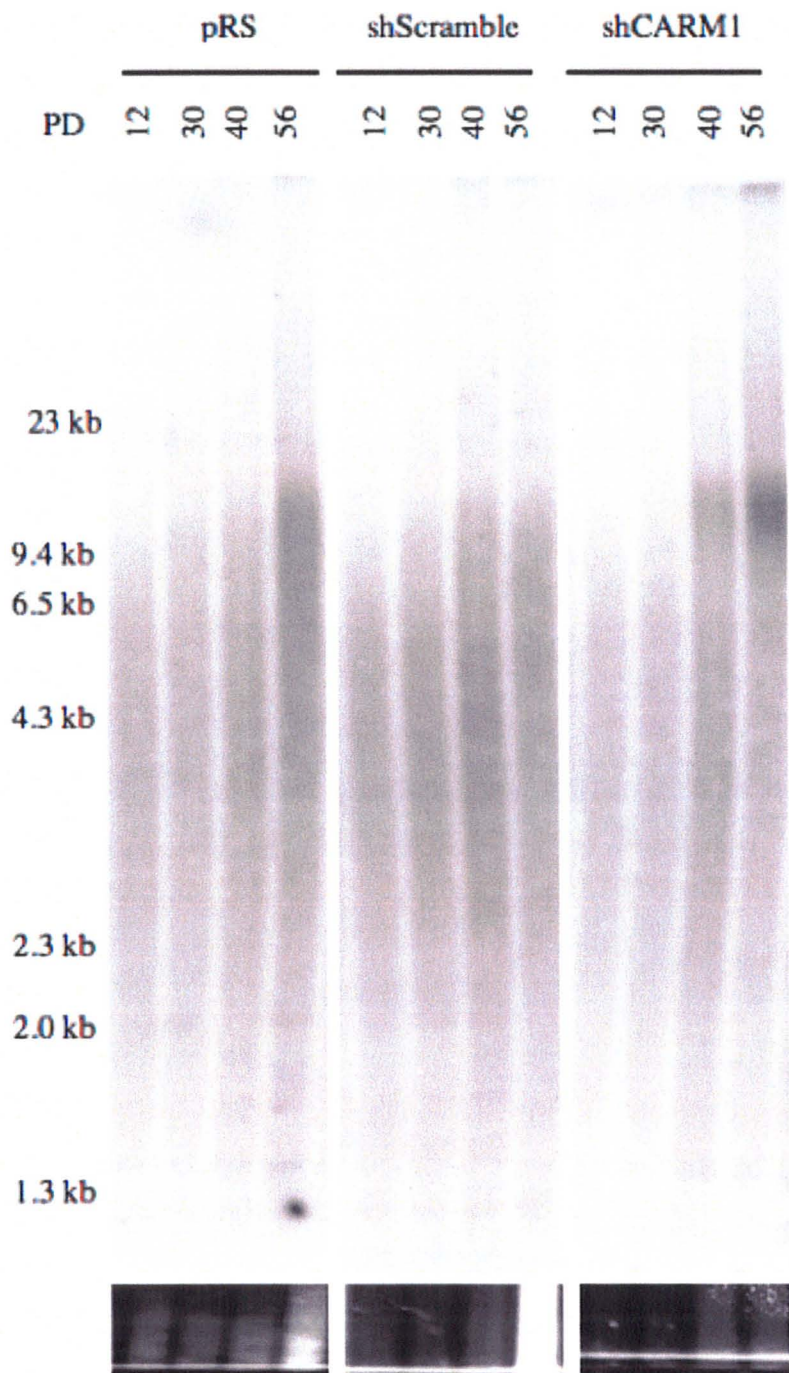
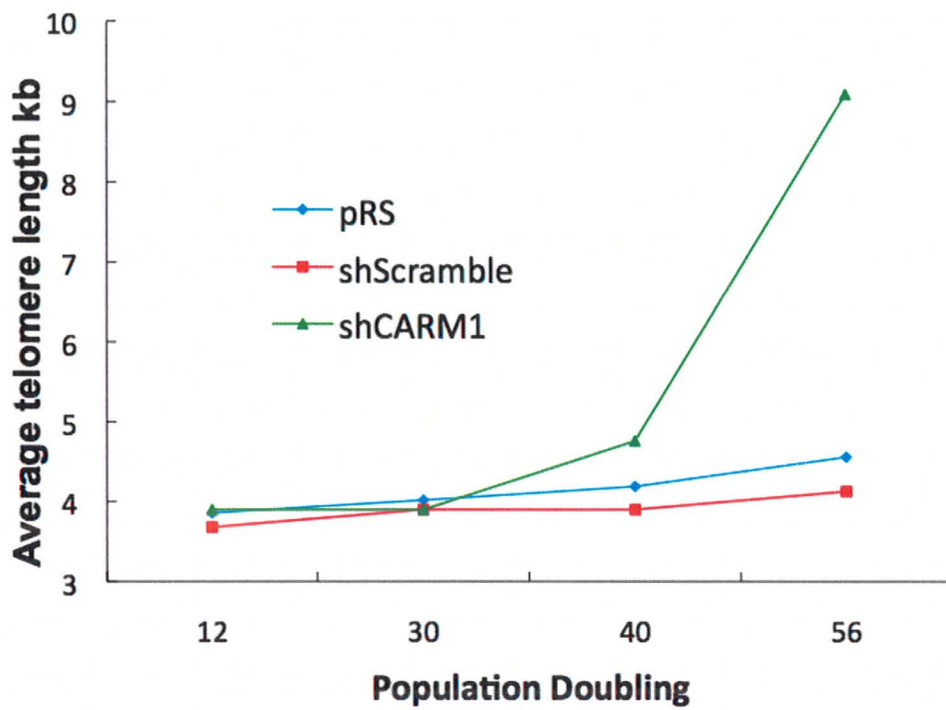


Figure 3.9: HeLaII cells depleted for CARM1 initially showed changes in telomere length dynamics; however, this datum was not reproducible. HeLaII cells infected with the indicated viruses were cultured long term. After 56 population doublings, a southern blot analysis was performed to determine if CARM1 plays a role in the regulation of telomere length. Genomic DNA was isolated from different population doublings and digested with frequent cutting restriction enzymes leaving the telomeres intact. The DNA was run on an agarose gel, the gel was dried, denatured, and probed with a radioactively labeled telomere specific probe. Southern blot analysis initially suggested that depletion of CARM1 resulted in telomere elongation. Figure A shows the southern blot and B is the quantification. In attempts to reproduce this phenotype, a different set of HeLaII cells were infected with shCARM1 along with shScramble and pRS controls. Genomic DNA was isolated from different population doublings, digested, and subjected to southern blot analysis. Southern blot analysis (C) and the quantification (D) reveal that depletion of CARM1 in HeLaII cells does not result in changes in telomere length dynamics overtime. Quantification in D is based on the average telomere length of two independent experiments. Loading control (ethidium bromide staining) is shown below the southern blot.

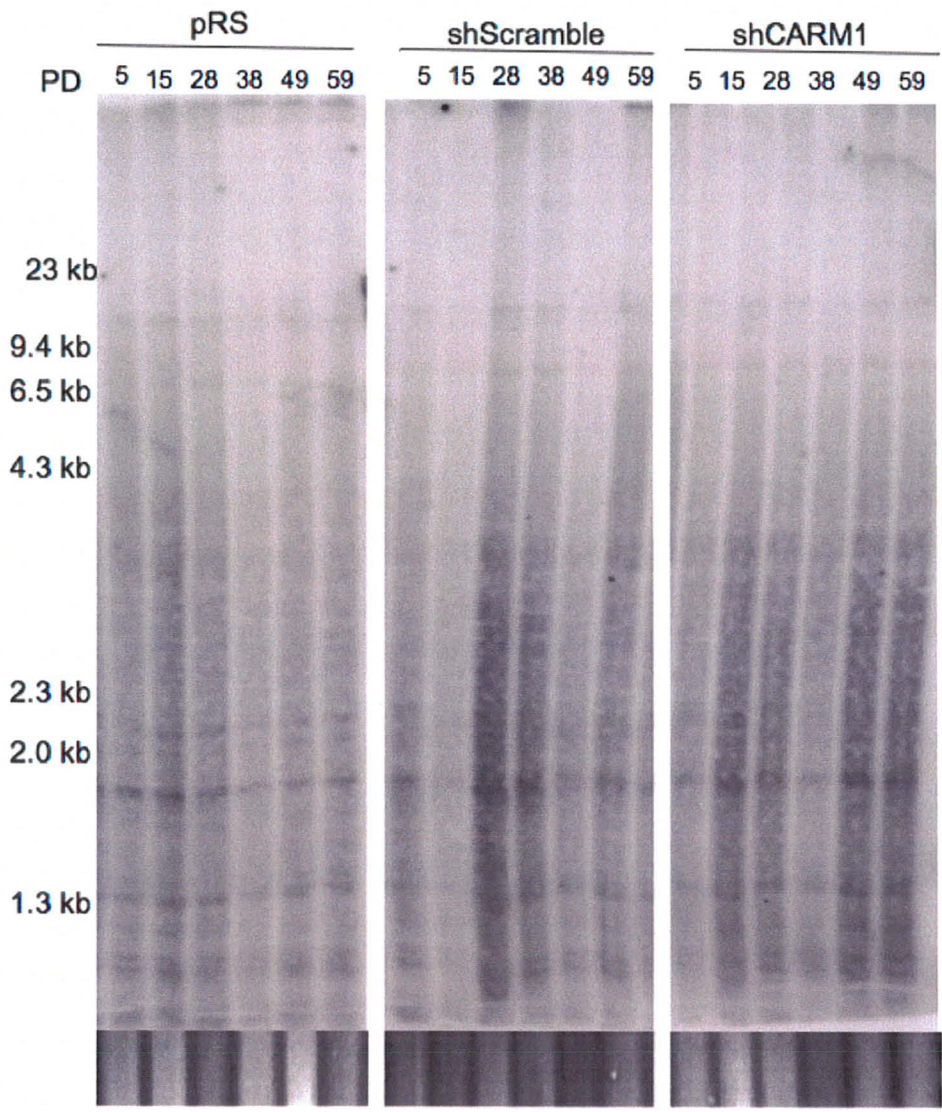
A



B



C



D

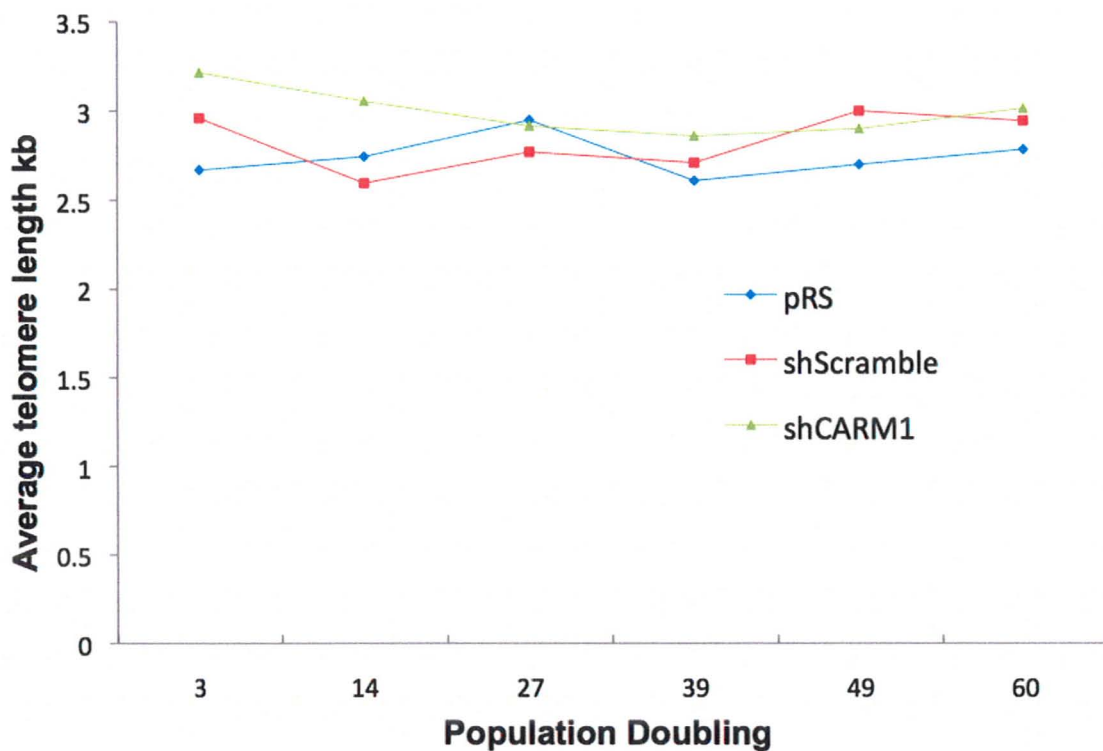


Figure 3.10: MCF-7 cells depleted of CARM1 show reduced levels of CARM1 knockdown at 40 population doublings compared to early population doublings. Protein extract was collected at early and late population doublings to compare the level of CARM1 knockdown.

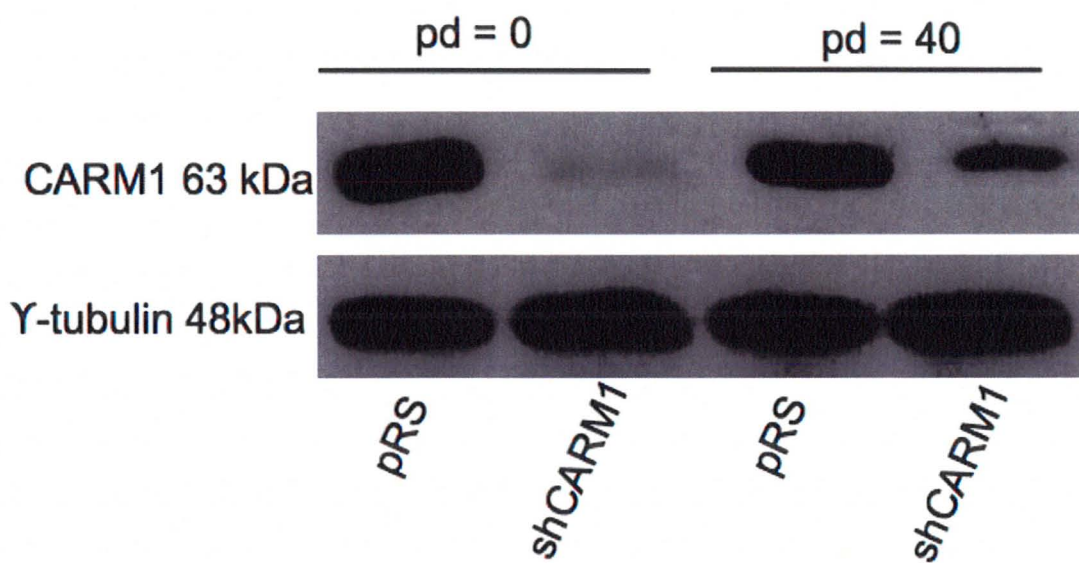


Figure 3.11: MCF-7 cells depleted of CARM1 do not exhibit defects in cell proliferation compared to control cells. MCF-7 cells infected with the indicated virus were cultured long term. Every four days the cells were counted and 750,000 cells were seeded. Number of population doublings was plotted against days in culture. Standard deviations derived from three independent experiments are shown.

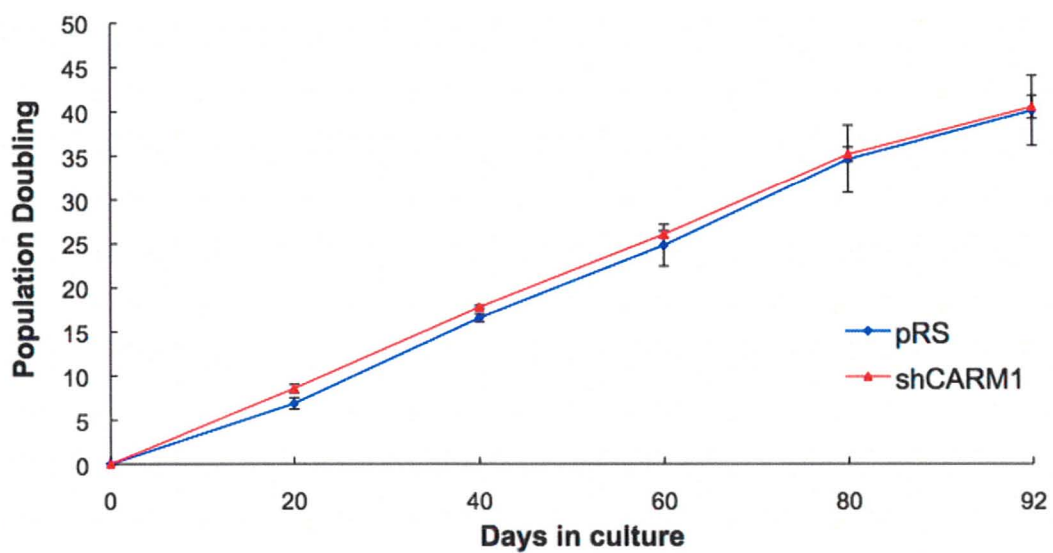
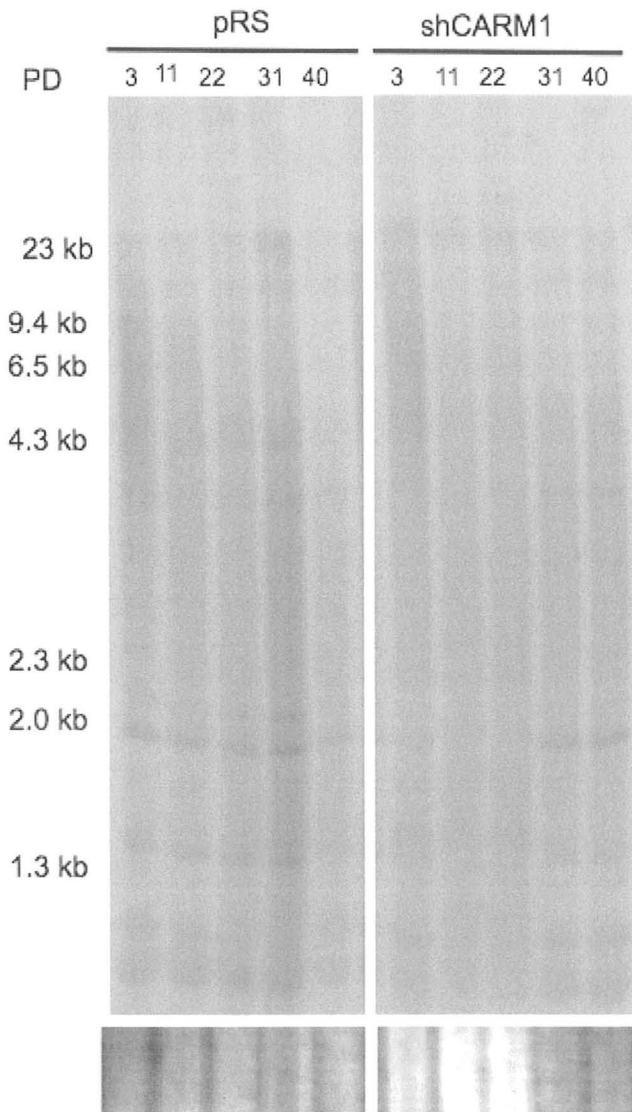


Figure 3.12: MCF-7 cells depleted for CARM1 do not show changes in telomere length dynamics. MCF-7 cells infected with the indicated viruses were cultured long term. After 40 population doublings, a southern blot analysis was performed to determine if CARM1 plays a role in the regulation of telomere length. Genomic DNA was isolated from different population doublings and digested with frequent cutting enzymes leaving the telomeres intact. The DNA was run on an agarose gel, the gel was dried, denatured, and probed with a radioactively labeled telomere specific probe. Southern blot analysis (A) and the quantification (B) reveal that depletion of CARM1 in MCF-7 cells does not result in changes in telomere length dynamics over time. Loading control (ethidium bromide staining) is shown below the southern blot.

A



B

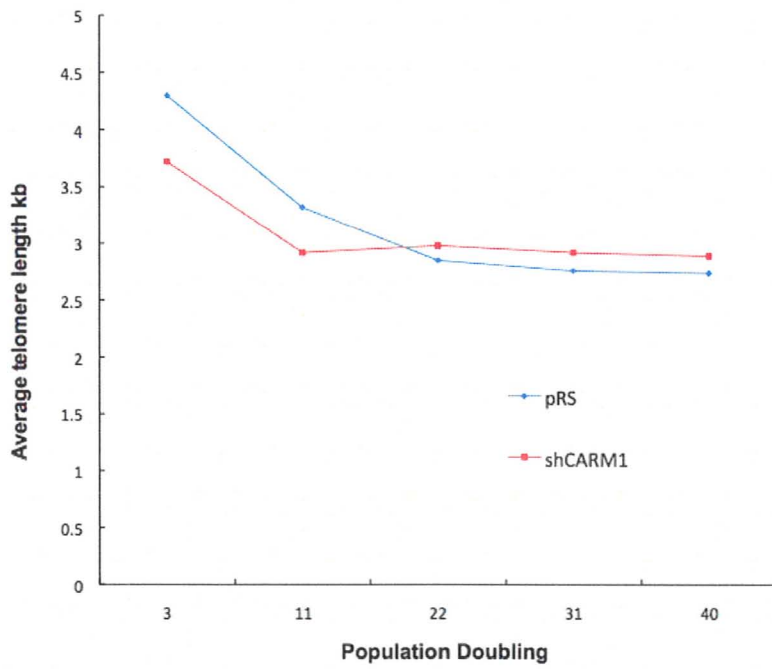


Figure 3.13: hTERT-BJ cells depleted of CARM1 show equal levels of CARM1 knockdown at early and late population doublings. Protein extract was collected at early and late population doublings to compare the level of CARM1 knockdown. As depicted, the level of knockdown appears to be stable from population doubling 0 to 30 compared to control cells.

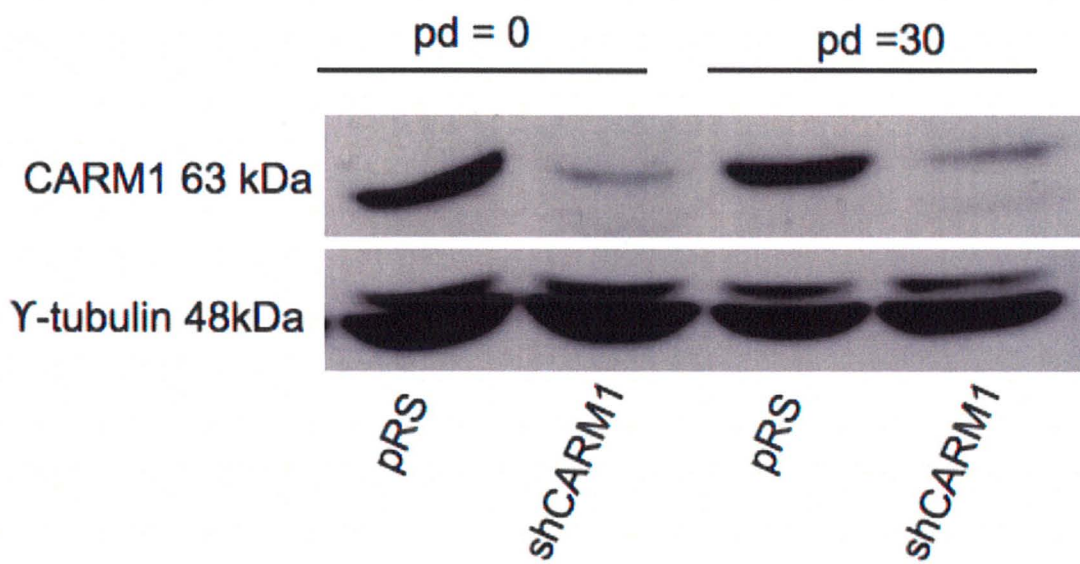


Figure 3.14: hTERT-BJ cells depleted of CARM1 do not exhibit defects in cell proliferation compared to control cells. hTERT-BJ cells infected with the indicated virus were cultured long term. Every four days the cells were counted and 750,000 cells were seeded. The number of population doublings was plotted against the number of days in culture. Standard deviations derived from three independent experiments are shown.

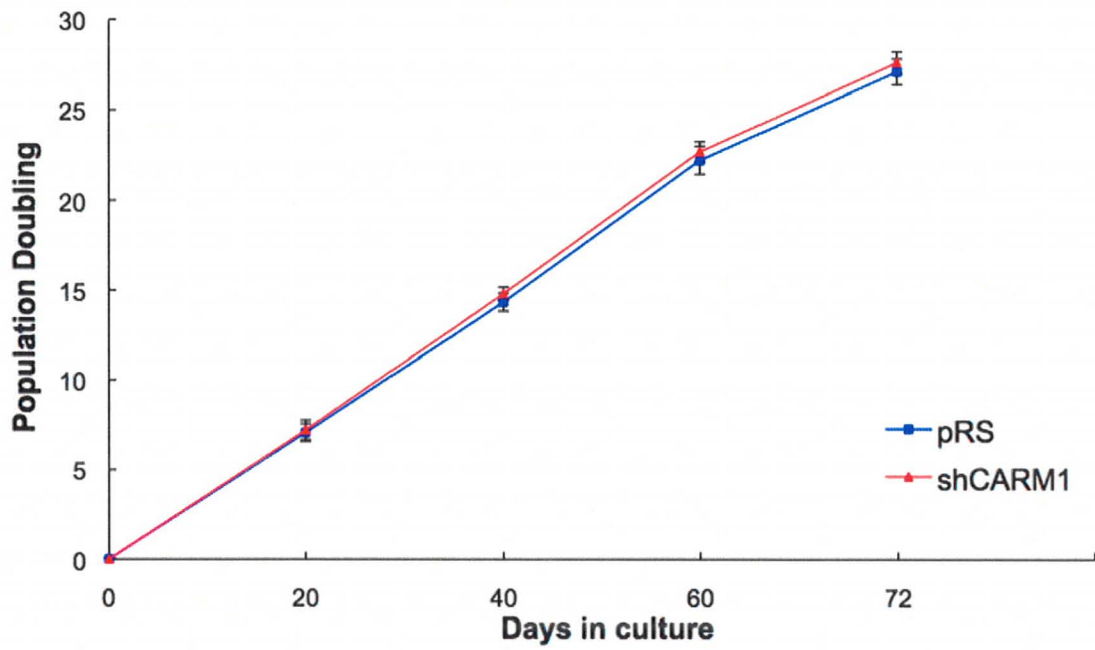
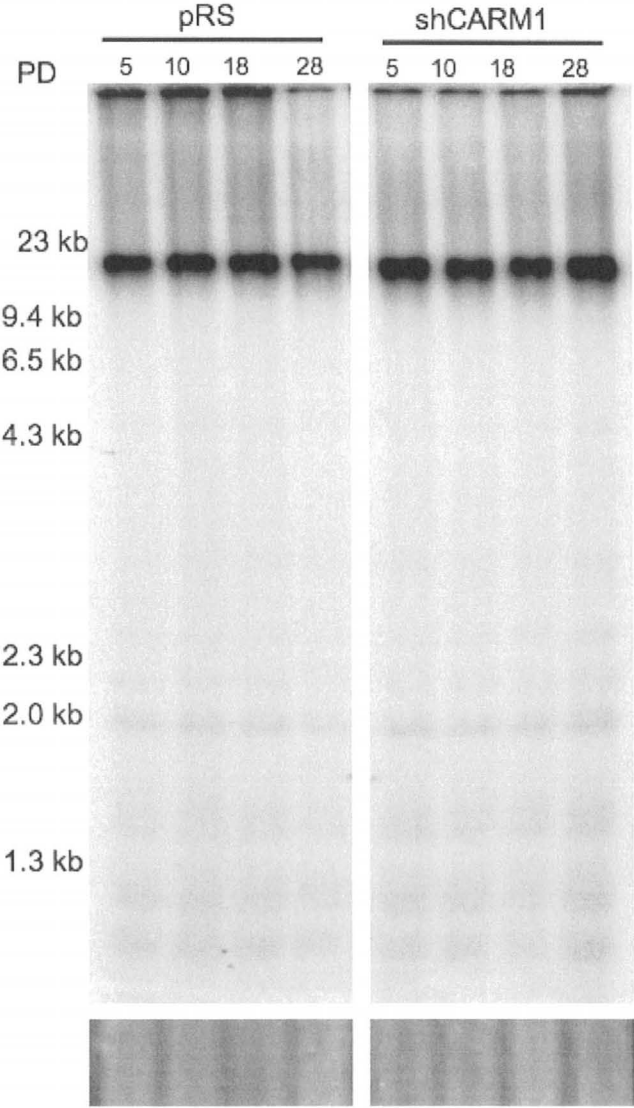


Figure 3.15: hTERT-BJ cells depleted for CARM1 do not show changes in telomere length dynamics. hTERT-BJ cells infected with the indicated viruses were cultured long term. After 28 population doublings, a southern blot analysis was performed to determine if CARM1 plays a role in the regulation of telomere length. Genomic DNA was isolated from different population doublings and digested with frequent cutting enzymes leaving the telomeres intact. The DNA was run on an agarose gel, the gel was dried, denatured, and probed with a radioactively labeled telomere specific probe. Southern blot analysis (A) and the quantification (B) reveal that depletion of CARM1 in hTERT-BJ cells does not result in changes in telomere length dynamics overtime. Loading control (ethidium bromide staining) is shown below the southern blot.

A



B

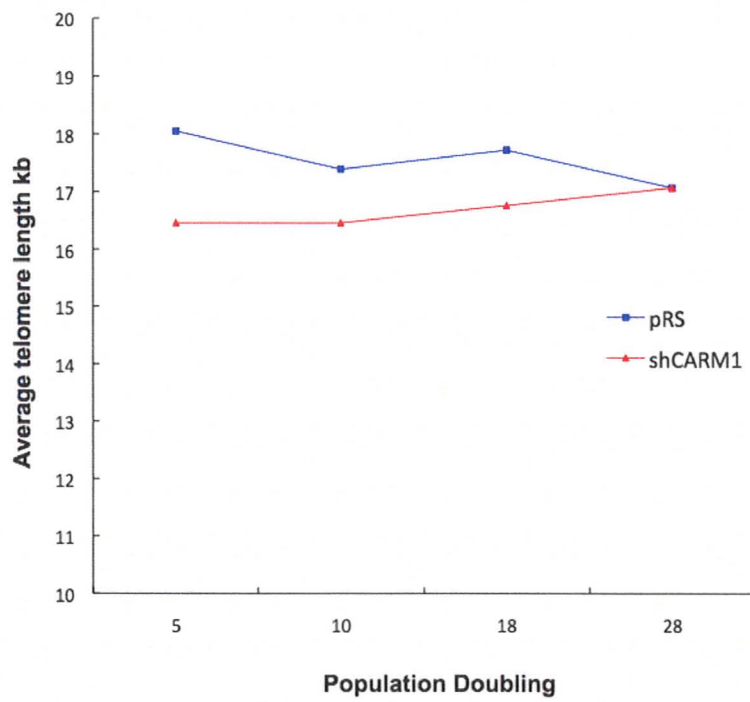
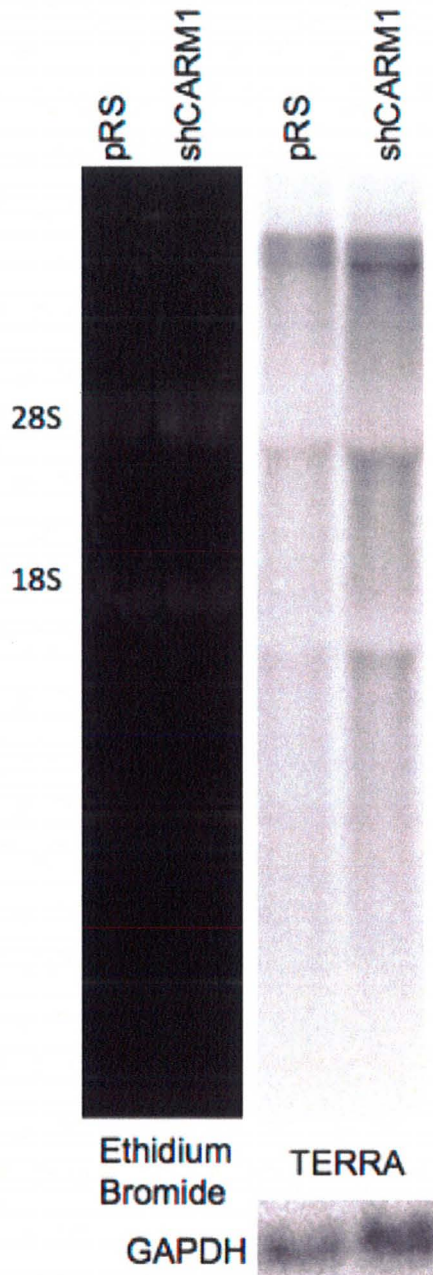


Figure 3.16: Depletion of CARM1 does not alter TERRA levels in MCF-7 cells. To determine if CARM1 plays a role in TERRA regulation, RNA was extracted from early passage MCF-7 cells depleted of CARM1 along with vector control cells. The RNA was run on an agarose gel, transferred to a nitrocellulose membrane, crosslinked, and probed with a telomere specific probe. GAPDH was used as a loading control and for normalization of TERRA levels. The ethidium bromide gel indicates the RNA quality. Figure A shows a depiction of the northern blot and figure B shows the quantification. Error bars represent 3 independent experiments.

A



B

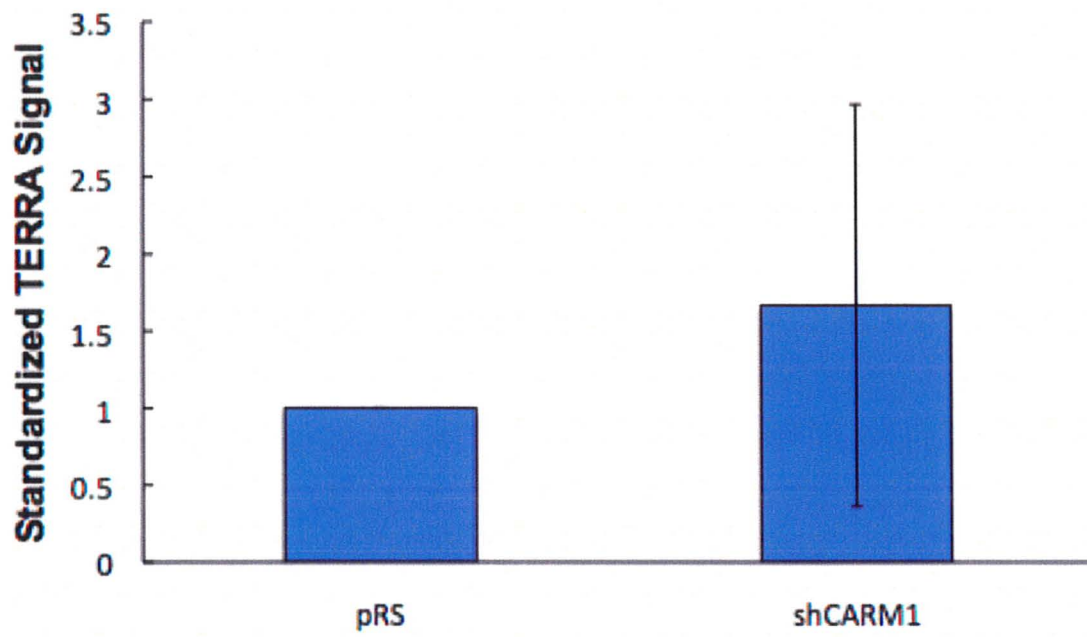
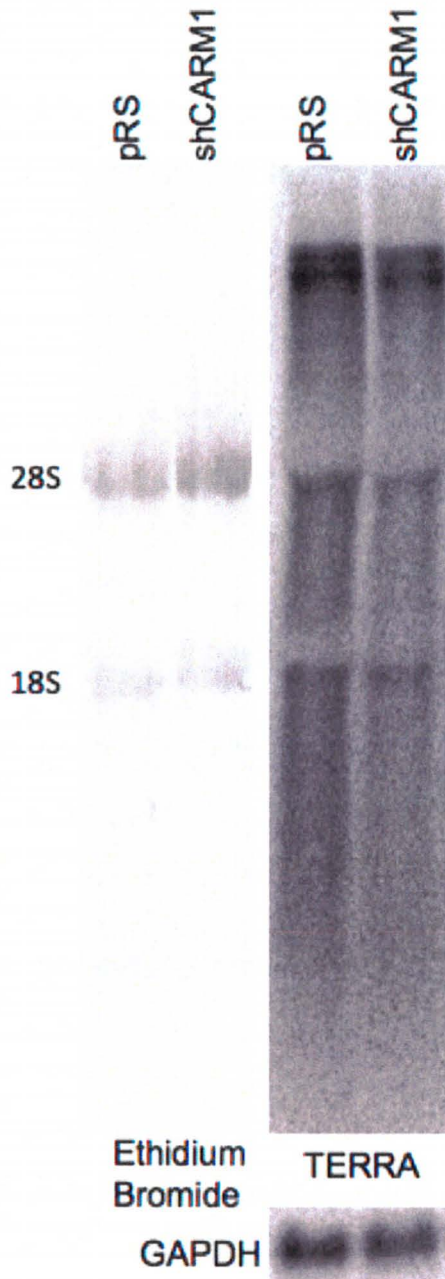
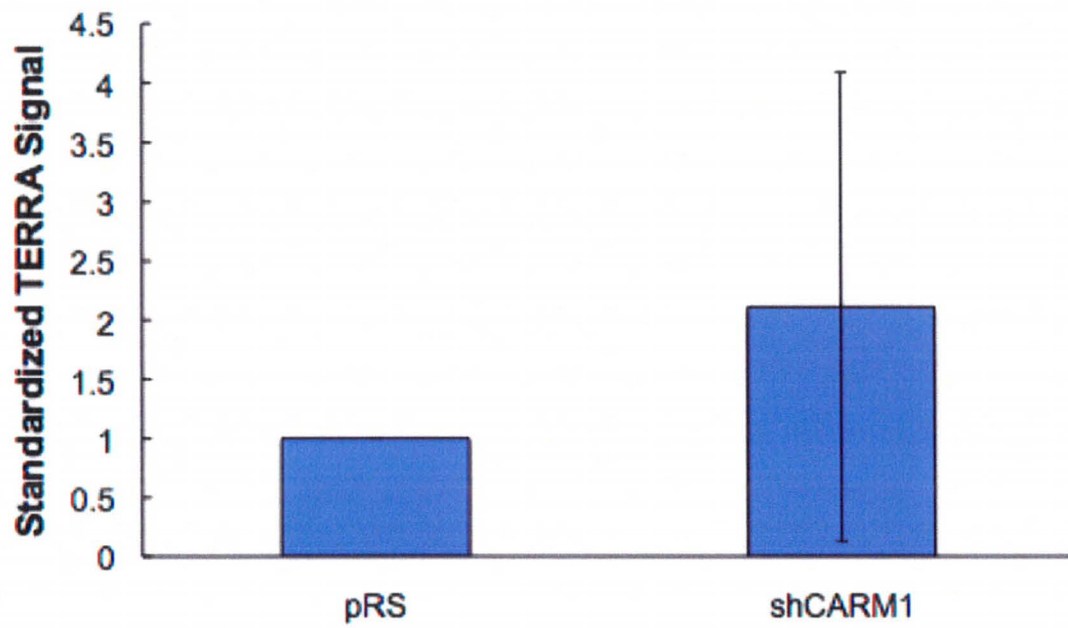


Figure 3.17: Depletion of CARM1 does not alter TERRA levels in hTERT-BJ cells. To determine if CARM1 plays a role in TERRA regulation, RNA was extracted from early passage hTERT-BJ cells depleted of CARM1 along with vector control cells. The RNA was run on an agarose gel, transferred to a nitrocellulose membrane, crosslinked, and probed with a telomere specific probe. GAPDH was used as a loading control and for normalization of TERRA levels. The ethidium bromide gel indicates the RNA quality. Figure A shows a depiction of the northern blot and B shows the quantification. Error bars represent three independent experiments.

A



B



4.0 Discussion:

4.1 Depletion of CARM1 initially induced cellular senescence:

The cellular senescence initially observed with depletion of CARM1 in hTERT-BJ cells was not reproducible. It is unknown as to why knockdown of CARM1 induced cellular senescence initially and why this phenotype was not subsequently reproducible. One possibility is that the initial senescent phenotype was an artifact. Alternatively, we consider the prospect that the senescent phenotype was caused by an unknown variable for which we could not account. It is likely that hTERT-BJ cells depleted for CARM1 are more sensitive compared to control cells and thus the applied conditions caused these cells to undergo senescence. Potentially the conditions with which the cells were handled and grown were not consistent causing an initial acute phenotype.

Subsequent experiments were completed in attempts to determine the cause of the initial senescence phenotype. Retroviral infections of shCARM1 along with shScramble and vector control were completed in hTERT-BJ cells. These cells did not exhibit signs of cellular senescence and this phenotype is consistent with a lack of genomic and telomere instability and a lack of growth defect.

4.2 CARM1 does not appear to play a role in telomere length dynamics:

I have shown that depletion of CARM1 initially led to telomere

elongation. However, such lengthening was not reproducible in subsequent experiments. In attempts to reproduce the elongation phenotype, telomere length experiments were performed in three different cell types. hTERT-BJ, HeLaII, and MCF-7 were cultured long term to determine if depletion of CARM1 alters telomere length dynamics. Southern blot analysis revealed that cells depleted of CARM1 maintain an average telomere length equal to that of the control cells. The cause of the initial telomere elongation phenotype observed in HeLaII cells is unknown. As with the initial senescent phenotype, it is possible that this result was due to an artifact or could have been caused by an unknown variable.

4.3 CARM1 does not appear to play a role in TERRA regulation:

The laboratory of Linger identified that telomeres are transcribed into UUAGGG repeat containing TERRA molecules (Azzalin *et al.*, 2007). The mechanism of TERRA regulation still needs to be elucidated. Caslini *et al.* identified a lysine methyltransferase, MLL, to contribute to TERRA transcription (Caslini *et al.*, 2009). Because CARM1 is a transcriptional coactivator, we decided to determine if CARM1 plays a role in TERRA transcription. Northern blot analysis conducted in both hTERT-BJ and MCF-7 cells revealed no change in TERRA levels upon depletion of CARM1. Although there appears to be a large standard error, repetition allowed us to conclude that CARM1 does not appear to be involved in the regulation of TERRA molecules.

4.4 Significance and Perspectives:

CARM1 has been shown to play a significant role in the establishment of breast and prostate cancers mainly through its function as a transcriptional coactivator (Pal and Sif, 2007). Telomere instability has been shown to be a characteristic of tumorigenesis. One member of the PRMT enzyme family, PRMT1 has been shown to contribute to telomere stability (Mitchell *et al.*, 2009). Depletion of PRMT1 leads to dysfunctional telomeres in primary cells and telomere shortening in cancer cells (Mitchell *et al.*, 2009). As a result, we aimed to determine if CARM1 parallels PRMT1 with respect to a role in telomere maintenance in the progression of cancer. My work is suggestive that CARM1 does not contribute to tumorigenesis through a role in telomere biology and thus does not parallel PRMT1.

My work also suggests that not all PRMT family members play a role in telomere biology. Although my findings do not give direct insight as to the role of arginine methylation at telomeres, these data suggest that CARM1 may not play a significant role in telomere regulation. By understanding which arginine methyltransferases do not play a role in telomere biology, we are closer to finding other potential PRMT enzymes that regulate telomeres.

To date, there are eleven known PRMT enzymes; however, not all of them have been shown to have methyltransferase ability (Pal *et al.*, 2007). In order to deduce which PRMT enzymes play a role at telomeres, our laboratory has created

various PRMT knockdown cell lines. These cells were cultured long term and southern blot analysis was performed to determine if these PRMT enzymes may play a role with respect to telomere length dynamics. The data presented in this report suggest that in the applied conditions CARM1 does not appear to play a role in telomere length maintenance and telomere transcription. Future experiments could be completed to determine if the other nine PRMT enzymes play a role in telomere biology. Cells could be depleted for each PRMT enzyme and if no acute phenotype is observed, cells could be cultured long term and southern blot analysis could be performed to determine if depletion of that specific PRMT enzyme alters telomere length dynamics. If these cells undergo an acute phenotype, such as apoptosis or cellular senescence, this phenotype can be further analyzed. One could perform terminal deoxynucleotidyl transferase dUTP nick end labeling or senescence assays as deemed appropriate. It would also be important to determine if lack of methylation increases the percentage of dysfunctional telomeres through TIF analysis or by fluorescence *in situ* hybridization of metaphase chromosomes using a telomere specific probe. Alternatively, one could harvest the cells for isolation of genomic DNA and perform southern blot analysis to determine if there is an acute change in telomere length.

4.5 Conclusion:

In conclusion, under the conditions outlined above, CARM1 does not

appear to play a role at telomeres. The initial senescence phenotype observed in hTERT-BJ cells was not reproducible for unknown reasons. Subsequent work suggested that depletion of CARM1 does not appear to play a role in genomic or telomere instability and that depletion of CARM1 does not appear to alter cellular proliferation. Southern blot analysis suggests that CARM1 does not appear to play a role in telomere maintenance in hTERT-BJ, HeLaII, or MCF-7 cells. Additionally, northern blot data indicated that depletion of CARM1 does not appear to alter the levels of TERRA transcripts within hTERT-BJ and MCF-7 cells.

5.0 References:

Abreu E, Aritonovska E, Reichenbach P, Cristofari G, Culp B, Terns RM, Lingner J, Terns MP. TIN2-tethered TPP1 recruits human telomerase to telomeres in vivo. *Mol Cell Biol*. 2010 Jun;30(12):2971-82.

Altucci L, Addeo R, Cicatiello L, Dauvois S, Parker MG, Truss M, Beato M, Sica V, Bresciani F, Weisz A. 17beta Estradiol induces cyclin D1 gene transcription, p36D1-p34cdk4 complex activation and p105Rb phosphorylation during mitogenic stimulation of G(1)-arrested human breast cancer cells. *Oncogene*. 1996 Jun 6;12(11):2315-24.

Amiard S, Doudeau M, Pinte S, Poulet A, Lenain C, Faivre-Moskalenko C, Angelov D, Hug N, Vindigni A, Bouvet P, Paoletti J, Gilson E, Giraud-Panis MJ. A topological mechanism for TRF2-enhanced strand invasion. *Nat Struct Mol Biol*. 2007 Feb;14(2):147-54.

An W, Kim J, Roeder RG. Ordered cooperative functions of PRMT1, p300, and CARM1 in transcriptional activation by p53. *Cell*. 2004 Jun 11;117(6):735-48.

Auboeuf D, Hönig A, Berget SM, O'Malley BW. Coordinate regulation of transcription and splicing by steroid receptor coregulators. *Science*. 2002 Oct 11;298(5592):416-9.

Azzalin CM, Reichenbach P, Khoriantseva L, Giulotto E, Lingner J. Telomeric repeat containing RNA and RNA surveillance factors at mammalian chromosome ends. *Science*. 2007 Nov 2;318(5851):798-801.

Azzalin CM, Lingner J. Telomeres: the silence is broken. *Cell Cycle*. 2008 May 1;7(9):1161-5.

Bachand F, Silver PA. PRMT3 is a ribosomal protein methyltransferase that affects the cellular levels of ribosomal subunits. *EMBO J*. 2004 Jul 7;23(13):2641-50.

Bae NS, Baumann P. A RAP1/TRF2 complex inhibits nonhomologous end-joining at human telomeric DNA ends. *Mol Cell*. 2007 May 11;26(3):323-34.

Baldwin AS Jr. The NF-kappa B and I kappa B proteins: new discoveries and insights. *Annu Rev Immunol*. 1996;14:649-83.

Bandyopadhyay D, Okan NA, Bales E, Nascimento L, Cole PA, Medrano EE.

Down-regulation of p300/CBP histone acetyltransferase activates a senescence checkpoint in human melanocytes. *Cancer Res.* 2002 Nov 1;62(21):6231-9.

Bauer UM, Daujat S, Nielsen SJ, Nightingale K, Kouzarides T. Methylation at arginine 17 of histone H3 is linked to gene activation. *EMBO Rep.* 2002 Jan;3(1):39-44.

Baumann P, Cech TR. Pot1, the putative telomere end-binding protein in fission yeast and humans. *Science.* 2001 May 11;292(5519):1171-5. Erratum in: *Science* 2001 Jul 13;293(5528):214.

Baumann P, Podell E, Cech TR. Human Pot1 (protection of telomeres) protein: cytolocalization, gene structure, and alternative splicing. *Mol Cell Biol.* 2002 Nov;22(22):8079-87.

Bedford MT, Richard S. Arginine methylation an emerging regulator of protein function. *Mol Cell.* 2005 Apr 29;18(3):263-72.

Bedford MT. Arginine methylation at a glance. *J Cell Sci.* 2007 Dec 15;120(Pt 24):4243-6.

Bianchi A, Smith S, Chong L, Elias P, de Lange T. TRF1 is a dimer and bends telomeric DNA. *EMBO J.* 1997 Apr 1;16(7):1785-94.

Bilaud T, Brun C, Ancelin K, Koering CE, Laroche T, Gilson E. Telomeric localization of TRF2, a novel human telobox protein. *Nat Genet.* 1997 Oct;17(2):236-9.

Blackburn EH, Greider CW, Henderson E, Lee MS, Shampay J, Shippen-Lentz D. Recognition and elongation of telomeres by telomerase. *Genome.* 1989;31(2):553-60.

Broccoli D, Smogorzewska A, Chong L, de Lange T. Human telomeres contain two distinct Myb-related proteins, TRF1 and TRF2. *Nat Genet.* 1997 Oct;17(2):231-5.

Caslini C, Connelly JA, Serna A, Broccoli D, Hess JL. MLL associates with telomeres and regulates telomeric repeat-containing RNA transcription. *Mol Cell Biol.* 2009 Aug;29(16):4519-26.

Celli GB, de Lange T. DNA processing is not required for ATM-mediated telomere damage response after TRF2 deletion. *Nat Cell Biol.* 2005 Jul;7(7):712-8.

Celli GB, Denchi EL, de Lange T. Ku70 stimulates fusion of dysfunctional telomeres yet protects chromosome ends from homologous recombination. *Nat Cell Biol.* 2006 Aug;8(8):885-90.

Chang W, Dynek JN, Smith S. TRF1 is degraded by ubiquitin-mediated proteolysis after release from telomeres. *Genes Dev.* 2003 Jun 1;17(11):1328-33.

Chen D, Ma H, Hong H, Koh SS, Huang SM, Schurter BT, Aswad DW, Stallcup MR. Regulation of transcription by a protein methyltransferase. *Science.* 1999 Jun 25;284(5423):2174-7.

Chen Y, Yang Y, van Overbeek M, Donigian JR, Baciú P, de Lange T, Lei M. A shared docking motif in TRF1 and TRF2 used for differential recruitment of telomeric proteins. *Science.* 2008 Feb 22;319(5866):1092-6.

Cheng D, Côté J, Shaaban S, Bedford MT. The arginine methyltransferase CARM1 regulates the coupling of transcription and mRNA processing. *Mol Cell.* 2007 Jan 12;25(1):71-83.

Chevillard-Briet M, Trouche D, Vandell L. Control of CBP co-activating activity by arginine methylation. *EMBO J.* 2002 Oct 15;21(20):5457-66.

Chiang YJ, Kim SH, Tessarollo L, Campisi J, Hodes RJ. Telomere-associated protein TIN2 is essential for early embryonic development through a telomerase-independent pathway. *Mol Cell Biol.* 2004 Aug;24(15):6631-4.

Chong L, van Steensel B, Broccoli D, Erdjument-Bromage H, Hanish J, Tempst P, de Lange T. A human telomeric protein. *Science.* 1995 Dec 8;270(5242):1663-7.

Colgin LM, Baran K, Baumann P, Cech TR, Reddel RR. Human POT1 facilitates telomere elongation by telomerase. *Curr Biol.* 2003 May 27;13(11):942-6.

Cook JR, Lee JH, Yang ZH, Krause CD, Herth N, Hoffmann R, Pestka S. FBXO11/PRMT9, a new protein arginine methyltransferase, symmetrically dimethylates arginine residues. *Biochem Biophys Res Commun.* 2006 Apr 7;342(2):472-81.

Counter CM, Avilion AA, LeFeuvre CE, Stewart NG, Greider CW, Harley CB, Bacchetti S. Telomere shortening associated with chromosome instability is arrested in immortal cells which express telomerase activity. *EMBO J.* 1992 May;11(5):1921-9.

Covic M, Hassa PO, Saccani S, Buerki C, Meier NI, Lombardi C, Imhof R,

Bedford MT, Natoli G, Hottiger MO. Arginine methyltransferase CARM1 is a promoter-specific regulator of NF-kappaB-dependent gene expression. *EMBO J.* 2005 Jan 12;24(1):85-96.

Cuthbert, G., Daujat, S., Snowden, A., Erdjument-Bromage, H., Hagiwara, T., Yamada, M., Schneider, R., Gregory, P., Tempst, P., Bannister, A. & Kouzarides, T. Histone deimination antagonizes methylation. *Cell.* 2004 118, 545-553.

Das BK, Xia L, Palandjian L, Gozani O, Chyung Y, Reed R. Characterization of a protein complex containing spliceosomal proteins SAPs 49, 130, 145, and 155. *Mol Cell Biol.* 1999 Oct;19(10):6796-802.

Daujat S, Bauer UM, Shah V, Turner B, Berger S, Kouzarides T. Crosstalk between CARM1 methylation and CBP acetylation on histone H3. *Curr Biol.* 2002 Dec 23;12(24):2090-7.

Déjardin J, Kingston RE. Purification of proteins associated with specific genomic Loci. *Cell.* 2009 Jan 9;136(1):175-86.

de Lange T, Shiue L, Myers RM, Cox DR, Naylor SL, Killery AM, Varmus HE. Structure and variability of human chromosome ends. *Mol Cell Biol.* 1990 Feb;10(2):518-27.

de Lange T. Shelterin: the protein complex that shapes and safeguards human telomeres. *Genes Dev.* 2005 Sep 15;19(18):2100-10.

de Lange T. Lasker Laurels for telomerase. *Cell.* 2006 Sep 22;126(6):1017-20.

Denchi EL, de Lange T. Protection of telomeres through independent control of ATM and ATR by TRF2 and POT1. *Nature.* 2007 Aug 30;448(7157):1068-71.

Deng Z, Norseen J, Wiedmer A, Riethman H, Lieberman PM. TERRA RNA binding to TRF2 facilitates heterochromatin formation and ORC recruitment at telomeres. *Mol Cell.* 2009 Aug 28;35(4):403-13.

Doisneau-Sixou SF, Sergio CM, Carroll JS, Hui R, Musgrove EA, Sutherland RL. Estrogen and antiestrogen regulation of cell cycle progression in breast cancer cells. *Endocr Relat Cancer.* 2003 Jun;10(2):179-86.

Eeckhoutte J, Carroll JS, Geistlinger TR, Torres-Arzayus MI, Brown M. A cell-type-specific transcriptional network required for estrogen regulation of cyclin D1 and cell cycle progression in breast cancer. *Genes Dev.* 2006 Sep 15;20(18):2513-26.

Eggert C, Chari A, Laggerbauer B, Fischer U. Spinal muscular atrophy: the RNP connection. *Trends Mol Med.* 2006 Mar;12(3):113-21.

El Messaoudi S, Fabrizio E, Rodriguez C, Chuchana P, Fauquier L, Cheng D, Theillet C, Vandell L, Bedford MT, Sardet C. Coactivator-associated arginine methyltransferase 1 (CARM1) is a positive regulator of the Cyclin E1 gene. *Proc Natl Acad Sci U S A.* 2006 Sep 5;103(36):13351-6.

Evans RM. The steroid and thyroid hormone receptor superfamily. *Science.* 1988 May 13;240(4854):889-95.

Fabrizio E, El Messaoudi S, Polanowska J, Paul C, Cook JR, Lee JH, Negre V, Rousset M, Pestka S, Le Cam A, Sardet C. Negative regulation of transcription by the type II arginine methyltransferase PRMT5. *EMBO Rep.* 2002 Jul;3(7):641-5.

Fouché N, Cesare AJ, Willcox S, Ozgür S, Compton SA, Griffith JD. The basic domain of TRF2 directs binding to DNA junctions irrespective of the presence of TTAGGG repeats. *J Biol Chem.* 2006 Dec 8;281(49):37486-95.

Frietze S, Lupien M, Silver PA, Brown M. CARM1 regulates estrogen-stimulated breast cancer growth through up-regulation of E2F1. *Cancer Res.* 2008 Jan 1;68(1):301-6.

Fujiwara T, Mori Y, Chu DL, Koyama Y, Miyata S, Tanaka H, Yachi K, Kubo T, Yoshikawa H, Tohyama M. CARM1 regulates proliferation of PC12 cells by methylating HuD. *Mol Cell Biol.* 2006 Mar;26(6):2273-85.

Ghosh S, May MJ, Kopp EB. NF-kappa B and Rel proteins: evolutionarily conserved mediators of immune responses. *Annu Rev Immunol.* 1998;16:225-60.

Greenwood J, Cooper JP. Trapping Rap1 at the telomere to prevent chromosome end fusions. *EMBO J.* 2009 Nov 4;28(21):3277-8.

Greider CW, Blackburn EH. The telomere terminal transferase of *Tetrahymena* is a ribonucleoprotein enzyme with two kinds of primer specificity. *Cell.* 1987 Dec 24;51(6):887-98.

Greider CW, Blackburn EH. A telomeric sequence in the RNA of *Tetrahymena* telomerase required for telomere repeat synthesis. *Nature.* 1989 Jan 26;337(6205):331-7.

Griffith J, Bianchi A, de Lange T. TRF1 promotes parallel pairing of telomeric tracts in vitro. *J Mol Biol.* 1998 Apr 24;278(1):79-88.

Griffith JD, Comeau L, Rosenfield S, Stansel RM, Bianchi A, Moss H, de Lange T. Mammalian telomeres end in a large duplex loop. *Cell*. 1999 May 14;97(4):503-14.

Hinman MN, Lou H. Diverse molecular functions of Hu proteins. *Cell Mol Life Sci*. 2008 Oct;65(20):3168-81.

Hockemeyer D, Sfeir AJ, Shay JW, Wright WE, de Lange T. POT1 protects telomeres from a transient DNA damage response and determines how human chromosomes end. *EMBO J*. 2005 Jul 20;24(14):2667-78.

Hockemeyer D, Daniels JP, Takai H, de Lange T. Recent expansion of the telomeric complex in rodents: Two distinct POT1 proteins protect mouse telomeres. *Cell*. 2006 Jul 14;126(1):63-77.

Hockemeyer D, Palm W, Else T, Daniels JP, Takai KK, Ye JZ, Keegan CE, de Lange T, Hammer GD. Telomere protection by mammalian Pot1 requires interaction with Tpp1. *Nat Struct Mol Biol*. 2007 Aug;14(8):754-61.

Hong H, Kao C, Jeng MH, Eble JN, Koch MO, Gardner TA, Zhang S, Li L, Pan CX, Hu Z, MacLennan GT, Cheng L. Aberrant expression of CARM1, a transcriptional coactivator of androgen receptor, in the development of prostate carcinoma and androgen-independent status. *Cancer*. 2004 Jul 1;101(1):83-9.

Houghtaling BR, Cuttonaro L, Chang W, Smith S. A dynamic molecular link between the telomere length regulator TRF1 and the chromosome end protector TRF2. *Curr Biol*. 2004 Sep 21;14(18):1621-31.

Huntriss JD, Barr JA, Horn DA, Williams DG, Latchman DS. Mice lacking Snrpn expression show normal regulation of neuronal alternative splicing events. *Mol Biol Rep*. 1994 Jul;20(1):19-25.

Jelinic P, Stehle JC, Shaw P. The testis-specific factor CTCFL cooperates with the protein methyltransferase PRMT7 in H19 imprinting control region methylation. *PLoS Biol*. 2006 Oct;4(11):e355.

Jenster G. The role of the androgen receptor in the development and progression of prostate cancer. *Semin Oncol*. 1999 Aug;26(4):407-21.

Kang Z, Jänne OA, Palvimo JJ. Coregulator recruitment and histone modifications in transcriptional regulation by the androgen receptor. *Mol Endocrinol*. 2004 Nov;18(11):2633-48.

Karlseder J, Broccoli D, Dai Y, Hardy S, de Lange T. p53- and ATM-dependent

apoptosis induced by telomeres lacking TRF2. *Science*. 1999 Feb 26;283(5406):1321-5.

Karlseder J, Kachatrian L, Takai H, Mercer K, Hingorani S, Jacks T, de Lange T. Targeted deletion reveals an essential function for the telomere length regulator Trf1. *Mol Cell Biol*. 2003 Sep;23(18):6533-41.

Keene JD. Why is Hu where? Shuttling of early-response-gene messenger RNA subsets. *Proc Natl Acad Sci U S A*. 1999 Jan 5;96(1):5-7.

Kibe T, Osawa GA, Keegan CE, de Lange T. Telomere protection by TPP1 is mediated by POT1a and POT1b. *Mol Cell Biol*. 2010 Feb;30(4):1059-66.

Kim D, Lee J, Cheng D, Li J, Carter C, Richie E, Bedford MT. Enzymatic activity is required for the in vivo functions of CARM1. *J Biol Chem*. 2010 Jan 8;285(2):1147-52.

Kim J, Lee J, Yadav N, Wu Q, Carter C, Richard S, Richie E, Bedford MT. Loss of CARM1 results in hypomethylation of thymocyte cyclic AMP-regulated phosphoprotein and deregulated early T cell development. *J Biol Chem*. 2004 Jun 11;279(24):25339-44.

Kim SH, Kaminker P, Campisi J. TIN2, a new regulator of telomere length in human cells. *Nat Genet*. 1999 Dec;23(4):405-12.

Kim SH, Han S, You YH, Chen DJ, Campisi J. The human telomere-associated protein TIN2 stimulates interactions between telomeric DNA tracts in vitro. *EMBO Rep*. 2003 Jul;4(7):685-91.

Kim SH, Beausejour C, Davalos AR, Kaminker P, Heo SJ, Campisi J. TIN2 mediates functions of TRF2 at human telomeres. *J Biol Chem*. 2004 Oct 15;279(42):43799-804.

Klinge CM. Estrogen receptor interaction with estrogen response elements. *Nucleic Acids Res*. 2001 Jul 15;29(14):2905-19.

Lakowski TM, Frankel A. Kinetic analysis of human protein arginine N-methyltransferase 2: formation of monomethyl- and asymmetric dimethyl-arginine residues on histone H4. *Biochem J*. 2009 Jun 26;421(2):253-61.

Latrick CM, Cech TR. POT1-TPP1 enhances telomerase processivity by slowing primer dissociation and aiding translocation. *EMBO J*. 2010 Mar 3;29(5):924-33.

Lee J, Bedford MT. PABP1 identified as an arginine methyltransferase substrate

using high-density protein arrays. *EMBO Rep.* 2002 Mar;3(3):268-73. Epub 2002 Feb 15.

Lee JH, Cook JR, Yang ZH, Mirochnitchenko O, Gunderson SI, Felix AM, Herth N, Hoffmann R, Pestka S. PRMT7, a new protein arginine methyltransferase that synthesizes symmetric dimethylarginine. *J Biol Chem.* 2005 Feb 4;280(5):3656-64.

Lee J, Sayegh J, Daniel J, Clarke S, Bedford MT. PRMT8, a new membrane-bound tissue-specific member of the protein arginine methyltransferase family. *J Biol. Chem.* 2005 Sep 23;280(38):32890-6.

Lejnine S, Makarov VL, Langmore JP. Conserved nucleoprotein structure at the ends of vertebrate and invertebrate chromosomes. *Proc Natl Acad Sci U S A.* 1995 Mar 14;92(6):2393-7.

Levine TD, Gao F, King PH, Andrews LG, Keene JD. Hel N1: an autoimmune RNA-binding protein with specificity for 3' uridylate-rich untranslated regions of growth factor mRNAs. *Mol Cell Biol.* 1993 Jun;13(6):3494-504.

Li B, Oestreich S, de Lange T. Identification of human Rap1: implications for telomere evolution. *Cell.* 2000 May 26;101(5):471-83.

Li B, de Lange T. Rap1 affects the length and heterogeneity of human telomeres. *Mol Biol Cell.* 2003 Dec;14(12):5060-8.

Li H, Park S, Kilburn B, Jelinek MA, Henschen-Edman A, Aswad DW, Stallcup MR, Laird-Offringa IA. Lipopolysaccharide-induced methylation of HuR, an mRNA-stabilizing protein, by CARM1. Coactivator-associated arginine methyltransferase. *J Biol Chem.* 2002 Nov 22;277(47):44623-30.

Liu D, Safari A, O'Connor MS, Chan DW, Laegeler A, Qin J, Songyang Z. PTPN12 interacts with POT1 and regulates its localization to telomeres. *Nat Cell Biol.* 2004 Jul;6(7):673-80.

Liu J, Dalmau J, Szabo A, Rosenfeld M, Huber J, Furneaux H. Paraneoplastic encephalomyelitis antigens bind to the AU-rich elements of mRNA. *Neurology.* 1995 Mar;45(3 Pt 1):544-50.

Loayza D, De Lange T. POT1 as a terminal transducer of TRF1 telomere length control. *Nature.* 2003 Jun 26;423(6943):1013-8.

Luke B, Panza A, Redon S, Iglesias N, Li Z, Lingner J. The Rat1p 5' to 3' exonuclease degrades telomeric repeat-containing RNA and promotes telomere

elongation in *Saccharomyces cerevisiae*. *Mol Cell*. 2008 Nov 21;32(4):465-77.

Luke B, Lingner J. TERRA: telomeric repeat-containing RNA. *EMBO J*. 2009 Sep 2;28(17):2503-10.

Ma H, Hong H, Huang SM, Irvine RA, Webb P, Kushner PJ, Coetzee GA, Stallcup MR. Multiple signal input and output domains of the 160-kilodalton nuclear receptor coactivator proteins. *Mol Cell Biol*. 1999 Sep;19(9):6164-73.

Ma WJ, Cheng S, Campbell C, Wright A, Furneaux H. Cloning and characterization of HuR, a ubiquitously expressed Elav-like protein. *J Biol Chem*. 1996 Apr 5;271(14):8144-51.

Majumder S, Liu Y, Ford OH 3rd, Mohler JL, Whang YE. Involvement of arginine methyltransferase CARM1 in androgen receptor function and prostate cancer cell viability. *Prostate*. 2006 Sep 1;66(12):1292-301.

Martínez P, Thanasoula M, Muñoz P, Liao C, Tejera A, McNees C, Flores JM, Fernández-Capetillo O, Tarsounas M, Blasco MA. Increased telomere fragility and fusions resulting from TRF1 deficiency lead to degenerative pathologies and increased cancer in mice. *Genes Dev*. 2009 Sep 1;23(17):2060-75.

McBride AE, Silver PA. State of the arg: protein methylation at arginine comes of age. *Cell*. 2001 Jul 13;106(1):5-8.

McClintock B. The Stability of Broken Ends of Chromosomes in *Zea Mays*. *Genetics*. 1941 Mar;26(2):234-82.

McElligott R, Wellinger RJ. The terminal DNA structure of mammalian chromosomes. *EMBO J*. 1997 Jun 16;16(12):3705-14.

Meyer R, Wolf SS, Obendorf M. PRMT2, a member of the protein arginine methyltransferase family, is a coactivator of the androgen receptor. *J Steroid Biochem Mol Biol*. 2007 Oct;107(1-2):1-14.

Miao F, Li S, Chavez V, Lanting L, Natarajan R. Coactivator-associated arginine methyltransferase-1 enhances nuclear factor-kappaB-mediated gene transcription through methylation of histone H3 at arginine 17. *Mol Endocrinol*. 2006 Jul;20(7):1562-73.

Mitchell TR, Glenfield K, Jeyanthan K, Zhu XD. Arginine methylation regulates telomere length and stability. *Mol Cell Biol*. 2009 Sep;29(18):4918-34.

Morrison AJ, Sardet C, Herrera RE. Retinoblastoma protein transcriptional

repression through histone deacetylation of a single nucleosome. *Mol Cell Biol.* 2002 Feb;22(3):856-65.

Musgrove EA, Hamilton JA, Lee CS, Sweeney KJ, Watts CK, Sutherland RL. Growth factor, steroid, and steroid antagonist regulation of cyclin gene expression associated with changes in T-47D human breast cancer cell cycle progression. *Mol Cell Biol.* 1993 Jun;13(6):3577-87.

Nergadze SG, Farnung BO, Wischniewski H, Khoriauli L, Vitelli V, Chawla R, Giulotto E, Azzalin CM. CpG-island promoters drive transcription of human telomeres. *RNA.* 2009 Dec;15(12):2186-94.

Nielsen SJ, Schneider R, Bauer UM, Bannister AJ, Morrison A, O'Carroll D, Firestein R, Cleary M, Jenuwein T, Herrera RE, Kouzarides T. Rb targets histone H3 methylation and HP1 to promoters. *Nature.* 2001 Aug 2;412(6846):561-5.

Nishioka K, Reinberg D. Transcription. Switching partners in a regulatory tango. *Science.* 2001 Dec 21;294(5551):2497-8.

O'Connor MS, Safari A, Liu D, Qin J, Songyang Z. The human Rap1 protein complex and modulation of telomere length. *J Biol Chem.* 2004 Jul 2;279(27):28585-91

O'Connor MS, Safari A, Xin H, Liu D, Songyang Z. A critical role for TPP1 and TIN2 interaction in high-order telomeric complex assembly. *Proc Natl Acad Sci U S A.* 2006 Aug 8;103(32):11874-9.

Ohkura N, Takahashi M, Yaguchi H, Nagamura Y, Tsukada T. Coactivator-associated arginine methyltransferase 1, CARM1, affects pre-mRNA splicing in an isoform-specific manner. *J Biol Chem.* 2005 Aug 12;280(32):28927-35.

Okano HJ, Darnell RB. A hierarchy of Hu RNA binding proteins in developing and adult neurons. *J Neurosci.* 1997 May 1;17(9):3024-37.

Olovnikov AM. [Principle of marginotomy in template synthesis of polynucleotides]. *Dokl Akad Nauk SSSR.* 1971;201(6):1496-9.

Olovnikov AM. A theory of marginotomy. The incomplete copying of template margin in enzymic synthesis of polynucleotides and biological significance of the phenomenon. *J Theor Biol.* 1973 Sep 14;41(1):181-90.

Onate SA, Boonyaratanakornkit V, Spencer TE, Tsai SY, Tsai MJ, Edwards DP, O'Malley BW. The steroid receptor coactivator-1 contains multiple receptor interacting and activation domains that cooperatively enhance the activation

function 1 (AF1) and AF2 domains of steroid receptors. *J Biol Chem.* 1998 May 15;273(20):12101-8.

Pal S, Sif S. Interplay between chromatin remodelers and protein arginine methyltransferases. *J Cell Physiol.* 2007 Nov;213(2):306-15.

Palm W, de Lange T. How shelterin protects mammalian telomeres. *Annu RevnGenet.* 2008;42:301-34.

Palm W, Hockemeyer D, Kibe T, de Lange T. Functional dissection of human and mouse POT1 proteins. *Mol Cell Biol.* 2009 Jan;29(2):471-82.

Paushkin S, Gubitza AK, Massenet S, Dreyfuss G. The SMN complex, an assembly of ribonucleoproteins. *Curr Opin Cell Biol.* 2002 Jun;14(3):305-12.

Pellizzoni L. Chaperoning ribonucleoprotein biogenesis in health and disease. *EMBO Rep.* 2007 Apr;8(4):340-5.

Qi C, Chang J, Zhu Y, Yeldandi AV, Rao SM, Zhu YJ. Identification of protein arginine methyltransferase 2 as a coactivator for estrogen receptor alpha. *J Biol Chem.* 2002 Aug 9;277(32):28624-30.

Redon S, Reichenbach P, Lingner J. The non-coding RNA TERRA is a natural ligand and direct inhibitor of human telomerase. *Nucleic Acids Res.* 2010 May 11.

Ruby SW, Abelson J. An early hierarchic role of U1 small nuclear ribonucleoprotein in spliceosome assembly. *Science.* 1988 Nov 18;242(4881):1028-35.

Sarthy J, Bae NS, Scraftford J, Baumann P. Human RAP1 inhibits non-homologous end joining at telomeres. *EMBO J.* 2009 Nov 4;28(21):3390-9.

Schoeftner S, Blasco MA. A 'higher order' of telomere regulation: telomere heterochromatin and telomeric RNAs. *EMBO J.* 2009 Aug 19;28(16):2323-36.

Schoeftner S, Blasco MA. Chromatin regulation and non-coding RNAs at mammalian telomeres. *Semin Cell Dev Biol.* 2010 Apr;21(2):186-93.

Schurter BT, Koh SS, Chen D, Bunick GJ, Harp JM, Hanson BL, Henschen-Edman A, Mackay DR, Stallcup MR, Aswad DW. Methylation of histone H3 by coactivator-associated arginine methyltransferase 1. *Biochemistry.* 2001 May 15;40(19):5747-56.

Selvi BR, Batta K, Kishore AH, Mantelingu K, Varier RA, Balasubramanyam K, Pradhan SK, Dasgupta D, Sriram S, Agrawal S, Kundu TK. Identification of a novel inhibitor of coactivator-associated arginine methyltransferase 1 (CARM1)-mediated methylation of histone H3 Arg-17. *J Biol Chem.* 2010 Mar 5;285(10):7143-52.

Sfeir A, Kosiyatrakul ST, Hockemeyer D, MacRae SL, Karlseder J, Schildkraut CL, de Lange T. Mammalian telomeres resemble fragile sites and require TRF1 for efficient replication. *Cell.* 2009 Jul 10;138(1):90-103.

Sfeir A, Kabir S, van Overbeek M, Celli GB, de Lange T. Loss of Rap1 induces telomere recombination in the absence of NHEJ or a DNA damage signal. *Science.* 2010 Mar 26;327(5973):1657-61.

Shirley SH, Rundhaug JE, Tian J, Cullinan-Ammann N, Lambertz I, Conti CJ, Fuchs-Young R. Transcriptional regulation of estrogen receptor-alpha by p53 in human breast cancer cells. *Cancer Res.* 2009 Apr 15;69(8):3405-14.

Smith S, de Lange T. TRF1, a mammalian telomeric protein. *Trends Genet.* 1997 Jan;13(1):21-6.

Smith S, Giriat I, Schmitt A, de Lange T. Tankyrase, a poly(ADP-ribose) polymerase at human telomeres. *Science.* 1998 Nov 20;282(5393):1484-7.

Smith S, de Lange T. Cell cycle dependent localization of the telomeric PARP, tankyrase, to nuclear pore complexes and centrosomes. *J Cell Sci.* 1999 Nov;112 (Pt 21):3649-56.

Smith JJ, Rücknagel KP, Schierhorn A, Tang J, Nemeth A, Linder M, Herschman HR, Wahle E. Unusual sites of arginine methylation in Poly(A)-binding protein II and in vitro methylation by protein arginine methyltransferases PRMT1 and PRMT3. *J Biol Chem.* 1999 May 7;274(19):13229-34.

Smith S, de Lange T. Tankyrase promotes telomere elongation in human cells. *Curr Biol.* 2000 Oct 19;10(20):1299-302.

Smogorzewska A, van Steensel B, Bianchi A, Oelmann S, Schaefer MR, Schnapp G, de Lange T. Control of human telomere length by TRF1 and TRF2. *Mol Cell Biol.* 2000 Mar;20(5):1659-68.

Smogorzewska A, de Lange T. Different telomere damage signaling pathways in human and mouse cells. *EMBO J.* 2002 Aug 15;21(16):4338-48.

Stack G, Kumar V, Green S, Ponglikitmongkol M, Berry M, Rio MC, Nunez AM,

Roberts M, Koehl C, Bellocq P, et al. Structure and function of the pS2 gene and estrogen receptor in human breast cancer cells. *Cancer Treat Res.* 1988;40:185-206.

Stansel RM, de Lange T, Griffith JD. T-loop assembly in vitro involves binding of TRF2 near the 3' telomeric overhang. *EMBO J.* 2001 Oct 1;20(19):5532-40.

Struhl K. Histone acetylation and transcriptional regulatory mechanisms. *Genes Dev.* 1998 Mar 1;12(5):599-606.

Suñé C, Garcia-Blanco MA. Transcriptional cofactor CA150 regulates RNA polymerase II elongation in a TATA-box-dependent manner. *Mol Cell Biol.* 1999 Jul;19(7):4719-28.

Szabo A, Dalmau J, Manley G, Rosenfeld M, Wong E, Henson J, Posner JB, Furneaux HM. HuD, a paraneoplastic encephalomyelitis antigen, contains RNA-binding domains and is homologous to Elav and Sex lethal. *Cell.* 1991 Oct 18;67(2):325-33.

Tadesse H, Deschênes-Furry J, Boisvenue S, Côté J. KH-type splicing regulatory protein interacts with survival motor neuron protein and is misregulated in spinal muscular atrophy. *Hum Mol Genet.* 2008 Feb 15;17(4):506-24.

Tang J, Gary JD, Clarke S, Herschman HR. PRMT 3, a type I protein arginine N-methyltransferase that differs from PRMT1 in its oligomerization, subcellular localization, substrate specificity, and regulation. *J Biol Chem.* 1998 Jul 3;273(27):16935-45.

Tejera AM, Stagno d'Alcontres M, Thanasoula M, Marion RM, Martinez P, Liao C, Flores JM, Tarsounas M, Blasco MA. TPP1 is required for TERT recruitment, telomere elongation during nuclear reprogramming, and normal skin development in mice. *Dev Cell.* 2010 May 18;18(5):775-89.

Torchia J, Glass C, Rosenfeld MG. Co-activators and co-repressors in the integration of transcriptional responses. *Curr Opin Cell Biol.* 1998 Jun;10(3):373-83.

Torres-Padilla ME, Parfitt DE, Kouzarides T, Zernicka-Goetz M. Histone arginine methylation regulates pluripotency in the early mouse embryo. *Nature.* 2007 Jan 11;445(7124):214-8.

Travers A. An engine for nucleosome remodeling. *Cell.* 1999 Feb 5;96(3):311-4.

Tsai MJ, O'Malley BW. Molecular mechanisms of action of steroid/thyroid

- receptor superfamily members. *Annu Rev Biochem.* 1994;63:451-86.
- van Steensel B, de Lange T. Control of telomere length by the human telomeric protein TRF1. *Nature.* 1997 Feb 20;385(6618):740-3.
- van Steensel B, Smogorzewska A, de Lange T. TRF2 protects human telomeres from end-to-end fusions. *Cell.* 1998 Feb 6;92(3):401-13.
- Wang F, Podell ER, Zaug AJ, Yang Y, Baciu P, Cech TR, Lei M. The POT1-TPP1 telomere complex is a telomerase processivity factor. *Nature.* 2007 Feb 1;445(7127):506-10.
- Wang RC, Smogorzewska A, de Lange T. Homologous recombination generates T-loop-sized deletions at human telomeres. *Cell.* 2004 Oct 29;119(3):355-68.
- Wang W, Dong L, Saville B, Safe S. Transcriptional activation of E2F1 gene expression by 17beta-estradiol in MCF-7 cells is regulated by NF-Y-Sp1/estrogen receptor interactions. *Mol Endocrinol.* 1999 Aug;13(8):1373-87.
- Wang Y, Wysocka J, Sayegh J, Lee YH, Perlin JR, Leonelli L, Sonbuchner LS, McDonald CH, Cook RG, Dou Y, Roeder RG, Clarke S, Stallcup MR, Allis CD, Coonrod SA. Human PAD4 regulates histone arginine methylation levels via demethylimination. *Science.* 2004 Oct 8;306(5694):279-83.
- Watson JD. Origin of concatemeric T7 DNA. *Nat New Biol.* 1972 Oct 18;239(94):197-201.
- Webb P, Nguyen P, Shinsako J, Anderson C, Feng W, Nguyen MP, Chen D, Huang SM, Subramanian S, McKinerney E, Katzenellenbogen BS, Stallcup MR, Kushner PJ. Estrogen receptor activation function 1 works by binding p160 coactivator proteins. *Mol Endocrinol.* 1998 Oct;12(10):1605-18.
- Wright WE, Tesmer VM, Huffman KE, Levene SD, Shay JW. Normal human chromosomes have long G-rich telomeric overhangs at one end. *Genes Dev.* 1997 Nov 1;11(21):2801-9.
- Wu L, Multani AS, He H, Cosme-Blanco W, Deng Y, Deng JM, Bachilo O, Pathak S, Tahara H, Bailey SM, Deng Y, Behringer RR, Chang S. Pot1 deficiency initiates DNA damage checkpoint activation and aberrant homologous recombination at telomeres. *Cell.* 2006 Jul 14;126(1):49-62.
- Wu Q, Bruce AW, Jedrusik A, Ellis PD, Andrews RM, Langford CF, Glover DM, Zernicka-Goetz M. CARM1 is required in embryonic stem cells to maintain pluripotency and resist differentiation. *Stem Cells.* 2009 Nov;27(11):2637-45.

Xin H, Liu D, Wan M, Safari A, Kim H, Sun W, O'Connor MS, Songyang Z. TPP1 is a homologue of ciliate TEBP-beta and interacts with POT1 to recruit telomerase. *Nature*. 2007 Feb 1;445(7127):559-62.

Xu W, Cho H, Kadam S, Banayo EM, Anderson S, Yates JR 3rd, Emerson BM, Evans RM. A methylation-mediator complex in hormone signaling. *Genes Dev*. 2004 Jan 15;18(2):144-56.

Xu Y, Kimura T, Komiyama M. Human telomere RNA and DNA form an intermolecular G-quadruplex. *Nucleic Acids Symp Ser (Oxf)*. 2008;(52):169-70.

Yadav N, Lee J, Kim J, Shen J, Hu MC, Aldaz CM, Bedford MT. Specific protein methylation defects and gene expression perturbations in coactivator-associated arginine methyltransferase 1-deficient mice. *Proc Natl Acad Sci U S A*. 2003 May 27;100(11):6464-8.

Yang H, Duckett CS, Lindsten T. iPABP, an inducible poly(A)-binding protein detected in activated human T cells. *Mol Cell Biol*. 1995 Dec;15(12):6770-6.

Yao TP, Ku G, Zhou N, Scully R, Livingston DM. The nuclear hormone receptor coactivator SRC-1 is a specific target of p300. *Proc Natl Acad Sci U S A*. 1996 Oct 1;93(20):10626-31.

Ye JZ, de Lange T. TIN2 is a tankyrase 1 PARP modulator in the TRF1 telomere length control complex. *Nat Genet*. 2004 Jun;36(6):618-23.

Ye JZ, Hockemeyer D, Krutchinsky AN, Loayza D, Hooper SM, Chait BT, de Lange T. POT1-interacting protein PIP1: a telomere length regulator that recruits POT1 to the TIN2/TRF1 complex. *Genes Dev*. 2004 Jul 15;18(14):1649-54.

Zhu XD, Küster B, Mann M, Petrini JH, de Lange T. Cell cycle-regulated association of RAD50/MRE11/NBS1 with TRF2 and human telomeres. *Nat Genet*. 2000 Jul;25(3):347-52.